UNIVERSITEIT GENT

FACULTY OF VETERINARY MEDICINE
approved by EAEVE

The Use and Advantages of Computed Tomography in Equine Medicine Evaluated by Clinical Studies

CASPER PAUL CRIJNS

Thesis submitted in fulfilment of the requirements for the degree of
Doctor of Philosophy (PhD) in Veterinary Sciences,
Faculty of Veterinary Medicine, Ghent University

2016

Promoters:
Dr. Ingrid Gielen
Prof. Dr. Ann Martens
Prof. Dr. Katrien Vanderperren

Department of Veterinary Medical Imaging and Small Animal Orthopaedics
Faculty of Veterinary Medicine
Ghent University

The Use and Advantages of Computed Tomography in Equine Medicine Evaluated by Clinical Studies

Casper Paul Crijns
Vakgroep Medische Beeldvorming van de Huisdieren en Orthopedie van de Kleine Huisdieren
Faculteit Diergeneeskunde
Universiteit Gent

Cover design by Marnix Verdonk: Merel Blom's Rumour Has It N.O.P. virtually jumping through a GE Revolution CT

"Make your passion your profession and you'll never work a day in your life"

EXAMINATION BOARD

Chairman: Prof. Dr. Patrick De Backer

Faculty of Veterinary Medicine, Ghent University, BE

Secretary: Prof. Dr. Lieven Vlaminck

Faculty of Veterinary Medicine, Ghent University, BE

Members: Em. Prof. Dr. Francis Verschooten

Faculty of Veterinary Medicine, Ghent University, BE

Prof. Dr. Renate Weller

Royal Veterinary College, UK

Prof. Dr. Frederik Pille

Faculty of Veterinary Medicine, Ghent University, BE

Prof. Dr. Pieter Cornillie

Faculty of Veterinary Medicine, Ghent University, BE

Prof. Dr. René van Weeren

Faculty of Veterinary Medicine, Utrecht University, NL

Drs. Leendert-Jan Hofland

DAP Bodegraven BV, NL

TABLE OF CONTENTS

LIST OF ABBREVIATIONS

AAEP	American Association of Equine Practitioners
ACTH	adrenocorticotropic hormone
CT	computed tomography
FPJ	femoropatellar joint
HU	Hounsfield Unit
IA	intra-arterial
IV	intravenous
K	Cohen's Kappa
kV	kilovoltage
LFTJ	lateral femorotibial joint
mAs	milliampere-seconds
MFTJ	medial femorotibial joint
mgI	milligram Iodine
MPR	multi-planar reconstruction
MRI	magnetic resonance imaging
OC	osteochondrosis
P:B ratio	pituitary gland height-to-brain area ratio
PEH	progressive ethmoidal haematoma
PI	pars intermedia
PPID	pituitary pars intermedia dysfunction
pQCT	peripheral quantitative computerised tomography
ROI	region of interest
wK	weighted Kappa
WL	window level
WW	window wide

PREFACE

In current equine practice, imaging modalities such as radiography and ultrasonography are widely used as diagnostic tools for musculoskeletal lesions. The advantages of these diagnostic-imaging tools include availability, mobility and ease of use, even in the horse's stable. However, interpretation of the images can be challenging due to superimposition of anatomical structure, a narrow imaging window and because of the complexity or discreteness of lesions. Therefore, cross sectional imaging modalities such as computed tomography (CT) and magnetic resonance imaging have been introduced in equine veterinary medicine to overcome these limitations. In order to choose the appropriate imaging modality in clinical situations, knowledge of their capacities and limitations is necessary.

This PhD thesis explores the use of computed tomography in equine medicine in various clinical studies. First, an assessment of the diagnostic value of CT compared to radiography was evaluated both for distal limb and head fractures. Secondly, the ability of CT compared to a clinical, radiographic, ultrasonographic and gross pathologic examination of a stifle-lameness case was documented. Thirdly, the ability to increase soft tissue contrast in the head was analysed by comparing two CT contrast enhancement protocols. Finally, the pituitary gland height-to-brain area ratio of healthy horses was determined on contrast-enhanced CT.

CHAPTER ONE

The Use and Advantages of Computed Tomography in Equine Medicine

Casper P. Crijns[1], Katrien Vanderperren[1], Renate Weller[2], Ann Martens[3], Lieven Vlaminck[3], Francis Verschooten[1], Henri J.J. van Bree[1], Ingrid M.V.L. Gielen[1]

[1] Department of Medical Imaging and Small Animal Orthopaedics, Ghent University, 9820 Merelbeke, Belgium
[2] Department of Veterinary Clinical Sciences, Royal Veterinary College, Hertfordshire AL9 7TA, United Kingdom
[3] Department of Surgery and Anaesthesiology of Domestic Animals, Ghent University, 9820 Merelbeke, Belgium

Adapted from:

Casper P. Crijns, Katrien Vanderperren, Renate Weller, Ann Martens, Lieven Vlaminck, Francis Verschooten, Henri J.J. van Bree, Ingrid M.V.L. Gielen. The use and advantages of computed tomography in equine medicine *(published in The Australian Equine Veterinarian (2016)* ***35*** *(2) 50-61)*

Summary

The use of computed tomography (CT) is becoming more common in equine medicine, as evidenced by the number of clinical papers published in recent years. Improvements in hardware (helical scanning, multiple detector rows, isotropic voxels and shorter scanning time), combined with software advances (multi-planar reformatting and volume rendering), and the use of new protocols (contrast-enhanced CT and standing CT) have increased the diagnostic value of CT in equine medicine. CT is used regularly for the indications described in this review (but it is not limited to these indications). To determine the additional value of CT, CT must be compared to the first-line diagnostic modalities such as radiography and ultrasonography, as well as to other advanced imaging modalities such as magnetic resonance imaging and scintigraphy. This review provides an introduction to CT in equine medicine and an overview of the comparative CT imaging studies available in the literature.

Introduction

The use of computed tomography (CT) in equine medicine has evolved substantially since its first use in equine medicine in 1984 by Professor Francis Verschooten (personal communication). Over the years, the basic technique has improved with faster scan-times and improved performance. CT scanners are now capable of producing much thinner slices, which provide superior information and allow for more accurate diagnosis. However, no data are available on the quantity of CT set-ups available for horses. An increasing amount of university teaching hospitals and private practices have installed CT scanners and provide simple and direct imaging examinations of referral patients (without intervention). In line, the amount of reports demonstrating the clinical usefulness of CT has increased in the last 10 years, with around 60 published reports prior to 2006 and about 250 published reports after 2006 (PubMed / Web of Science).

After acquisition, the raw data can be processed in a variety of ways to improve the diagnostic capabilities and the radiologist's ability to visualise structures/lesions. Depending on the tissue of interest (bone, soft tissue, brain, lung, etc.), different image reconstruction algorithms are used to emphasise these specific tissues. The contrast scale (window width and window level) can be manipulated digitally to optimise the contrast latitude for these different tissues [1]. Multi-planar reconstruction (MPR) allows the orientation of the source images to be manipulated, so that the different structures can be reviewed in any plane (Figure 1). MPR also allows the slice thickness to be adjusted to depict curved structures more easily and to reduce the effects of certain artefacts on image quality. For example: beam-hardening and partial volume artefacts at the level of the thick petrous part of the temporal bones of the caudal cranial fossa are mainly caused by small, highly attenuating structures. Reducing the slice thickness of the scan reduces these artefacts but increases image noise. Re-sampling the thinner slices (0.6 mm) into thicker slices (2 mm) reduces this image noise (noise cancelation by averaging) [2] and the re-sampled images contain both fewer artefacts and less noise. Finally, volume-rendering software allows 3-dimensional visualisation of the surfaces of the structures of interest (Figure 1e). Although volume rendering often presents helpful

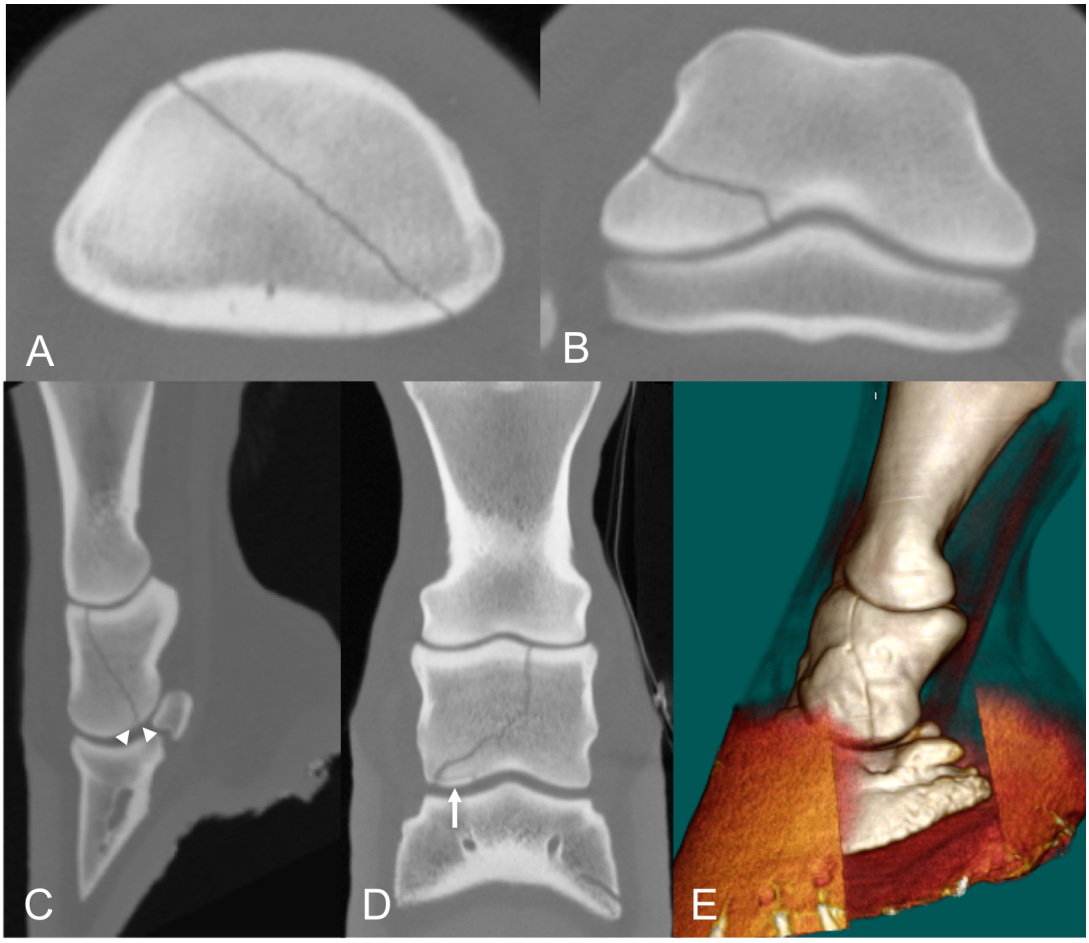

Figure 1: Transverse, sagittal, dorsal and 3D reconstructed CT images of a 15-year-old Irish pony gelding with a simple, acute, biarticular, complete, closed, not displaced spiral fracture of P2 (medial or dorsal is to the left). A fracture line (<1mm) is visible, starting in the pastern joint and is oriented in a dorsomedial-plantarolateral direction (A). The fracture runs distally in a spiral (B) and ends as 2 fracture lines (arrow points) in the coffin joint in the plantar part of the medial condyl (C), separating an intra-articular non-displaced fragment (arrow) (D). 3D representation of the fracture from a dorsomedial direction (E). Several coalescing cracks are visible along the fracture line.

images of the lesions (e.g. fractures), the diagnostic value is limited due to the loss of data available for evaluation (only the outer shell of data is used to construct the images).

In addition to post-processing, iodine-based contrast media can be used to better characterise and differentiate normal from pathological structures. These contrast media can be used intravascularly (intra-venously or intra-arterially) [3, 4] or intrathecally, intra-articularly or intra-synovially [5-8]. Intrathecal, intra-articular and intra-synovial contrast administration is based on the delineation of normal anatomical structures (e.g. joint cartilage) and infiltration of contrast into lesions

(e.g. a tear in a cruciate ligament in the stifle) [5]. Intravascular contrast enhancement is based on the increased opacity of (neo-) vascularised structures (e.g. tendon, ligaments and the soft tissue structures in the head) [4, 9]. The uptake of iodine contrast media is influenced by the iodine dosage per kilogram body weight, the rate of injection, the product's osmolarity and viscosity, the variability in heart rate and blood pressure during anaesthesia, and the patient's positioning (lateral or dorsal recumbency) [10, 11]. Normally the protocol used in small animals would be extrapolated and used in horses (600 mgI/kg injected at a rate of 2 ml/s) [12-14]. However, administering a comparable amount of contrast in horses is considered impractical and costly. Several protocols with variable enhancement are described in the literature [4, 9, 10, 15, 16], but further research has yet to determine the optimal contrast dosage and administration technique for equine patients.

Detailed descriptions of the normal CT anatomy of the head and most regions of the limb has been published [3, 4, 5, 6, 7, 8, 17, 18, 19]. In these studies the benefits of CT arthrography [5-8] and/or intra-vascular contrast-enhanced CT [4], to visualise and characterise normal soft tissue anatomy are described. These anatomical studies are useful references guides highlighting possibilities, variations and shortcomings of CT in combination with contrast enhanced CT in these regions.

CT studies in equine practice are performed on recumbent horses under general anaesthesia or on sedated, standing horses (Figure 2).

Specifically, for the use of CT in horses, beside a CT scanner and associated equipment additional adaptations of the facilities are needed to accommodate horses. To perform CT examinations under general anaesthesia, an induction and recovery box (preferably one that allows assisted recovery), equipment for maintaining general anaesthesia and patient monitoring, and a hoist to transport the horse and lift it onto the custom-made table are needed [20]. For standing CT of the equine head, the CT scanner is reversed to accommodate an equine platform. Moreover, to allow the horse to place its head horizontally on the CT couching, the CT scanner has to be raised in relation to the equine platform [21]. Each technique has its own advantages and disadvantages. However, general anaesthesia in horses has always been a concern, due to the risks and the additional costs [22]. Thus,

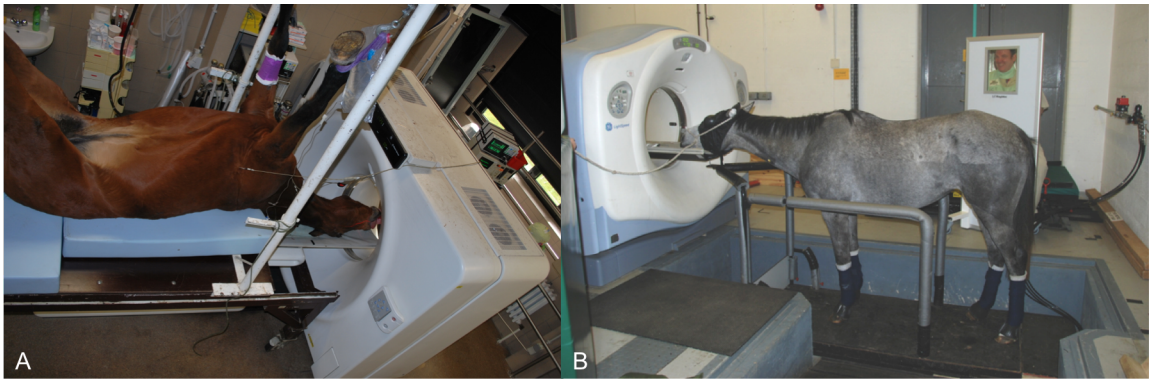

Figure 2: Photographs of head CT's performed on a recumbent horse under general anaesthesia at Ghent University (A) and on a standing, sedated horse at the Royal Veterinary College (B). The horse is placed in dorsal recumbency on a custom-made table, the equipment to maintain and monitor the general anaesthesia are placed behind the scanner (A). The horse is standing in a pit on a platform which is connected to the CT couch, allowing the horse to rest it's head on the CT couch, note the blinkers, rope head collar and earplugs (B).

scanning the head while the horse is standing is becoming more popular. The primarily disadvantages of this technique however are: the inability to scan limbs, the increased probability of motion artefacts that necessitate re-scanning and the radiation exposure of the handler holding the horse. A secondary disadvantage of this technique is the inability of producing topographic scans as many horses oppose the higher table speeds during these scans [21, 23].

Indications

CT in horses is primarily focused on musculoskeletal injuries of the limbs, head and cranial neck, dental pathology, and sinonasal disease. The size of the patient relative to the size of the gantry (variable between 50 to 85 cm) is the limiting factor for CT in horses. Reports on adult horses illustrate that extremities can be scanned up to the stifle and the head and neck to C4 [24] (in individual cases, to C7-T1 [25]). In foals and miniature horses, size restriction does not apply, and scanning of thorax, abdomen or pelvis is possible [26-29].

Musculoskeletal injuries of the limbs

Lameness is a common cause of performance-related wastage in equines. Radiography and ultrasonography are widely used by general practitioners to detect and diagnose musculoskeletal disease [1]. However, the limitations of these modalities must be considered, an accurate diagnosis is essential for an optimal

treatment, management plan, and realistic prognosis, to allow the horse the best chance of returning to its previous athletic level. Advanced imaging modalities, such as CT, scintigraphy and magnetic resonance imaging (MRI), add important diagnostic information to the traditionally used radiography and ultrasonography. The advantage of CT used in combination with contrast-enhanced CT in orthopaedic cases is that it allows complete evaluation of all structures (bone, cartilage, tendon and ligament), even the structures previously obstructed by bony superimposition or a narrow imaging window.

Navicular disease

The interpretation of the clinical relevance of radiographic changes in the navicular bone differs among clinicians. Several studies on navicular disease, comparing CT to plain radiographs, have illustrated the limitations of the latter technique: on a lateromedial radiographic projection, the indistinct demarcation between compact and spongiform bone and bone densification of the spongiform bone is prone to over interpretation [30]. Conversely, the detection of distal border fragments is underestimated on the dorsoproximal-palmarodistal oblique radiographic projection [30]. The radiographic evaluation of the number and depth of the synovial invaginations in the distal navicular border is also underestimated [19]. These specific radiographic changes are commonly used for grading navicular disease and assessing the risk factors for future sport performances. Due to disadvantages as general anaesthesia and the higher costs of a CT examination, CT will not replace radiography as a screening test for navicular disease. Further research involving more advanced imaging modalities, as CT, however could indirectly help diminish the existing variability in interpreting these specific changes and evaluating risk factors, especially in the early stages of navicular disease.

Bone trauma

The advantages of CT in pre- or intra-operative fracture evaluation have been repeatedly reported [31-35]. The limited ability to determine fracture length, complexity and orientation on radiographs has been observed during surgery [36]. Detecting additional fracture lines during surgery complicated and lengthened the procedure and general anaesthesia time. Therefore, it is hypothesised that the

ability to plan surgery thoroughly with CT helps improve the quality of surgical repair and ensures a more accurate pre-operative prognosis (Figure 1).

Articular lesions

Osteoarthritis, a degenerative process affecting joints, is frequently encountered in horses. The presence of osteophytes, enthesiophytes, sclerosis, osteolytic lesions and cartilage defects constitute the major changes observed in osteoarthritis. Even in an anatomically relatively simple joint such as the fetlock, these changes are easily missed or underestimated with radiography [37]. In fact, to overcome the limited contrast resolution of radiography, the mineral content of a bony lesion has to change by at least 30% to become visible [38]. Compared to radiography, CT is able to detect subtler changes and changes in an earlier stage [37] (Figure 3).

Comparing CT to MRI, the studies of Olive et al. [37] and O'brien et al. [39] focused on the cartilaginous and non-cartilaginous structures of the metacarpophalangeal joint. Subchondral bone lesions were detected similarly with CT and MRI, although some differences were present. Compared to MRI, CT had a higher correlation score between osteophytosis and the grossly evaluated cartilage damage scores. However, the sentinels of osteophytes, not detected with CT, were possibly detected using a special MRI sequence – a sagittal 3D spoiled gradient recalled echo with fat saturation. The presence of these small changes was not confirmed on gross pathology and other (more routinely used) MRI sequences could not replicate these results. As histopathology was not performed, and other characteristics of osteoarthrosis were absent, the clinical relevance of these suspected lesions is questionable [37].

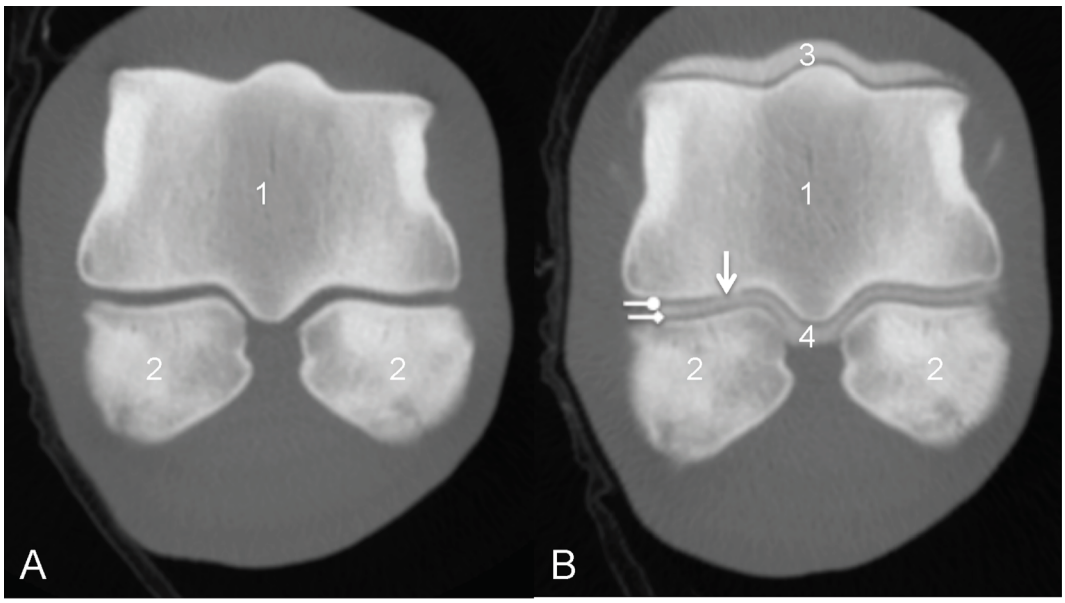

Figure 3: Transverse CT (A) and transverse CT arthrogram (B) images of a left metacarpophalangeal joint (medial is to the left). The joint cartilage of the condyles of the third metacarpal bone and the proximal sesamoid bones separated by the palmar synovial recess cannot be differentiated from each other (A); the CT arthrogram (same level as A) shows contrast medium (arrow) in the joint cartilage of the medial palmar condyle of the third metacarpal bone, representing a full-thickness cartilage lesion. 1 distal condyles of the third metacarpal bone; 2 proximal sesamoid bones; 3 dorsal synovial recess of the metacarpophalangeal joint; 4 palmar synovial recess of the metacarpophalangeal joint, separating cartilage of the palmar aspect of the medial palmar condyl (round arrow) and cartilage of the medial proximal sesamoid bone (diamond arrow).

The study of Hontoir et al. [40] showed that CT arthrography is a valuable tool for assessing cartilage defects. Compared to specific high field MRI sequences (3D fast spin echo or dual echo in the steady state sequences), CT arthrography has better contrast resolution, higher spatial resolution, and less limitation due to artefacts. This results in a better correlation between imaging findings and macroscopic findings of cartilage defects [40]. Similar results are reported in the human medicine literature [41]. When comparing CT arthrography and conventional MRI, CT arthrography has proven to be superior in detecting especially small surface lesions. When comparing CT arthrography and MRI arthrography, both modalities have similar specificity and sensitivity for the detection of cartilage lesions, even in joints with thin cartilage [41].

Tendon and ligament lesions

Ultrasonography is the standard imaging modality used for tendon and ligament lesions in horses. In cases of an ultrasonographic inconclusive diagnosis (e.g. vague suspensory ligament injury or involving structures within the hoof capsule) the use of MRI has been documented in the literature [42-45]. However, when MRI is not available, CT in combination with intra-arterial contrast-enhanced CT has been suggested as an alternative (Figure 4).

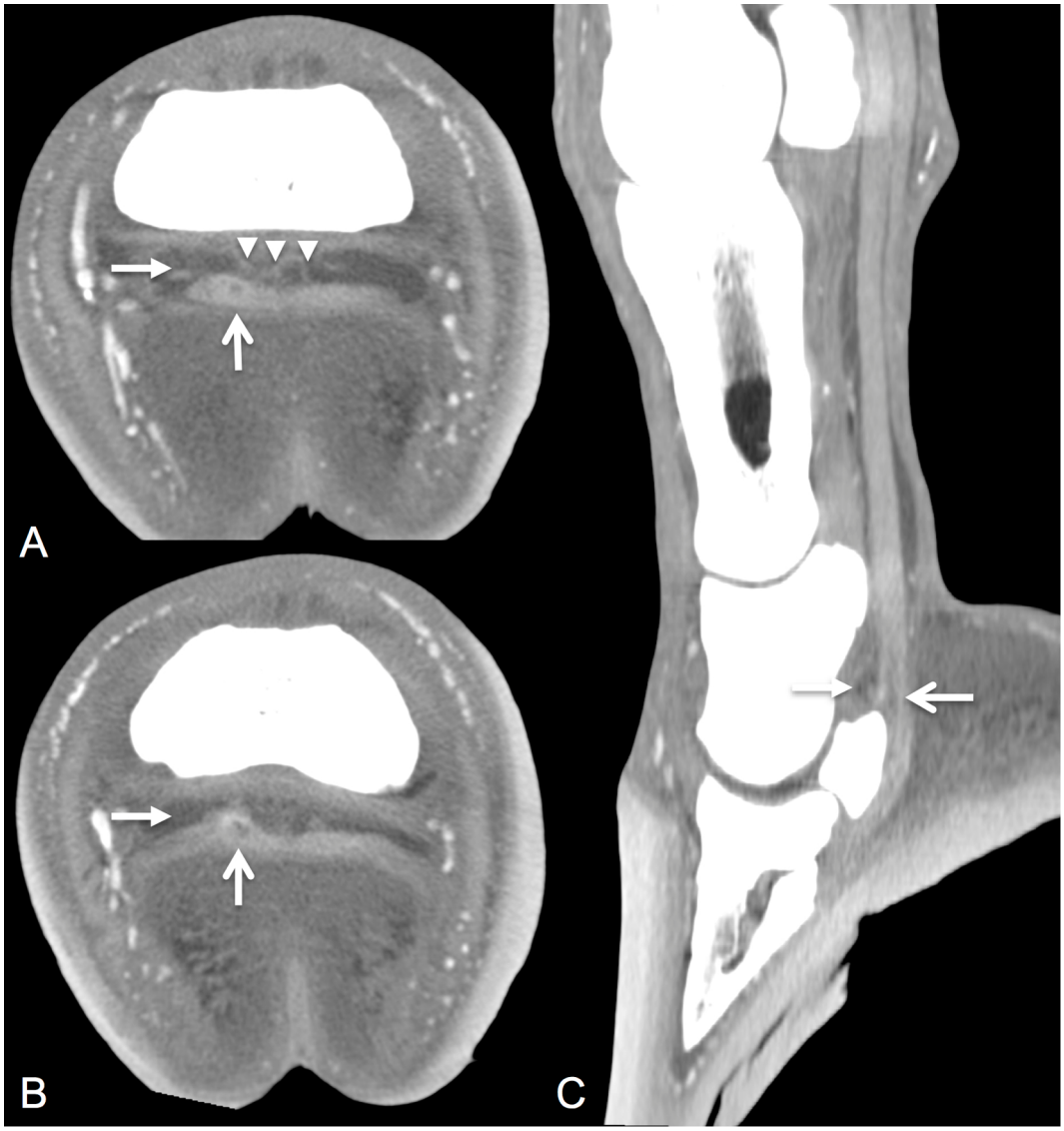

Figure 4: Transverse (A and B) and sagittal (C) post-intra-arterial contrast CT images of the distal limb of a 7 year-old Warmblood gelding (medial or dorsal is left). A core to dorsal border lesion with peripheral enhancement is present in the medial lobe of the DDFT (open arrow) just proximal to the navicular bone. A concurrent navicular bursa effusion with slight synovial enhancement (closed arrow) and new vessel formation at the level of the lesion (arrowheads) are present.
Images courtesy of Dr HJ Bergman (Lingehoeve Diergeneeskunde).

The studies of Vallance et al. [46, 47] and the study of Puchalski et al. [9], which focused on the soft tissue structures of the foot, show that CT combined with contrast-enhanced CT has higher visibility scores for the distal phalanx, whereas standing low-field MRI could better visualise the impar ligament, the synovial structures (except for the tendon sheath), and the distal part of the deep digital flexor tendon, with no significant difference for the remaining ligamentous structures in the foot [47].

Identified lesions showed a similar pattern with both modalities. Lesions located proximal to the navicular bone were often identified only with CT, whereas lesions distal to the navicular bone were frequently detected only with low-field MRI [46]. CT scans a volume (e.g. the distal limb) homogeneously, whereas in MRI studies the image quality is best in the centre of the image (in the focus of the region of interest) and image quality decreases towards the periphery of the field of view. Thus, structures in the periphery of the image are less easy to detect or evaluate. If the focus of the MRI study had been on structures other than the foot, the structures in this focus of the field of view would probably have been detected/diagnosed more easily.

The additional use of contrast-enhanced CT, in combination with multiplanar reformatting tools and decreased slice thickness, improved CT's ability to identify a lesion at the insertion of the deep digital flexor tendon [4, 46]. Therefore, contrast-enhanced CT can be considered a good alternative to MRI for diagnosing tendinopathy of the deep digital flexor tendon (Figure 4) [9].

Head

CT has proven useful for diagnosing sinus and dental disease, head trauma, bone pathology [17, 48, 49] and, to a lesser extent, intra-cranial disease [11]. The normal anatomical CT appearance and lesion-specific CT characteristics have been described for most lesions, but accurately interpreting CT images of the equine head requires some experience [10]. In contrast to musculoskeletal injuries of the limbs, the use of CT in head pathology (with the exception of intra-cranial lesions) is applied far more frequently than MRI and is considered to be the advanced imaging modality of choice. Comparing CT and MRI for the diagnosis of most head diseases,

CT has the advantage that it can be performed in standing horses, thus avoiding general anaesthesia. This is especially useful, as in most cases treatment does not require general anaesthesia either. When general anaesthesia is required, the shorter study time associated with CT compared to MRI facilitates diagnosis and treatment during the same general anaesthesia session [50]. To date, MRI of the head requires general anaesthesia, and the long scanning times usually result in a second general anaesthesia session when surgical treatment is required [51].

Bone trauma

The bony skull of the horse is very prone to trauma − e.g. from falling over backwards, direct kicks from other animals, or running into stationary objects [52, 53]. In these cases, it is important to obtain specific and thorough information about the lesion's type, localisation, extent, severity, and the involvement of brain and other soft tissue. A presumptive diagnosis based on clinical history, physical examination, radiography and endoscopy can be made, but several reports have mentioned the risk of overlooking, or underestimating the extent of lesions [52-54]. CT has proven to be very sensitive and reliable in visualising bony trauma to the head, especially in regions (such as the ventral cranium or the temporomandibular joint) that are less accessible via other imaging modalities (Figure 5) [52, 53-55].

Larger case studies comparing the capabilities of the different imaging modalities are lacking. Unpublished data have shown that, when radiography and CT are compared to a gold standard such as surgery or gross pathology, the true extent of a traumatic lesion can only be appreciated with CT (Figure 5) (Casper P. Crijns, unpublished data).

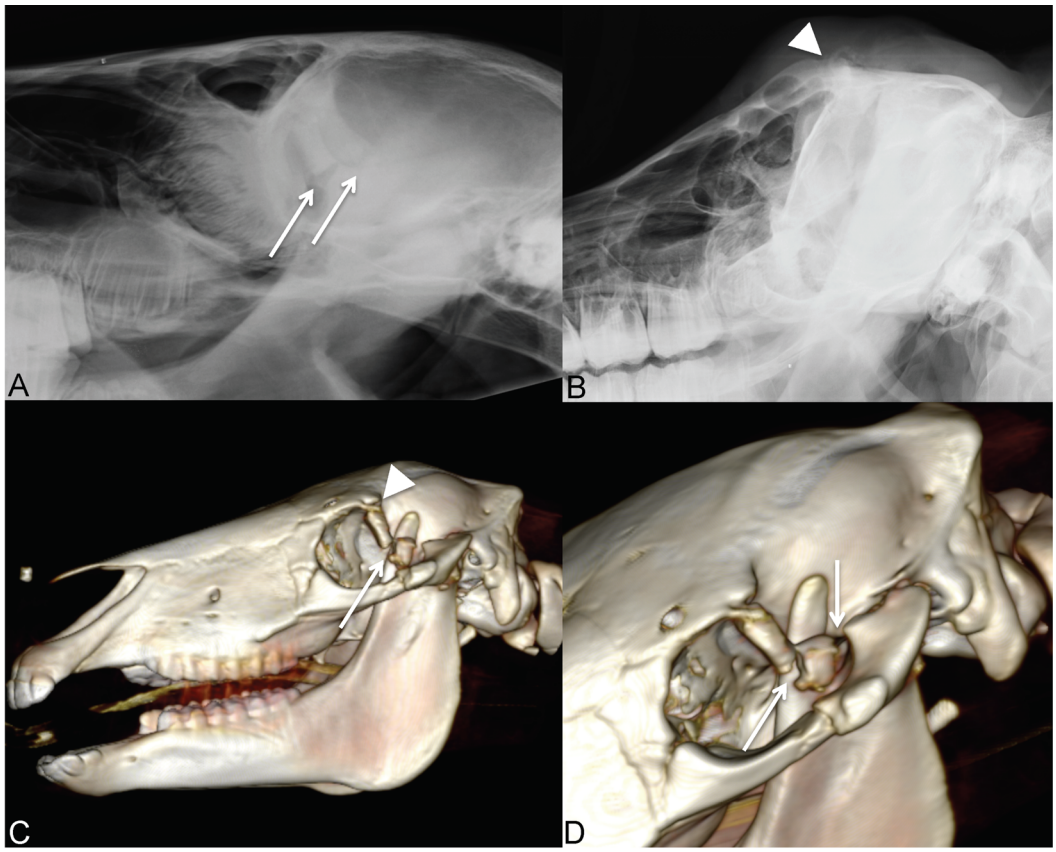

Figure 5: Laterolateral (A) and leftventral-rightdorsal-oblique (B) radiographic images and 3-dimensional volume rendered CT images of the complete head (C) and close-up (D) of a 3 month-old foal (rostral is to the left). A double fracture of the zygomatic bone (A: arrows) and suspicion of a fracture of the base of the zygomatic process of the frontal bone (B: arrow point) are detected (A and B). Multiple fractures are visible surrounding the left orbita (C and D). The fractures included the mandibular fossa and temporomandibular joint, the zygomatic process of the frontal bone, the zygomatic arch and the zygomatic bone down to the alveolus of element 109 (not visible on the image). The arrows and arrow point similarly annotate the fractures previously detected on radiographs.

Hyoid apparatus

The hyoid apparatus can be affected by equine temporohyoid osteoarthropathy, a progressive disease characterised by osseous proliferation of the temporohyoid articulation and the surrounding structures [48, 57, 58]. An acute onset can be recognised by vestibular and/or facial nerve signs due to petrous temporal bone fractures through the ankylosed joint [48, 58]. Diagnosis is traditionally made through endoscopic evaluation of the stylohyoid bones in the guttural pouches, which is usually combined with radiography [48, 57, 58]. However, when the endoscopic and radiographic diagnosis was compared to the CT diagnosis,

10 of the 16 cases of temporohyoid osteoarthropathy described in the study were diagnosed only with CT [48]. CT is able to identify previously undiagnosed stress fractures of the temporal and stylohyoid bone, lytic osseous changes and thickening of the ceratohyoid bone, and the presence of subclinical bilateral disease and other abnormalities of adjacent structures [48]. The study of Hilton et al. [48] has also shown an age-associated increase of the lesions' severity and an increased level of neurologic dysfunction associated with the increased width of the styloid bone, which has been confirmed by the study of Naylor et al. [58]. Although the aetiology has not been established, the additional evidence from CT supports the theory of a degenerative process [48, 57, 58]. With the more complete evaluation that CT provides, diagnosis of bilateral disease can be made at an early (subclinical) stage in unilateral clinically affected horses. The treatment plan and a more deliberate prognosis can be made based on these additional findings [48].

Dental disease

Dental disease is common in horses. After a clinical examination, radiography is the primary diagnostic modality used – but it is an imprecise method for diagnosing dental disease, mainly because of superimposition [54]. CT has been shown to be very helpful in detecting changes in the cheek teeth that are not detected with radiography [54, 59]. Computed tomographic studies report a high prevalence of infundibular changes in both normal and diseased cheek teeth, which has raised questions about the clinical relevance of the changes encountered [59, 60]. Studies describing the normal anatomic and physiologic appearance of the cheek teeth have systematically identified age-dependent pulpar anatomy and enamel morphology with CT [61] and have been able to differentiate between patterns of normal physiologic appearance and pathologic lesions in maxillary cheek teeth [59].

The following criteria are used for a reliable evaluation of a tooth's health: the extent of the loss of definition of the laminae dura dentes, the amount of periapical lysis, the progressive demineralisation of the dental cementum, enamel and dentin, the presence of gas in the pulp cavity, widening of the pulp canal and pulp chamber, and infundibular changes (Figure 6a) [54, 59, 60]. Compared to

radiography or MRI, CT is the only modality that enables all of these criteria to be evaluated and dental lesions in earlier stages to be diagnosed [59, 62].

Dentigerous cysts

CT has also contributed to the diagnosis of dentigerous cysts, which are not painful, but are usually associated with a persistent fistulous tract located distal at the base of the ear [63]. Radiography is used primarily to visualise and identify the location of the associated ectopic tooth [64], but superimposition of the petrous part of the temporal bone, in particular, can make it difficult to localise those ectopic teeth. Computed tomography is recommended to confirm the diagnosis, localise the teeth, or exclude the presence of ectopic tooth tissue in these cases [63]. CT allows a more thorough preoperative planning and prediction of the feasibility of surgery, especially when the ectopic tooth is close to, or in contact with, the calvarium or the temporomandibular joint (Figure 6b) [63].

Paranasal sinuses

The horse has a complex paranasal sinus system, which consists of air-filled spaces lined with a thin respiratory epithelium. The different sinuses communicate with each other or with the nasal cavity through small or large openings that form two separate cavities in each half of the head. CT imaging techniques have been used to describe the complex anatomy of the equine paranasal sinus system in detail (Figure 7) [65, 66].

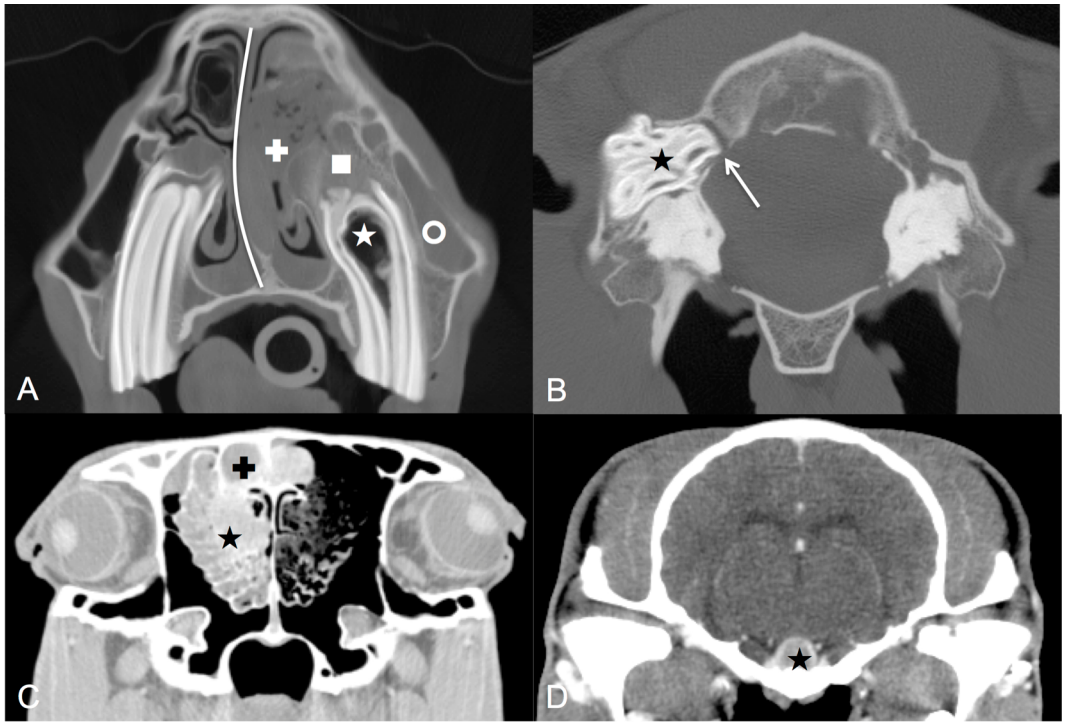

Figure 6: A: Transverse CT image of a 5 year-old Warmblood horse at the level of the fourth premolars visualising an alveolitis and infundibulum necrosis of element 208 with secondary sinusitis in bone algorithm (right is to the left). Element 208 shows a widened, hypodense infundibulum with a apical spherical lesion (star). The surrounding alveolar bone (square) is thickened and shows a sclerotic appearance. The ventral conchal sinus is filled with heterogeneous soft tissue / air opacities (cross) and is causing a deviation of the nasal septum (curved line). The rostral maxillary sinus is fluid-filled (circle).
B: Transverse CT image at the level of the petrous part of the temporal bones of a 3 year-old Warmblood horse in bone algorithm (right is to the left). A dentigerous cyst (ectopic tooth)(star) is visible dorsolaterally to the right petrosal bone extending in the occipital bone, with interruptions (arrow) of the bony outlining of the cerebellum.
C: Transverse CT image at the level of the ethmoid of a 13 year-old Warmblood horse in soft tissue algorithm (rostral or right is to the left). A heterogeneous soft tissue mass (most likely an ethmoid hematoma) is originating from the right ethmoid turbinates (star) and extending to the frontal sinus (cross).
D: Transverse, post-contrast CT image of a 6 year-old Shetland pony at the level of the pituitary gland in a soft-tissue algorithm (right is to the left). The pituitary gland (star) seems mildly enlarged and spherical with a distinct ring enhancement and only a moderate enhancement at the centre. Image strongly indicative for a pituitary pars intermedia dysfunction (pituitary adenoma).

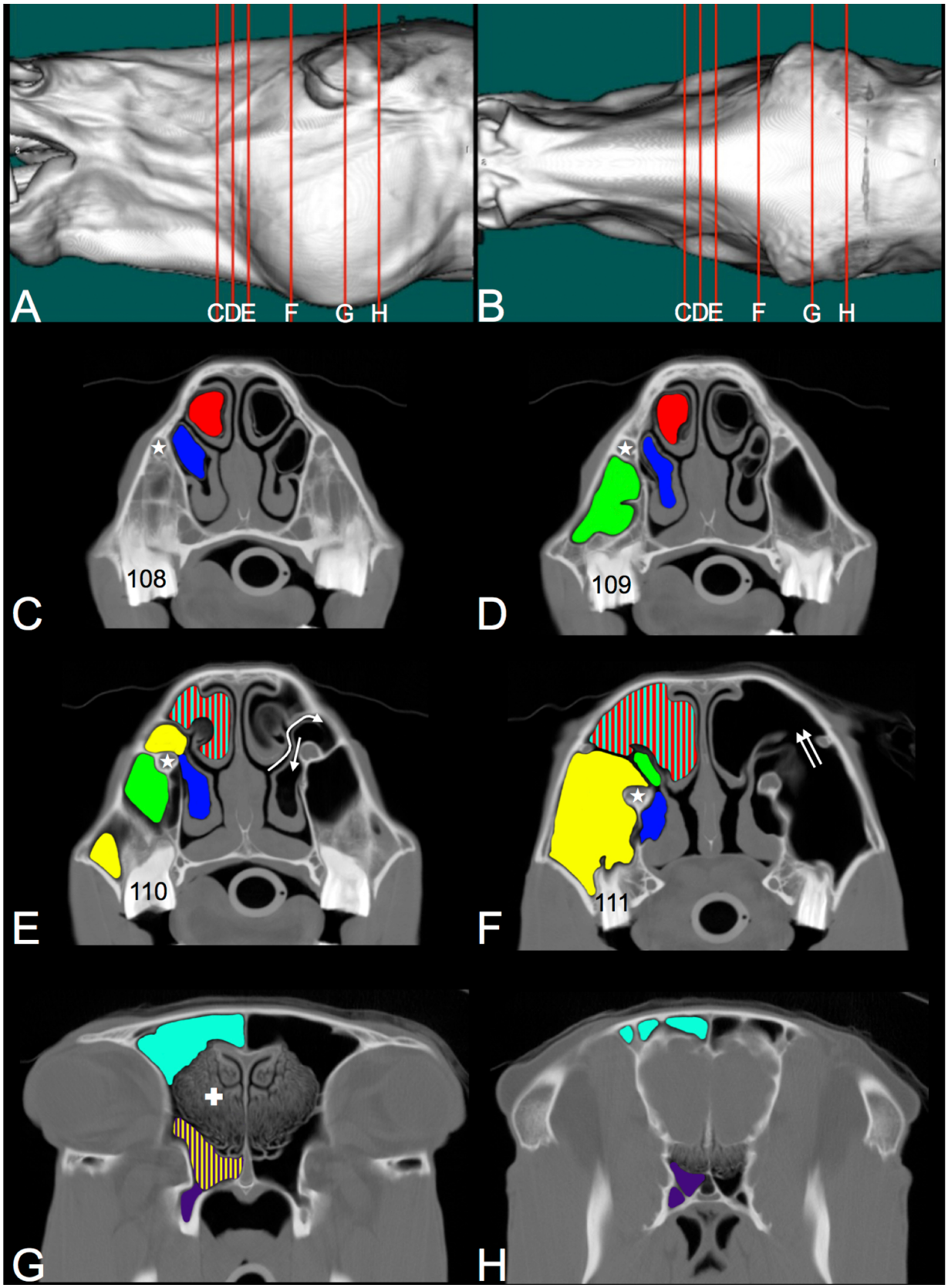

Figure 7: legend on next page

Figure 7: Lateral (A) and dorsal (B) 3-dimensional volume rendered CT images of an equine head with indications of the level representing the transverse CT images (C, D, E, F, G and H) of the paranasal sinuses without pathology of a 19 year-old Warmblood horse (rostral or right is to the left). At the level of element 108, the most rostrally located sinuses are visible. The ventral (dark blue) and dorsal (red) conchal sinuses are located in the most caudal portions of the ventral and dorsal nasal conchae, respectively. The rostral maxillary sinus (green), first visible at the level of element 109, lies lateral to the ventral conchal sinus and ventral to the infraorbital canal (star). The caudal maxillary sinus (yellow) and frontal sinus (light blue) appear simultaneously at the level of element 110. The slit-like nasomaxillary opening (long curved arrow) is the connection of the nasal cavity and the caudal maxillary sinus and the conchomaxillary opening (straight arrow) connects the ventral conchal sinus with the caudal maxillary sinus. In the literature, the frontal and dorsal conchal sinuses are sometimes united as the frontalconchal sinus illustrated by the red/light-blue striation at the level of elements 110 and 111. The caudal maxillary sinus is connected to the frontal sinus by a large frontomaxillary opening (double arrow). At the level of the ethmoid (cross), the sphenopalatinal opening (yellow/pink striation) is a broad connection between the caudal maxillary sinus and the sphenopalatinal sinus (pink). Note the difference in localisation of the sinuses relative to the teeth compared to anatomical textbook.

Radiography is a screening tool to identify space-occupying processes in this region [67, 68]. Equine paranasal sinus disease can be divided into two categories: primary sinusitis, caused by viral or bacterial infections, and secondary sinusitis, which is most often caused by a tooth problem or space-occupying mass (e.g. sinus cyst) [50, 68]. However, the complexity of the area in combination with subtle changes and the inability of completely visualising all structures (e.g. the sphenopalatine sinus) on standard radiographs should be considered [69]. An accurate diagnosis of the underlying cause and the structures involved is necessary in order to treat a sinus lesion successfully and avoid recurrence of the symptoms [70]. The normal air and bone interface present in the paranasal sinuses improves the CT image contrast to a degree that allows even the soft-tissue structures (such as the mucous membranes) to be evaluated [66, 69, 70], enabling CT to identify the different structures involved in the pathology [69, 71].

Ethmoids

Progressive ethmoidal haematoma (PEH) in horses, a chronic lesion that causes intermittent epistaxis, is well documented [72]. The appearance of PEH on CT is a mild to moderately heterogeneous soft tissue mass, slightly hyper-attenuating

relative to muscle tissue, with no (or only mild) anatomic distortion and, on rare occasions, bone destruction (Figure 6c). While endoscopy and/or radiography will often enable the presence of PEH to be identified, CT is invaluable in showing its true extent and exact localisation [72, 73]. CT can detect bilateral occurrence, identify paranasal sinus involvement (sphenopalatine sinus involvement, in particular, is often missed), and show whether PEH is in close proximity to the cribriform plate or whether the optic canal is eroded.

Knowing the full extent of PEH is important, because there is less likelihood of recurrence when all of the lesions are treated appropriately [72]. The lesions in the sphenopalatine sinuses, in particular, cause recurrence of PEH more often, due to the impossible surgical approach with rhinolaryngoscopy, unless part of the medial wall of the dorsal concha has been removed. Direct sinus access is indicated, and CT has been very useful in planning surgery for these cases [72].

Intra-cranial lesions

Normal brain anatomy can be visualised on native CT images in both adult horses and foals [18, 74, 75], and it is possible to distinguish between grey and white brain matter when the window width and window level are chosen [74]. CT's ability to visualise intracranial lesions when used in combination with IV contrast has been reported [11], as well as CT-guided brain biopsy (a technique that allows *in vivo* histopathologic diagnosis of intracranial lesions) [76], but these are case reports. Limited capabilities using CT to diagnose brain parenchyma lesions, such as multifocal, diffuse, abnormal brain parenchyma and meningeal inflammation or non-acute haemorrhage − should be considered [10, 11]. To be visualised on pre-contrast images, an intracranial lesion should have an abnormal opacity, such as acute haemorrhage and focal hyperdense structures in fluid-filled densities (cholesterol granulomata), or an abnormal appearance, such as a midline shift, distortion of the lateral ventricles, hydrocephalus and sometimes bone lysis [10, 11, 23, 75]. Contrast-enhancement CT can help differentiate between brain abscesses, neoplasms and infarction areas, and meningeal congestion can be diagnosed [10, 11]. Contrast-enhancement CT is also an established method for visualising and measuring an enlarged pituitary gland to diagnose pituitary pars intermedia dysfunction (Figure

6d). When comparing CT with gross- and histopathology, researchers found analogous lesions and concluded that CT diagnosis was comparable [10, 11, 15]. Histopathology also demonstrated additional lesions in CT-negative examinations. Therefore, CT can demonstrate intra-cranial lesions, but cannot exclude them. In human and small animal medicine, MRI has proven to be more sensitive and specific in detecting central nervous system lesions [49]. In equine medicine, the specificity and sensitivity of MRI for intra-cranial lesions has not yet been compared with CT [10].

Conclusion

The diagnostic possibilities of CT have been shown to be very versatile, and the evolution towards standing head CT has led to an increase in CT examinations of horses. The use of CT in equine medicine is limited by the size of the horse in relation to the size of the CT gantry. The increase of CT scanners available for horses and new technical developments specifically targeting size issues (gantry opening of 125 cm) and further increasing possibilities of scanning standing sedated horses (neck and limbs) shows the increase in interest and appreciation for CT. As the limits of CT's diagnostic possibilities have not yet been reached, research in this field is on-going. Especially research describing the limitations of CT and comparing CT to other (advanced) imaging modalities would help substantiate the clinical decision making further.

REFERENCES:

1. Kraft, S.L. and Gavin, P. (2001) Physical principles and technical considerations for equine computed tomography and magnetic resonance imaging. *Vet Clin N Am-Equine* **17**, 115-130.

2. Porat-Mosenco, Y., Schwarz, T. and Kass, P.H. (2004) Thick-section reformatting of thinly collimated computed tomography for reduction of skull-base-related artifacts in dogs and horses. *Vet Radiol Ultrasound* **45**, 131-135.

3. Collins, J.N., Galuppo, L.D., Thomas, H.L., Wisner, E.R. and Hornof, W.J. (2004) Use of computed tomography angiography to evaluate the vascular anatomy of the distal portion of the forelimb of horses. *Am J Vet Res* **65**, 1409-1420.

4. Puchalski, S.M., Galuppo, L.D., Hornof, W.J. and Wisner, E.R. (2007) Intraarterial contrast-enhanced computed tomography of the equine distal extremity. *Vet Radiol Ultrasound* **48**, 21-29.

5. Gray, S.N., Puchalski, S.M. and Galuppo, L.D. (2013) Computed tomographic arthrography of the intercarpal ligaments of the equine carpus. *Vet Radiol Ultrasound* **54**, 245-252.

6. Raes, E.V., Bergman, E.H.J., van der Veen, H., Vanderperren, K., Van der Vekens, E. and Saunders, J.H. (2011) Comparison of cross-sectional anatomy and computed tomography of the tarsus in horses. *Am J Vet Res* **72**, 1209-1221.

7. Van der Vekens, E., Bergman, E.H.J., Vanderperren, K., Raes, E.V., Puchalski, S.M., van Bree, H.J.J. and Saunders, J.H. (2011) Computed tomographic anatomy of the equine stifle joint. *Am J Vet Res* **72**, 512-521.

8. Vanderperren, K., Ghaye, B., Snaps, F.R. and Saunders, J.H. (2008) Evaluation of computed tomographic anatomy of the equine metacarpophalangeal joint. *Am J Vet Res* **69**, 631-638.

9. Puchalski, S.M., Galuppo, L.D., Drew, C.P. and Wisner, E.R. (2009) Use of contrast-enhanced computed tomography to assess angiogenesis in deep digital flexor tendonopathy in a horse. *Vet Radiol Ultrasound* **50**, 292-297.

10. Lacombe, V.A., Sogaro-Robinson, C. and Reed, S.M. (2010) Diagnostic utility of computed tomography imaging in equine intracranial conditions. *Equine Vet J* **42**, 393-399.

11. Sogaro-Robinson, C., Lacombe, V.A., Reed, S.M. and Balkrishnan, R. (2009) Factors predictive of abnormal results for computed tomography of the head

in horses affected by neurologic disorders: 57 cases (2001-2007). *J Am Vet Med Assoc* **235**, 176-183.

12. Kromhout, K., Gielen, I., De Cock, H.E., Van Dyck, K. and van Bree, H. (2012) Magnetic resonance and computed tomography imaging of a carotid body tumor in a dog. *Acta Vet Scand* **54**.

13. Collins, S.P., Matheson, J.S., Hamor, R.E., Mitchell, M.A., Labelle, A.L. and O'Brien, R.T. (2013) Comparison of the diagnostic quality of computed tomography images of normal ocular and orbital structures acquired with and without the use of general anesthesia in the cat. *Vet Ophthalmol* **16**, 352-358.

14. Paul, A.E., Lenard, Z. and Mansfield, C.S. (2010) Computed tomography diagnosis of eight dogs with brain infarction. *Aust Vet J* **88**, 374-380.

15. Pease, A.P., Schott, H.C., Howey, E.B. and Patterson, J.S. (2011) Computed tomographic findings in the pituitary gland and brain of horses with pituitary pars intermedia dysfunction. *J Vet Intern Med* **25**, 1144-1151.

16. Crijns, C.P., Vlaminck, L., Verschooten, F., van Bergen, T., de Cock, H.E., Huylebroek, F., Pool, R. and Gielen, I. (2015) Multiple mandibular ossifying fibroma in a yearling belgian draught horse filly. *Equine Vet Educ* **27**, 11-15.

17. Solano, M. and Brawer, R.S. (2004) Ct of the equine head: Technical considerations, anatomical guide, and selected diseases. *Clin Tech equine Pract* **3**, 374-388.

18. Smallwood, J.E., Wood, B.C., Taylor, E. and Tate, L.P. (2002) Anatomic reference for computed tomography of the head of the foal. *Vet Radiol Ultrasound* **43**, 99-117.

19. Claerhoudt, S., Bergman, H.J., van der Veen, H., Duchateau, L., Raes, E.V., Vanderperren, K. and Saunders, J.H. (2012) Morphology of distal border synovial invaginations of the equine distal sesamoid bone comparison between computed tomography and a hoof-specific radiographic projection. *Vet Comp Orthop Traumatol* **25**, 453-459.

20. Barbee, D.D., Allen, J.R. and Gavin, P.R. (1987) Computed tomography in horses *Vet Radiology* **28**, 144-151.

21. Dakin, S.G., Lam, R., Rees, E., Mumby, C., West, C. and Weller, R. (2014) Technical set-up and radiation exposure for standing computed tomography of the equine head. *Equine Vet Educ* **26**, 208-215.

22. Czupalla, I. and Gerhards, H. (2013) Risk of general anesthesia in horses - a retrospective study on 1.989 cases. *Pferdeheilkunde* **29**, 729-738.

23. Finding, E., Fletcher, N., Avella, C., Naylor, R.J., Volk, H.A., Weller, R., Dunkel, B. and Piercy, R.J. (2012) Standing ct and clinical progression of equine cholesterol granulomata. *Vet Rec* **170**, 289-290.

24. De Zani, D., Zani, D.D., Borgonovo, S., Di Giancamillo, M., Rondena, M. and Verschooten, F. (2011) An undifferentiated sarcoma in the cervical region in a horse. *Equine Vet Educ* **23**, 138-141.

25. Kristoffersen, M., Puchalski, S., Skog, S. and Lindegaard, C. (2014) Cervical computed tomography (ct) and ct myelography in live horses: 16 cases. *Equine Vet J* **46**, 11.

26. Lempe, A., Heine, M., Bosch, B., Mueller, K. and Brehm, W. (2012) Imaging diagnosis and clinical presentation of a chiari malformation in a Thoroughbred foal. *Equine Vet Educ* **24**, 618-623.

27. Rebsamen, E., Gygax, D., Dennler, M., Jud, R. and Kummer, M. (2010) External infiltrating lipoma in a two-week-old foal: Computed tomographic evaluation for the assessment of the extension and invasiveness of the tumour. *Equine Vet Educ* **22**, 602-607.

28. Stewart, A.J., Salazar, P., Waldridge, B.M., Hathcock, J., Whitley, E.M. and Welles, E.G. (2007) Computed tomographic diagnosis of a pathological fracture due to rhodococcal osteomyelitis and spinal abscess in a foal. *Equine Vet Educ* **19**, 231-235.

29. Barba, M. and Lepage, O.M. (2013) Diagnostic utility of computed tomography imaging in foals: 10 cases (2008-2010). *Equine Vet Educ* **25**, 29-38.

30. Claerhoudt, S., Bergman, H.J., Van Der Veen, H., Duchateau, L., Raes, E.V. and Saunders, J.H. (2012) Differences in the morphology of distal border synovial invaginations of the distal sesamoid bone in the horse as evaluated by computed tomography compared with radiography. *Equine Vet J* **44**, 679-683.

31. Debrosse, F.G., Vandeweerd, J.-M.E.F., Perrin, R.A.R., Clegg, P.D., Launois, M.T., Brogniez, L. and Gehin, S.P. (2008) A technique for computed tomography (ct) of the foot in the standing horse. *Equine Vet Educ* **20**, 93-98.

32. Kelmer, G., Wilson, D.A. and Essman, S.C. (2008) Computed tomography assisted repair of a central tarsal bone slab fracture in a horse. *Equine Vet Educ* **20**, 284-287.

33. May, K.A., Holmes, L.C., Moll, H.D. and Jones, J.C. (2001) Computed tomographic imaging of comminuted carpal fractures in a gelding. *Equine Vet Educ* **13**, 303-308.

34. Perrin, R.A.R., Launois, M.T., Brogniez, L., Clegg, P.D., Coomer, R.P.C., Desbrosse, F.G. and Vandeweerd, J.M.E.F. (2011) The use of computed tomography to assist orthopaedic surgery in 86 horses (2002-2010). *Equine Vet Educ* **23**, 306-313.

35. Waselau, M., Bertone, A.L. and Green, E.M. (2006) Computed tomographic documentation of a comminuted fourth carpal bone fracture associated with carpal instability treated by partial carpal arthrodesis in an arabian filly. *Vet Surg* **35**, 618-625.

36. Smith, M.R. and Wright, I.M. (2014) Radiographic configuration and healing of 121 fractures of the proximal phalanx in 120 Thoroughbred racehorses (2007-2011). *Equine Vet J* **46**, 81-87.

37. Olive, J., d'Anjou, M.A., Alexander, K., Laverty, S. and Theoret, C. (2010) Comparison of magnetic resonance imaging, computed tomography, and radiography for assessment of noncartilaginous changes in equine metacarpophalangeal osteoarthritis. *Vet Radiol Ultrasound* **51**, 267-279.

38. Raes, E., Bergman, H.J., Van Ryssen, B., Vanderperren, K., Stock, E. and Saunders, J.H. (2014) Computed tomographic features of lesions detected in horses with tarsal lameness. *Equine Vet J* **46**, 189-193.

39. O'brien, T., Baker, T.A., Brounts, S.H., Sample, S.J., Markel, M.D., Scollay, M.C., Marquis, P. and Muir, P. (2011) Detection of articular pathology of the distal aspect of the third metacarpal bone in Thoroughbred racehorses: Comparison of radiography, computed tomography and magnetic resonance imaging. *Vet Surg* **40**, 942-951.

40. Hontoir, F., Nisolle, J.F., Meurisse, H., Simon, V., Tallier, M., Vanderstricht, R., Antoine, N., Piret, J., Clegg, P. and Vandeweerd, J.M. (2014) A comparison of 3-t magnetic resonance imaging and computed tomography arthrography to identify structural cartilage defects of the fetlock joint in the horse. *Vet J* **199**, 115-122.

41. Waldt, S., Bruegel, M., Ganter, K., Kuhn, V., Link, T.M., Rummeny, E.J. and Woertler, K. (2005) Comparison of multislice ct arthrography and mr arthrography for the detection of articular cartilage lesions of the elbow. *Eur Radiol* **15**, 784-791.

42. Dyson, S. and Murray, R. (2007) Magnetic resonance imaging evaluation of 264 horses with foot pain: The podotrochlear apparatus, deep digital flexor tendon and collateral ligaments of the distal interphalangeal joint. *Equine Vet J* **39**, 340-343.

43. Gutierrez-Nibeyro, S.D., White, N.A., Werpy, N.M., Tyrrell, L., Allen, K.A., Sullins, K.E. and Mitchell, R.D. (2009) Magnetic resonance imaging findings of desmopathy of the collateral ligaments of the equine distal interphalangeal joint. *Vet Radiol Ultrasound* **50**, 21-31.

44. Schramme, M., Josson, A. and Linder, K. (2012) Characterization of the origin and body of the normal equine rear suspensory ligament using ultrasonography, magnetic resonance imaging, and histology. *Vet Radiol Ultrasound* **53**, 318-328.

45. Werpy, N.M., Denoix, J.M., McIlwraith, C.W. and Frisbie, D.D. (2013) Comparison between standard ultrasonography, angle contrast ultrasonography, and magnetic resonance imaging characteristics of the normal equine proximal suspensory ligament. *Vet Radiol Ultrasound* **54**, 536-547.

46. Vallance, S.A., Bell, R.J.W., Spriet, M., Kass, P.H. and Puchalski, S.M. (2012) Comparisons of computed tomography, contrast-enhanced computed tomography and standing low-field magnetic resonance imaging in horses with lameness localised to the foot. Part 2: Lesion identification. *Equine Vet J* **44**, 149-156.

47. Vallance, S.A., Bell, R.J.W., Spriet, M., Kass, P.H. and Puchalski, S.M. (2012) Comparisons of computed tomography, contrast enhanced computed tomography and standing low-field magnetic resonance imaging in horses with lameness localised to the foot. Part 1: Anatomic visualisation scores. *Equine Vet J* **44**, 51-56.

48. Hilton, H., Puchalski, S.M. and Aleman, M. (2009) The computed tomographic appearance of equine temporohyoid osteoarthropathy. *Vet Radiol Ultrasound* **50**, 151-156.

49. Tucker, R.L. and Farrell, E. (2001) Computed tomography and magnetic resonance imaging of the equine head. *Vet Clin N Am-Equine* **17**, 131-144.

50. Henninger, W., Frame, E.M., Willmann, M., Simhofer, H., Malleczek, D., Kneissl, S.M. and Mayrhofer, E. (2003) CT features of alveolitis and sinusitis in horses. *Vet Radiol Ultrasound* **44**, 269-276.

51. Tessier, C., Bruhschwein, A., Lang, J., Konar, M., Wilke, M., Brehm, W. and Kircher, P. (2013) Magnetic resonance imaging features of sinonasal disorders in horses. *Vet Radiol Ultrasound* **54**, 54-60.

52. Beccati, F., Angeli, G., Secco, I., Contini, A., Gialletti, R. and Pepe, M. (2011) Comminuted basilar skull fracture in a colt: Use of computed tomography to aid the diagnosis. *Equine Vet Educ* **23**, 327-332.

53. Ramirez, O., Jorgensen, J.S. and Thrall, D.E. (1998) Imaging basilar skull fractures in the horse: a review. *Vet Radiol Ultrasound* **39**, 391-395.

54. Huggons, N.A., Bell, R.J.W. and Puchalski, S.M. (2011) Radiography and computed tomography in the diagnosis of nonneoplastic equine mandibular disease. *Vet Radiol Ultrasound* **52**, 53-60.

55. Pownder, S., Scrivani, P.V., Bezuidenhout, A., Divers, T.J. and Ducharme, N.G. (2010) Computed tomography of temporal bone fractures and temporal region anatomy in horses. *J Vet Intern Med* **24**, 398-406.

56. Avella, C.S. and Perkins, J.D. (2011) Computed tomography in the investigation of trauma to the ventral cranium. *Equine Vet Educ* **23**, 333-338.

57. Palus, V., Bladon, B., Brazil, T., Cherubini, G.B., Powell, S.E., Greet, T.R.C. and Marr, C.M. (2012) Retrospective study of neurological signs and management of seven english horses with temporohyoid osteoarthropathy. *Equine Vet Educ* **24**, 415-422.

58. Naylor, R.J., Perkins, J.D., Allen, S., Aldred, J., Draper, E., Patterson-Kane, J. and Piercy, R.J. (2010) Histopathology and computed tomography of age-associated degeneration of the equine temporohyoid joint. *Equine Vet J* **42**, 425-430.

59. Windley, Z., Weller, R., Tremaine, W.H. and Perkins, J.D. (2009) Two- and three-dimensional computed tomographic anatomy of the enamel, infundibulae and pulp of 126 equine cheek teeth. Part 2: Findings in teeth with macroscopic occlusal or computed tomographic lesions. *Equine Vet J* **41**, 441-447.

60. Veraa, S., Voorhout, G. and Klein, W.R. (2009) Computed tomography of the upper cheek teeth in horses with infundibular changes and apical infection. *Equine Vet J* **41**, 872-876.

61. Windley, Z., Weller, R., Tremaine, W.H. and Perkins, J.D. (2009) Two- and three-dimensional computed tomographic anatomy of the enamel, infundibulae and pulp of 126 equine cheek teeth. Part 1: Findings in teeth without macroscopic occlusal or computed tomographic lesions. *Equine Vet J* **41**, 433-440.

62. Gerlach, K., Ludewig, E., Brehm, W., Gerhards, H. and Delling, U. (2013) Magnetic resonance imaging of pulp in normal and diseased equine cheek teeth. *Vet Radiol Ultrasound* **54**, 48-53.

63. Smith, L.C.R., Zedler, S.T., Gestier, S., Keane, S.E., Goodwin, W. and van Eps, A.W. (2012) Bilateral dentigerous cysts (heterotopic polyodontia) in a yearling standardbred colt. *Equine Vet Educ* **24**, 573-578.

64. Hunt, R.J., Allen, D. and Mueller, P.O.E. (1991) Intracranial trauma associated with extraction of a temporal ear tooth (dentigerous cyst) in a horse. *Cornell Vet* **81**, 103-108.

65. De Zani, D., Borgonovo, S., Biggi, M., Vignati, S., Scandella, M., Lazzaretti, S., Modina, S. and Zani, D. (2010) Topographic comparative study of paranasal sinuses in adult horses by computed tomography, sinuscopy, and sectional anatomy. *Vet Res Commun* **34 (Suppl. 1)**, S13-S16.

66. Probst, A., Henninger, W. and Willmann, M. (2005) Communications of normal nasal and paranasal cavities in computed tomography of horses. *Vet Radiol Ultrasound* **46**, 44-48.

67. Park, R.D. (1993) Radiographic examination of the equine head. *Vet Clin North Am Equine Pract* **9**, 49-74.

68. Dixon, P.M., Parkin, T.D., Collins, N., Hawkes, C., Townsend, N., Tremaine, W.H., Fisher, G., Ealey, R. and Barakzai, S.Z. (2012) Equine paranasal sinus disease: A long-term study of 200 cases (1997-2009): ancillary diagnostic findings and involvement of the various sinus compartments. *Equine Vet J* **44**, 267-271.

69. Cissell, D.D., Wisner, E.R., Textor, J., Mohr, F.C., Scrivani, P.V. and Theon, A.P. (2012) Computed tomographic appearance of equine sinonasal neoplasia. *Vet Radiol Ultrasound* **53**, 245-251.

70. Dixon, P.M., Parkin, T.D., Collins, N., Hawkes, C., Townsend, N., Tremaine, W.H., Fisher, G., Ealey, R. and Barakzai, S.Z. (2012) Equine paranasal sinus disease: A long-term study of 200 cases (1997-2009): treatments and long-term results of treatments. *Equine Vet J* **44**, 272-276.

71. Veraa, S., Dijkman, R., Klein, W.R. and van den Belt, A.J.M. (2009) Computed tomography in the diagnosis of malignant sinonasal tumours in three horses. *Equine Vet Educ* **21**, 284-288.

72. Textor, J.A., Puchalski, S.M., Affolter, V.K., MacDonald, M.H., Galuppo, L.D. and Wisner, E.R. (2012) Results of computed tomography in horses with ethmoid hematoma: 16 cases (1993-2005). *J Am Vet Med Assoc* **240**, 1338-1344.

73. Tremaine, W.H. (2009) The diagnosis and treatment of progressive ethmoidal haematomas. *Equine Vet Educ* **21**, 582-583.

74. Arencibia, A., Vazquez, J.M., Rivero, M., Latorre, R., Sandoval, J.A., Vilar, J.M. and Ramirez, J.A. (2000) Computed tomography of normal cranioencephalic structures in two horses. Anat Histol Embryol **29**, 295-299.

75. Morrow, K.L., Park, R.D., Spurgeon, T.L., Stashak, T.S. and Arceneaux, B. (2000) Computed tomographic imaging of the equine head. *Vet Radiol Ultrasound* **41**, 491-497.

76. Vanschandevijl, K., Gielen, I., Nollet, H., Vlaminck, L., Deprez, P. and van Bree, H. (2008) Computed tomography-guided brain biopsy for in vivo diagnosis of a cholesterinic granuloma in a horse. *J Am Vet Med Assoc* **233**, 950-954.

CHAPTER TWO

Scientific Aims

The general aim of this PhD thesis was to evaluate the use of computed tomography (CT) in equine medicine based on various clinical and research studies. CT is an axial imaging modality not limited by superimposition of structures. Additionally, in combination with contrast-enhancement, CT is able to visualise bone and certain soft tissue structures with a diagnostic acceptable contrast resolution. To be able to warrant a correct diagnostic decision in equine patients, the advantages of CT however have to be weighed against the (higher) costs, the increase in exposure to ionising radiation and (often) the need for general anaesthesia.

- Therefore, the aim of the first part of this thesis was to **compare radiography and CT in their ability to detect, describe and diagnose bony lesions** occurring in horses. Several case reports in equine literature describe fractures diagnosed with CT, but no studies comparing the diagnostic capabilities of radiography and CT have been performed in equine medicine.
    - The specific aim of the first and second study was to document the agreement between radiography and CT in visualising fracture characteristics in (retrospectively) selected clinical cases of **1: distal limb fractures** and **2: head fractures**.
    - The third study was an unusual **case report of a horse suffering from lameness originating from the stifle,** to demonstrate the abilities of physical, radiographic, ultrasonographic, and CT examinations and compare them to gross pathologic evaluation.
- The aim of the second part of this thesis was to **evaluate contrast-enhanced CT protocols and applications** for the equine head.
    - The specific aim of the fourth study was to describe and compare physiologic contrast enhancement of the soft tissue structures after **systemic intravenous and direct intra-arterial administration of contrast medium.**
    - The specific aim of the fifth study was to determine **a pituitary gland height-to-brain area ratio** using contrast-enhanced CT in healthy horses without pituitary pars intermedia dysfunction.

CHAPTER THREE

Intra-Modality and Inter-Modality Agreement in Radiography and Computed Tomography of Equine Distal Limb Fractures

Casper P. Crijns[1], Ann Martens[2], Hendrik-Jan Bergman[3], Henk van der Veen[3], Luc Duchateau[4], Henri J.J. van Bree[1], Ingrid M.V.L. Gielen[1]

[1] Department of Medical Imaging and Small Animal Orthopaedics, Ghent University, 9820 Merelbeke, Belgium
[2] Department of Surgery and Anaesthesiology of Domestic Animals, Ghent University, 9820 Merelbeke, Belgium
[3] Lingehoeve Diergeneeskunde, 4033 AK Lienden, The Netherlands
[4] Department of Comparative Physiology and Biometrics, Ghent University, 9820 Merelbeke, Belgium

Adapted from:

Casper P. Crijns, Ann Martens, Hendrik-Jan Bergman, Henk van der Veen, Luc Duchateau, Henri J.J. van Bree, Ingrid M.V.L. Gielen. Intra-modality and inter-modality agreement in radiography and computed tomography of equine distal limb fractures *(published in Equine Veterinary Journal (2014) **46** (1) 92-96)*

Summary

Case reports suggest that CT is more sensitive than radiography in visualising distal limb fractures and their anatomic characteristics in horses. So far, this is not supported by evidence from studies comparing both imaging modalities. A retrospective study of the image records of a population of horses that underwent radiographic and CT evaluation for suspected distal limb fracture was conducted. Twenty-seven patients and three negative controls were included. Using Cohen's kappa and weighted kappa analysis, the level of agreement between four different observers for a predefined set of radiological characteristics, was documented for radiography and CT separately, as well as the level of agreement for these parameters between the two imaging modalities. The visualisation of fractures showed very good intra-modality agreement (0.8<kappa<1) for both CT and radiography, but moderate inter-modality agreement only (0.4<kappa<0.6). The anatomic localisation showed very good inter-modality and intra-modality agreement. Fracture displacement showed good inter-modality and intra-modality agreement (0.6<kappa<0.8). For articular involvement, fracture comminution and fracture fragment number, all agreement levels bordered on the lower limit of good agreement. Documentation of fracture orientation, fracture width and coalescing cracks showed poor (0<kappa<0.2) to fair (0.2<kappa<0.4) inter-modality agreement levels; for these three parameters, intra-modality agreement was higher for CT than for radiography.

In conclusion, although for various parameters the agreement profile is similar, the data suggest that CT may offer added value in diagnosing distal limb fractures in horses. This study provides the rationale for a prospective controlled study on the agreement and the relative sensitivity of CT and radiography for this purpose.

Introduction

Distal limb fractures constitute a relatively common and well-described disorder in horses [1-3]. Accurate diagnosis of such fractures is critical in directing treatment, indicating a prognosis and preventing complications [4, 5]. Generally, radiography is used as a first line diagnostic modality to visualise fractures in lame horses. Although two or more projections can be taken, accurate interpretation of such radiographs may be challenging due to the complexity of this type of fracture and the anatomical superimposition of the bones [4-11]. It is well known that, overall, computed tomography provides images with a higher contrast resolution than radiographic images [12-14]. With CT, cross-sectional images are acquired which eliminates superimposition of structures [12-14]. In humans, CT is therefore considered the gold standard for the diagnosis of bone injuries [15]. Although in horses, CT can be used to visualise the head, the neck and the limb up to the stifle, the physical dimensions of the animal, the need for general anaesthesia, as well as the high cost of CT are limiting factors in clinical use of CT in this species [13, 16]. Literature on the use of CT to explore fractures in lame horses is scarce and concerns mostly single cases [5, 7-10, 17] as well as a few small case series [4, 11, 18]. These studies suggest that CT may be more sensitive in detecting distal limb fractures and may facilitate the evaluation of fracture size, orientation and opening, indicating that CT may have value in accurately diagnosing fractures of the equine distal limb [4-11, 17, 18]. Along this line, there is increasing interest in CT as a clinical diagnostic modality in horses [13, 16, 18]. However, evidence from comparative studies to support the presumed superiority of CT over radiography in diagnosing distal limb fractures in horses is not available.

As a first step towards this goal, the objective of the current study was to document the agreement between radiography and CT in visualising equine distal limb fractures and their anatomic characteristics. A retrospective study of a population of horses that underwent radiographic and CT evaluation for suspected distal limb fracture was conducted. The level of agreement between four different observers, separately for radiography and CT, was documented for a predefined set

of radiological characteristics. In addition, the level of agreement for these parameters between the two imaging modalities was documented.

Materials and Methods

Study population

The study population was selected at two different clinical centres: the Department of Medical Imaging and Small Animal Orthopaedics of the Faculty of Veterinary Medicine of Ghent University, Belgium and the private clinic, Lingehoeve Diergeneeskunde, The Netherlands. Through retrospective medical record analysis, all horses that presented with a suspected distal limb fracture and those subsequently underwent evaluation with radiography as well as with CT were identified. At the Department of Medical Imaging and Small Animal Orthopaedics of the Faculty of Veterinary Medicine of Ghent University, Belgium all records between 1998 and 2010 were reviewed, and nine horses were identified. At Lingehoeve Diergeneeskunde, The Netherlands, all records between 2003 and 2010 were reviewed, and eighteen horses were identified. In addition, at Lingehoeve Diergeneeskunde, The Netherlands, all horses that underwent radiography and CT of the distal limb for suspected soft tissue injury during the study period were reviewed. Three such cases, showing neither previous nor current bone injury, were included as negative controls. The total study population therefore was composed of thirty horses.

Radiography

For all thirty study subjects, radiographic images of various projections were available for evaluation, all of which were used for this study. At the Department of Medical Imaging and Small Animal Orthopaedics of the Faculty of Veterinary Medicine of Ghent University, Belgium conventional radiography was used between 1998 and March 2007, these radiographic films were digitised for the purpose of this study. Since March 2007 a computed radiography system (Konica Minolta[1]) was used. At Lingehoeve Diergeneeskunde, The Netherlands all radiographs were

acquired with a computed radiography system (FujiFilm[2]). All radiographs were taken with the horses standing.

Computed tomography

At the Department of Medical Imaging and Small Animal Orthopaedics of the Faculty of Veterinary Medicine of Ghent University, Belgium, the earliest cases were examined using a single slice axial CT scanner (GE Medical Systems Pace Plus[3]), and for the purpose of this study, these analogue images were digitised; multiplanar reformatting options for these image records were restricted. For the subsequent cases, a single slice, helical CT scanner (GE Medical Systems Prospeed single slice[3]) was used. At Lingehoeve Diergeneeskunde, The Netherlands, a 4-slice, helical CT scanner (Philips Mx8000 Quad multislice CT-scanner[4]) was used.

Data evaluation

All radiographic and CT images were blinded and randomly evaluated digitally, by four different observers each having a record of 10 to 15 years of daily practice experience in evaluating skeletal radiography and CT images of horses. In a first phase, all radiographic images were evaluated; in a second phase all CT images. Transverse images of CT exams were used as a basis for evaluation; observers used Osirix[5] or Efilm[6] software according to their preference, and used multiplanar reconstruction if judged necessary. Observers used a standardised scoring form to evaluate ten radiological criteria, the possible outcomes of which were predefined and precoded: detectable injury, definition of involved bone(s), localisation of injury on the bone, articular involvement, comminution, number of fragments, orientation of the fracture line(s), fracture opening, displacement and presence of small or coalescing cracks. All parameters and coded possible outcomes are represented in Table 1.

CODE	0	1	2	3	4	5	6	7	8
OBSERVER		EB	HvdV	AM	IG				
IMAGING MODALITY		radiography	CT						
FRACTURE		Yes	No						
FRACTURE CHARACTERISTICS									
Bone involved		tibia / fibula radius / ulna	carpus/ tarsus	metacarpus/ metatarsus	proximal sesamoid	phalanx 1	phalanx 2	navicular bone	phalanx 3
Localisation		proximal	corpus	distal	whole bone				
Articular involvement	no	yes							
Comminution	no	yes							
Number of fragments		1	2	3					
Orientation		fissure	longitudinal	transverse	spiral	oblique	infarction		
Fracture opening		1 mm	2 mm	3mm	...				
Displacement	no	yes							
Coalescing cracks	no	yes							

Table 1: Codes used to categorize data for analysis. Numerical codes were assigned to the 4 observers, 2 image-modalities and the categories of possible answers for each radiological feature.

Statistical Analysis

Cohen's kappa (κ) and weighted kappa (wκ) was used to quantify intra-modality agreement for the different responses (separately for CT and radiography). Furthermore, Cohen's kappa and weighted kappa was used to quantify agreement between radiography and CT (comparing within the different observer-case combinations). Cohen's kappa and weighted kappa is a measurement of the difference between the observers, with a κ value ranging from -1 to 1. Zero is exactly what would be expected by chance and 1 would be a perfect agreement. The Cohen's kappa and weighted kappa values were interpreted as described by Altman, <0.2 indicating poor agreement, 0.20 to 0.40 fair agreement, 0.40 to 0.60 moderate agreement, 0.60 to 0.80 good agreement and 0.80 to 1 very good agreement [19]. Additionally, for response variables which could be considered to be continuous (number of fragments and fracture opening), the average difference (+/- s.d.) between observers was calculated for CT and radiography separately, as well as the average difference (+/- s.d.) between radiography and CT within the different observer-fracture combinations; a paired t-test at the 5% significance level was used to assess the difference between radiography and CT.

Results

The study population included 6 stallions, 10 geldings and 14 mares, with a median age of 8 years (range: 2m–26y). There were 20 Warmbloods, 5 ponies, 2 French Trotter, 2 Arabians and 1 Thoroughbred.

Review of the medical records showed that for eighteen horses the radiographic examination consisted of three standard projections (latero-medial, dorso-palmar/plantar, dorsolateral-palmaro-/plantaromedial oblique and dorsomedial-palmaro-/plantarolateral oblique projection), whereas in nine cases on a latero-medial and dorso-palmar/plantar projection and in three cases only a dorsolateral-palmaro-/plantaromedial oblique and dorsomedial-palmaro-/plantarolateral oblique projection were taken. In 28 out of thirty cases, the initial evaluation was followed by additional projections: several repeat projections in fifteen cases, projections at slightly different angles in seven cases, a navicular skyline projection in five cases and a latero-medial flexed projection in one case.

For all horses, at least a native CT scan was available for evaluation. Four cases were evaluated using a single slice axial CT scanner, acquiring transverse slices of 2 mm thickness. Five cases were evaluated using a single slice, helical CT scanner and 21 cases were evaluated using a four-slice, helical CT scanner, all acquiring the scans helically.

In this study were included: one distal tibia fracture, three fractures involving the tarsus, one fracture of the metacarpus, one fracture of a proximal sesamoid bone, eleven fractures of P1, three fractures of P2, one fracture of the navicular bone and six fractures of P3.

A graphic overview of the kappa values for each radiographic parameter is given in Figure 1.

Presence of a fracture and its anatomic location

When answering the question whether or not images showed the presence of bone injury, the results showed a *very good* (radiography: κ= 0.98; CT: κ= 1.00) intra-modality agreement for each imaging modality. For radiography, the observers failed to agree in one single case. The observers agreed for radiography and CT about the absence of bony injuries in the three negative controls. The inter-modality agreement between CT and radiography was reflecting *moderate* (κ= 0.56) agreement only. In five cases, the observers detected injury on CT images but failed to do so on the radiographs. These cases involved one fracture of the tarsus, two fractures of P1, one fracture of P2 and one fracture of P3. The images of two such representative cases are shown in Figure 2 and Figure 3.

Diagnosing the anatomic localisation of the fracture showed a *very good* intra-modality agreement for radiography (κ= 0.82) and CT (κ= 0.83). In addition, *very good* (κ= 0.91) inter-modality agreement was documented between radiography and CT. Similarly, the localisation of the fracture on the involved bone showed *very good* (radiography: κ= 0.91; CT: κ= 0.90) intra-modality agreement for both modalities. The inter-modality agreement was equally *very good* (κ= 0.93).

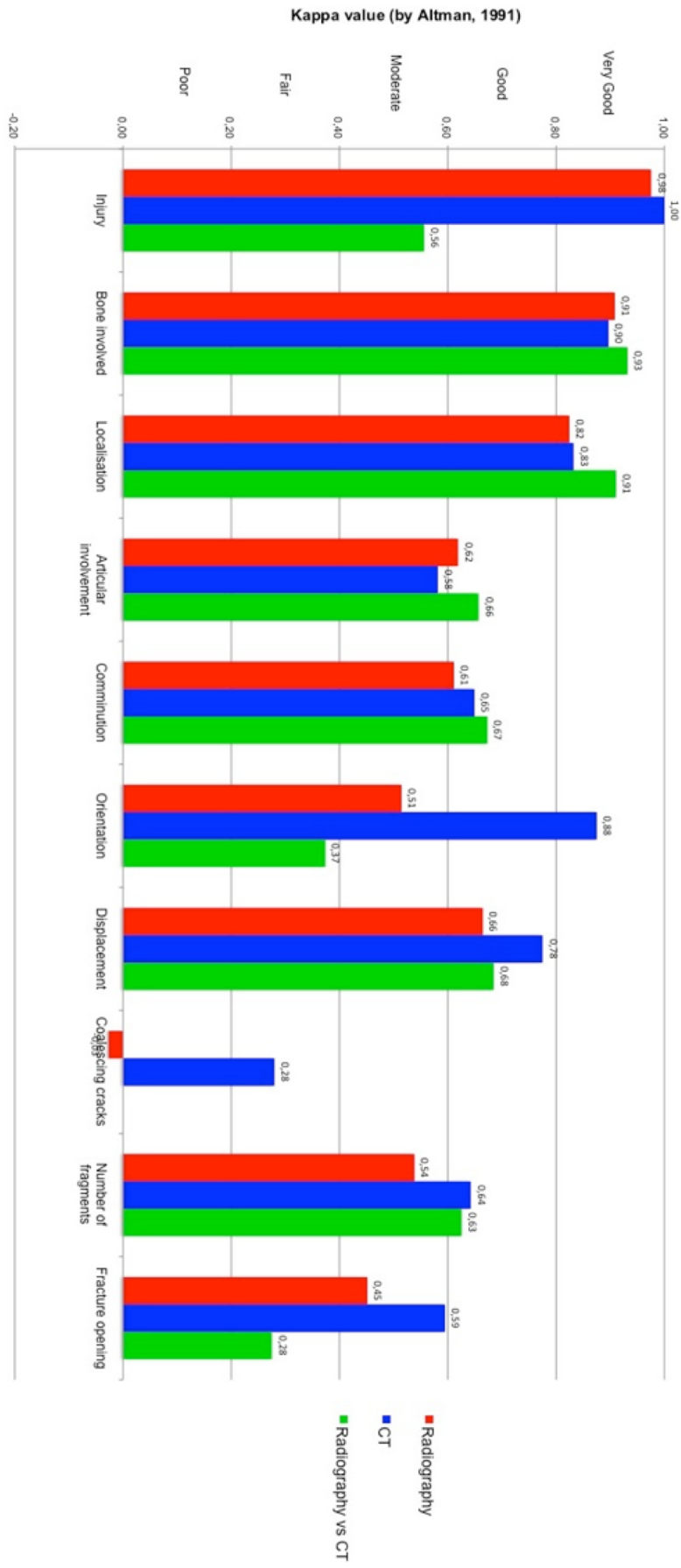

Figure 1: Cohen's kappa and weighted kappa values obtained for the different fracture characteristics evaluated: for the intra-modality agreement for radiography, the intra-modality agreement for CT, and agreement between CT and radiography

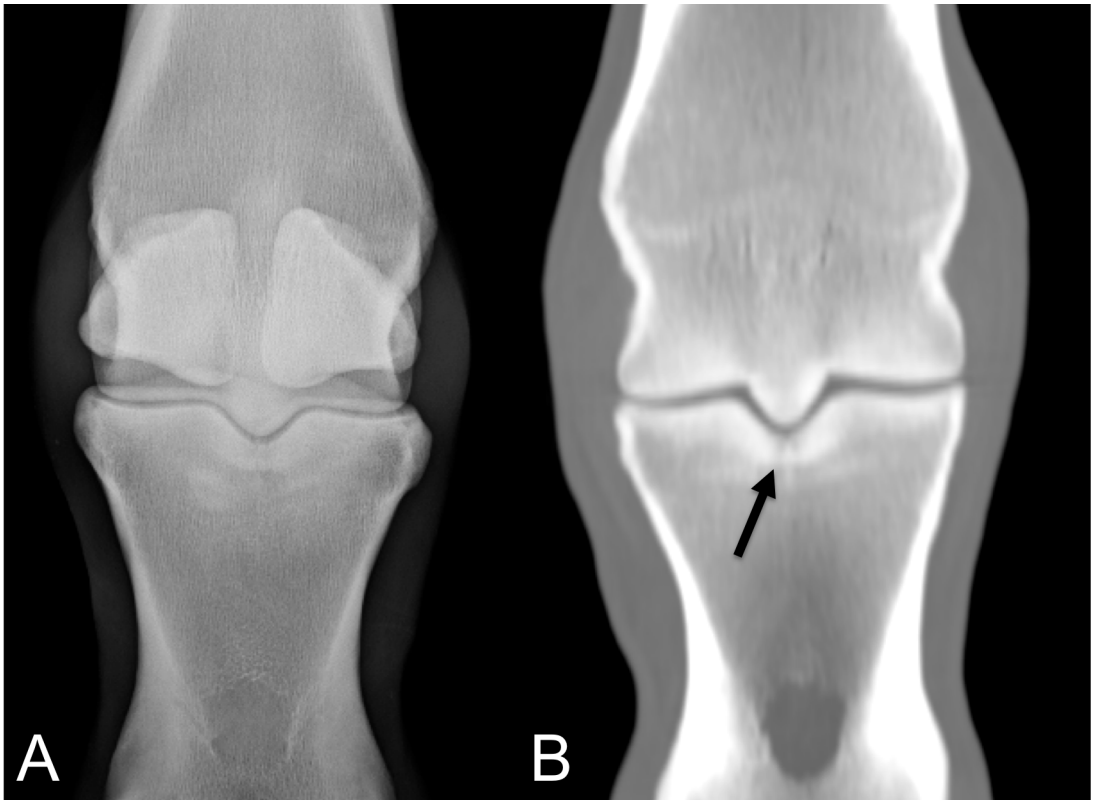

Figure 2: Radiograph and CT image of the fetlock of a horse with a proximal P1 fissure in the sagittal groove. Dorsoplantar projection (a) of the fetlock (medial is to the left), showing no significant bony abnormalities, according to the observers. Retrospectively, a fissure line may be visible in the sagittal groove of P1. Dorsal reconstructed (b) CT image (medial is to the left), showing a clear fissure line in the sagittal groove of P1 (arrow).

Fracture characteristics

Documenting whether or not the fracture involved the joint showed *good* levels of intra-modality agreement (radiography: κ= 0.62; CT: κ= 0.58). A *good* level of inter-modality agreement (κ= 0.66) was also documented between CT and radiography for this parameter.

When evaluating whether the fragments of the fracture showed displacement relative to the original position, the different observers showed a *good* level of intra-modality agreement for radiography (κ= 0.66) and CT (κ= 0.78). Along this line, a *good* level of inter-modality agreement (κ= 0.68) was documented when CT and radiography were compared.

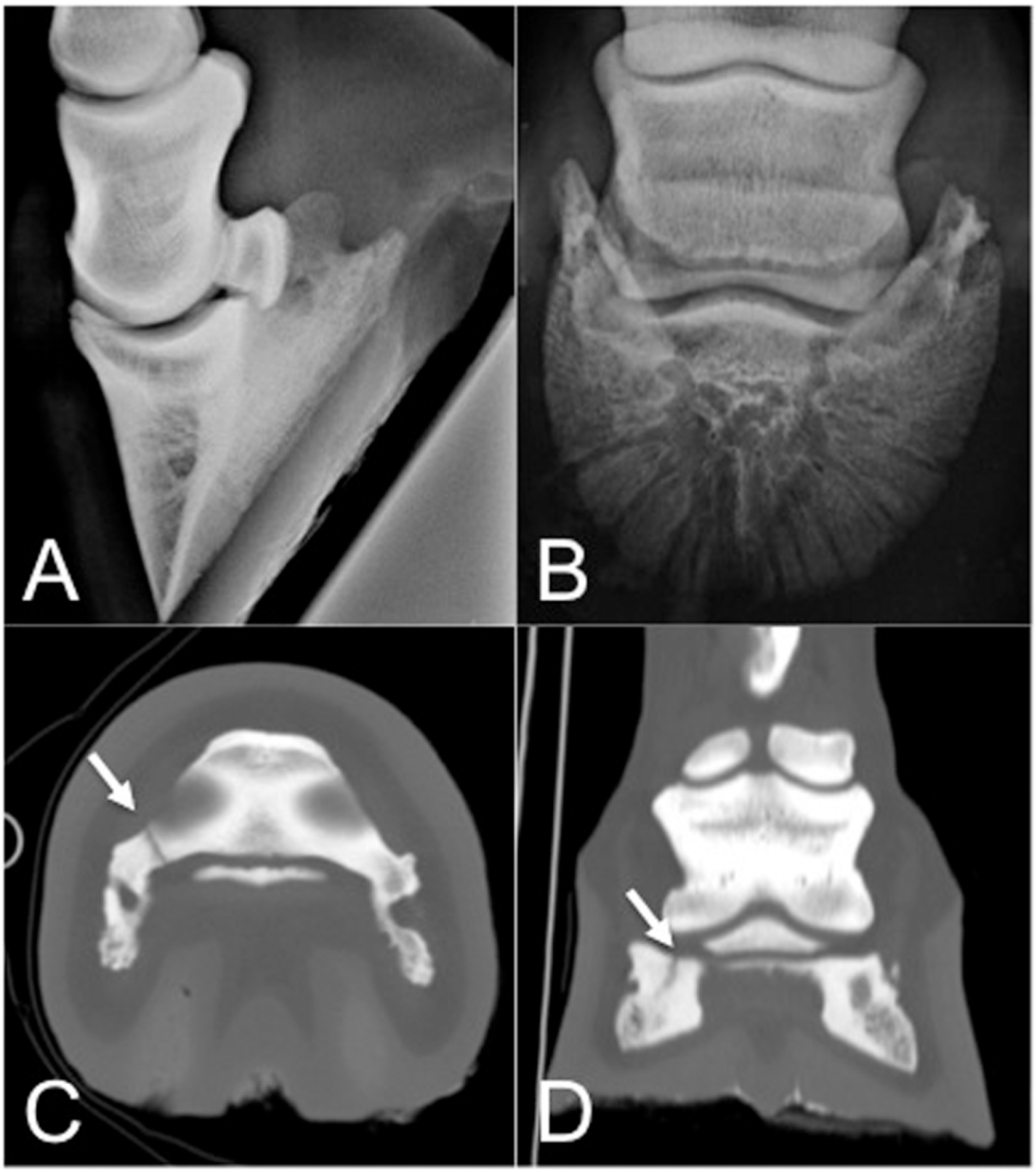

Figure 3: Radiographs and CT images of the foot of a horse suffering from a fracture in the third phalanx. Lateromedial projection (A) and dorso65proximal-palmarodistal oblique projection (B) of the foot (medial is to the left) showing no evidence of bony injury. Transverse CT (medial is to the left) (C) and dorsal reconstructed CT image (medial is to the left) (D), showing a clear fracture line running through the medial palmar process of P3 (arrow).

The level of intra-modality agreement for diagnosing a fracture as comminuted was *good* for radiography (κ= 0.61) and CT (κ= 0.65); similarly, a *good* level of inter-modality agreement (κ= 0.67) between CT and radiography.

The evaluation of the orientation of the fracture showed a very good intra-modality agreement for CT (κ= 0.88), but in contrast, only a moderate intra-modality

agreement for radiography (κ= 0.51). Along this line, it showed only a fair inter-modality agreement (κ= 0.37) between CT and radiography for this parameter.

When scoring for the presence of coalescing cracks, observers showed no intra-modality agreement for radiography (κ= -0.03), and fair intra-modality agreement for CT (κ= 0.28).

The mean difference of the number of fragments counted by two observers equalled 0.41 (s.d. +/-1.13) for radiography and showed a moderate intra-modality agreement (wκ= 0.54). The mean difference of the number of fragments counted by two observers equalled 0.35 (s.d. +/-1.15) for CT and showed a good intra-modality agreement (wκ= 0.64). The mean difference in number of fragments counted by two observers between CT and radiography was 0.11 fragments (s.d. +/-1.43) (p=0.38) and had a good inter-modality agreement (wκ= 0.63). The mean difference between two observers in measuring the fracture opening on the radiographs was 0.05mm (s.d. +/-1.45) and reflecting a moderate intra-modality agreement (wκ= 0.45). For CT the mean difference between two observers in measuring the fracture opening was 0.15mm (s.d. +/-1.17mm) and reflecting a good intra-modality agreement (wκ= 0.59). The mean difference between two observers in measuring the fracture opening between CT and radiography was -0.49mm (s.d. +/-2.30) (p=0.06) and indicating a fair inter-modality agreement (wκ= 0.28).

Discussion

In this study we comparatively investigated the inter-modality agreement between radiography and CT in visualising equine distal limb fractures, as well as the intra-modality agreement for each modality. We found that CT and radiography agreed only to a moderate level in detecting the presence of a fracture, with CT visualising a higher number of fractures than radiography. For crude anatomic radiological parameters of these fractures, the two modalities showed good to very good inter-modality agreement. However, for detailed fracture characteristics, the level of inter-modality agreement between CT and radiography was fair to poor, the level of intra-modality agreement for CT being higher than for radiography. The data therefore indicate that CT may have added value in diagnosing detailed radiological characteristics of distal limb fractures in horses.

Although the definitive diagnosis of any skeletal lesion is obtained by gross inspection during surgery, the specific aim of this study was to document the inter-modality and intra-modality agreement of CT and radiography in the diagnosis of distal limb fractures in horses. It was not the aim to take the definitive diagnosis into account. This study therefore does not aim at or allow judging on the relative sensitivity of either modality. It should also be noted that the positions during radiography and CT, which were standing and recumbent, respectively, may influence the eventual visualisation of fractures and several of their characteristics. In theory this represents a confounding factor if one were to evaluate the intrinsic agreement between the two imaging modalities. However, for the comparisons in this study to yield clinically relevant conclusions, it is felt appropriate to rely on images that are taken in the standard position used in clinical practice for either imaging modality.

Radiography visualised fewer fractures than CT. Although both imaging modalities showed almost perfect intra-modality agreement, five out of 27 fractures that were visible on CT were not reported based on radiographs. This is in line with previous reports showing that fracture trauma became apparent during surgery in animal patients with negative preoperative radiographic evaluations [4-6, 17]. This discrepancy may be attributed to the physical principles of radiography. For radiography to visualise a fracture line, the x-ray beam should be oriented parallel to the fracture line; in addition, radiographic images reflect the superimposition of all the tissues the x-rays have penetrated, and this may obscure discrete fracture lines. Although radiography allows for multiple projections under varying angles of obliquities, these factors may cause selected fracture lines to go unnoticed [5, 9]. At this moment there is no standard radiographic protocol described in literature for fracture diagnosis. Including all radiographic images in this study and not only the standard protocol reflects the reality of the decision making of the treating veterinarian for the cases used in this study.

Radiography and CT appeared to have similar ability in visualising the anatomic localisation of a fracture, as evident from a high level of inter-modality agreement and similarly high intra-modality agreement levels for each method. Radiography and CT also agreed well with respect to the visualisation of

displacement of the fracture fragments. Determining whether or not a fracture is displaced is important to direct appropriate surgical treatment and to allow appropriate fracture reduction to prevent the development of osteoarthritis [4-6, 17, 18, 20, 21].

For the visualisation of articular involvement, comminution of the fracture and the number of fracture fragments, all agreement levels bordered on the lower limit of good agreement. The number of fracture fragments counted with CT was not statistically different from that counted with radiography. These data indicate that interpretation of these fracture characteristics shows some variability, not only between CT and radiography, but also between observers using one and the same modality.

Finally, the results indicate that radiography and CT show fair or poor inter-modality agreement only in visualising detailed fracture characteristics, and that CT identified more details of the fractures than radiography with this respect.

First, when determining the orientation of a fracture, which is of capital relevance in directing surgical treatment [4-6, 10, 11, 18, 22], inter-modality agreement was fair whereas clearly, CT produced little intra-modality variability as opposed to radiography. In this study, we investigated the visualisation of fracture orientation making use of a categorical classification of orientation types, to allow statistical analysis. However, good clinical practice requires every lesion to be evaluated with a detailed description of its individual anatomy, as subtle differences may influence the treatment approach and prognosis [6, 22]. One should, therefore, interpret these results with some caution. It can be anticipated that if CT could provide more accurate information on fracture configuration, this would result in a shorter surgery time.

Second, when measuring the width of a fracture opening, CT scored a borderline good level, and radiography a borderline fair level of intra-modality agreement. Although both fell within the ‘moderate’ agreement category, the difference does seem to indicate that CT is more precise than radiography in measuring the fracture width. We found that the average fracture opening measured on CT images was 0.5mm smaller than that measured on radiographic images. The aforementioned standing versus recumbent position during radiography

and CT, respectively, may in particular account for differences in measured fracture width between radiography and CT. Alternatively, overestimation of the fracture width on radiography may be due to measurement error and/or magnification artefact. Along this line, the data do indicate that very small fracture openings may not be visible on radiographs. Indeed, in this study, the observed discrepancy between radiography and CT in visualising the presence of injury mostly concerned discrete fracture lesions (Figure 2 and Figure 3).

Third, along the same line, the results indicated that CT has the potential to visualise small fissures around the fracture (coalescing cracks), whereas radiography has not. Although the intra-modality agreement for CT reached a fair level only, indicating that strong variability does exist between observers, the level of agreement was clearly higher than the level documented for radiography. This observation may be relevant for the diagnosis of other types of bone lesions, such as stress fractures [3, 23, 24]. Currently, scintigraphy is the method of choice to diagnose bone lesions at an early stage [10, 24], when changes have taken place at the histopathological level but can as yet not be seen radiographically [1]. For this reason, scintigraphy is regarded the gold standard for identifying scaphoid fractures in people [15]. Catastrophic fractures are often preceded by subtle changes, such as a linear defect in the joint cartilage and subchondral bone, localised necrosis, cysts, cortical remodelling but also small fissures [1, 6, 9]. Our data indicate that CT may be helpful in diagnosing early prodromal changes, not radiographically visible. The ability of CT relative to radiography in visualising fine radiological characteristics of a fracture can be ascribed to the known technical features of computed tomography. Firstly, CT inherently produces superior contrast resolution than radiography does, and is very sensitive in visualising changes in tissue density [9, 18]. Secondly, CT visualises the anatomical structures in cross-sectional slices, which avoids superimposition of tissue images. These advantages may account for the ability of CT to visualise small distal limb fractures and the fine radiological features of such lesions. In contrast, as has been reported, CT holds the disadvantage of potentially missing a lesion that is too small in comparison to the slice thickness, due to volume averaging artefact [6]. With multislice CT scanners, however, this risk can be minimised since they allow customising the slice thickness with isotropic voxels.

Currently, both CT and magnetic resonance imaging are used to visualise bone lesions and both methods are known to present with advantages and disadvantages. Computed tomography is the method of choice for detecting the earliest sign of fatigue damage of cortical bone [23]. In contrast, MRI has shown the ability of visualising subtle bony lesions and the ability of visualising bony oedema in human [23] and in equine medicine [25]. MRI also has the advantage of better visualising the regional soft tissue [23]. In a veterinary clinic, however, the choice for either method will critically depend on the availability of the imaging equipment. If general anaesthesia is needed, the owners should be advised in advance to let a positive diagnosis be followed by a surgical treatment. Standing MRI [25] and standing CT [14], can be performed on the sedated horse; both techniques avoid the need for general anaesthesia but both also have a longer acquisition time.

This retrospective study inevitably presents with certain limitations. First, the study population consisted exclusively of patients for which radiography was felt insufficient to investigate the clinical problem. The distal limb fractures studied here may therefore represent a subgroup of lesions, in particular, the subtler and complex ones. In the absence of a gold standard as intra-operative or post mortem findings and the exclusion of fracture cases not fulfilling the inclusion criteria, sensitivity, specificity, positive predictive value and negative predictive value were not calculated. Second, we considered both digitised conventional and primary digital radiographs together and the variable level of detail provided by these images was not taken into account. This is a consequence of the continuous advance in radiological techniques used in routine clinical practice. Limiting the comparative analysis in this retrospective study to one of either method would have adversely affected the sample size of the study.

While taking these limitations into account, we would like to draw the following careful conclusions. In agreement with what is suggested by a number of case reports and small case series [4, 5, 7-11, 17, 18], this first comparative study seems to provide support for the hypothesis that CT may offer added value in diagnosing equine distal limb fractures. However, the profile of agreement levels for various aspects was strikingly similar. The value of this study therefore lies in providing the rationale for a prospective controlled study on the agreement, and

more importantly on the relative sensitivity, of CT and radiography techniques in the diagnosis of distal limb fractures in horses. Ideally such a study would compare the current state of the art techniques in radiography and CT and document not only the definitive diagnosis on gross inspection but also the clinical outcome to allow determining if the use of either radiological method may steer prognosis.

Footnotes

[1]Konica Minolta, Zaventem, Belgium.

[2]FujiFilm, Sint Niklaas, Belgium.

[3]GE Medical Systems, Milwaukee, Wisconsin, United States of America.

[4]Philips, Eindhoven, The Netherlands.

[5]OsiriX, Open Source, http://www.osirix-viewer.com.

[6]Merge Healthcare, Mississauga, Canada.

References

1. Riggs, C.M. (2002) Review Fractures- A preventable hazard of racing Thoroughbreds?. *Vet J* **163**, 19-29.

2. Parkin, T.D.H., Clegg, P.D., French, N.P., Proudman, C.J., Riggs, C.M., Singer, E.R., Webbon, P.M. and Morgan, K.L. (2004) Horse-level risk factors for fatal distal limb fracture in racing Thoroughbreds in the UK. *Equine Vet J* **36**, 513-519.

3. Kuemmerle, J.M., Auer, J.A., Rademacher, N., Lischer, C.J., Bettschart-Wolfensberger, R. and Fürst, A.E. (2008) Short incomplete sagittal fractures of the proximal phalanx in ten horses not used for racing. Vet *Surg* **37**, 193-200.

4. Rose, P.L, Seeherman, H. and O'Callaghan, M. (1997) Computed tomographic evaluation of comminuted middle phalangeal fractures in the horse. *Vet Radiol Ultrasound* **38**, 424-429.

5. May, K.A., Holmes, L.C., Moll, H.D. and Jones, J.C. (2001) Computed tomographic imaging of comminuted carpal fractures in a gelding. *Equine Vet Educ* **13**, 303-308.

6. Morgan, J.W., Santschi, E.M., Zekas, L.J., Scollay-Ward, M.C., Markel, M.D., Radtke, C.L., Sample, S.J., Keuler, N.S. and Muir, P. (2006) Comparison of radiography and computed tomography to evaluate metacarpo/metatarsophalangeal joint pathology of paired limbs of Thoroughbred racehorses with severe condylar fracture. *Vet Surg* **35**, 611-617.

7. Martens, P., Ihler, C.F. and Rennesund, J. (1999) Detection of a radiographically occult fracture of the lateral palmar process of the distal phalanx in a horse using computed tomography. *Vet Radiol Ultrasound* **40**, 346-349.

8. Waselau, M., Bertone, A.L. and Green, E.M. (2006) Computed tomographic documentation of a comminuted fourth carpal bone fracture associated with carpal instability treated by partial carpal arthrodesis in an Arabian filly. *Vet Surg* **35**, 618-625.

9. Del Chicca, F., Kuemmerle, J.M., Ossent, P., Nitzl, D., Fuerst, A. and Ohlerth, S. (2008) Use of computed tomography to evaluate a fracture associated with a subchondral pedal bone cyst in a horse. *Equine Vet Educ* **20**, 515-519.

10. Kelmer, G., Wilson, D.A. and Essman, S.C. (2008) Computed tomography assisted repair of a central tarsal bone slab fracture in a horse. *Equine Vet Educ* **20**, 284-287.

11. Perrin, P.R., Launois, T., Vandeweerd, J-M, Brogniez, L. and Debrosse, F. (2009) CT-assisted surgical treatment of equine digit fractures. *Bull Acad Vét France* **162**, 327-333.

12. Bienert, A. and Stadler, P. (2006) Computertomographische untersuchungen am Bewegungsapparat des Pferdes – eine Übersicht. *Pferdeheilkunde* **22**, 218-226.

13. Puchalski, S.M. (2007) Computed tomography in equine practice. *Equine Vet Educ* **19**, 207-209.

14. Debrosse, F.G., Vandeweerd, J.M.E.F., Perrin, R.A.R., Clegg, P.D., Launois, M.T., Brogniez, L. and Gehin, S.P. (2008) A technique for computed tomography (CT) of the foot in the standing horse. *Equine Vet Educ* **20**, 93-98.

15. Temple, C.L.F., Ross, D.C., Bennett, J.D., Garvin, G.J., King G.J.W. and Faber, K.J. (2005) Comparison of sagittal computed tomography and plain film radiography in a scaphoid fracture model. *J Hand Surg Am* **30A**, 534-542.

16. Crijns, C.P., Gielen, I.M.V.L., Van Bree, H.J.J. and Bergman, E.H.J. (2010) Case report the use of CT and CT arthrography in diagnosing equine stifle injury in a Rheinlander gelding. *Equine Vet J* **42**, 367-371.

17. Whitton, R.C., Buckley, C., Donovan, T., Wales, A.D. and Dennis, R. (1998) The diagnosis of lameness associated with distal limb pathology in a horse: a comparison of radiography, computed tomography and magnetic resonance imaging. *Vet J* **155**, 223-229.

18. Perrin, R.A.R., Launois, M.T., Brogniez, L., Clegg, P.D., Coomer R.P.C., Debrosse, F.G. and Vandeweerd, J.M.E.F. (2011) The use of computed tomography to assist orthopaedic surgery in 86 horses (2002-2010). *Equine Vet Educ* **23**, 306-313.

19. Altman, D.G. (1991). In: Practical statistic for medical research. London: Chapman and Hall.

20. Huggons, N.A., Bell, R.J.W. and Puchalski, S.M. (2011) Radiography and computed tomography in the diagnosis of nonneoplastic equine mandibular disease. *Vet Radiol Ultrasound* **52**, 53-60.

21. Perrin, P.R. (2008) Computer-assisted orthopaedic surgery in horses. *Bull Acad Vét France* **161**, 359-364.

22. MacDonald, M.H., Galuppo, L.D. and Puchalski, S.M. (2009) Assessment of the utility of preoperative computed tomography in surgical planning for the equine distal extremity. *Proceedings of ACVS Congress.*

23. Moran, D.S., Evans, K. and Hadad, E. (2008) Imaging of lower extremity stress fracture injuries. *Sports Med* **38**, 345-356.

24. Archer, D.C., Boswell, J.C., Voute, L.C. and Clegg, P.D. (2007) Skeletal scintigraphy in the horse: current indications and validity as a diagnostic test. *Vet J* **173**, 31-44.

25. Dyson, S., Nagy, A. and Murray R. (2011) Clinical and diagnostic imaging findings in horses with subchondral bone trauma of the sagittal groove of the proximal phalanx. *Vet Radiol Ultrasound* **52**, 596-604.

CHAPTER FOUR

Comparison Between Radiography and Computed Tomography for Diagnosis of Equine Head Fractures

Casper P. Crijns[1], Renate Weller[2], Lieven Vlaminck[3], Francis Verschooten[1], Stijn Schauvliege[3], Sarah E. Powell[4], Henri J.J. van Bree[1], Ingrid M.V.L. Gielen[1]

[1] Department of Medical Imaging and Small Animal Orthopaedics, Ghent University, 9820 Merelbeke, Belgium
[2] Department of Veterinary Clinical Sciences, Royal Veterinary College, Hertfordshire AL9 7TA, United Kingdom
[3] Department of Surgery and Anaesthesiology of Domestic Animals, Ghent University, 9820 Merelbeke, Belgium
[4]Rossdales Equine Diagnostic Centre, Cotton End Road, Exning, United Kingdom

Adapted from:

Casper P. Crijns, Renate Weller, Lieven Vlaminck, Francis Verschooten, Stijn Schauvliege, Sarah E. Powell, Henri J.J. van Bree, Ingrid M.V.L. Gielen. Comparison between radiography and computed tomography for diagnosis of equine head fractures *(in preparation)*

Summary

The equine head is a complex structure prone to traumatic injuries. To determine the value and limitations of radiography for the diagnosis of head fracture, the differences with CT images were described in 18 horses. Two observers retrospectively reviewed the radiographic and CT images of these horses. To allow direct comparison between the two modalities, a simplified fracture classification system was used. In 3/18 cases the evaluations of the radiographic examination concluded no injuries visible. In 2/15 cases soft tissue involvement was not detected and in 7/15 cases the extent of the fracture was underestimated. Radiography classified 4/10 multiple fractures incorrectly as single fractures and 5/15 comminuted fractures as simple fractures. In line with this last finding, the number of fragments was underestimated with radiography in 14/15 cases.

In conclusion, radiography enables to diagnose a head fracture in most cases. Head fractures however are not similarly classified after radiographic and CT evaluation, which causes a difference in interpretation and perception of the fractures.

Introduction

The equine head is a complex structure, with a skull that surrounds and protects the brain, sensory organs and upper airway tracts. Traumatic injuries to the head are relatively common in horses[1-11]. The most frequently described causes are blunt trauma and injuries from collisions, entrapment of the rostral part of the mandible, and falling over backwards [1, 6, 8, 10, 11]. Injured horses are often unwilling to cooperate; rendering a thorough physical examination of an area that is already hard to access even more difficult [1, 4, 8, 12]. Diagnosis and treatment planning is therefore typically based on diagnostic imaging findings [4, 8, 9]. Radiographic examination is most often used as a first investigation modality to visualise bony trauma. However, superimposition of the complex bony structures is a major disadvantage and limits a complete evaluation of the potentially affected areas [1, 4, 8, 12]. With complex, unstable and/or displaced skull fractures [1], more sophisticated cross-sectional imaging modalities, such as computed tomography (CT), have been suggested for diagnostic purposes, as in human medicine [13-15], allowing greater recognition of normal anatomy and pathology.

To our knowledge, no studies have compared the diagnostic value of different imaging modalities for the evaluation of head fractures in horses, although information is available in small animal and human literature [15-17].

The objective of this study was to compare bony fractures of the horse's head using radiography and CT and to provide insight into the value and limitations of radiography and CT for the diagnosis of head fractures. The hypothesis was that radiography would be able to detect the presence of head fractures, but CT would provide more detailed information about the fracture configuration, extent, comminution and involvement of surrounding structure in horses.

Materials and Methods

Study population

All horses that underwent a radiographic and computed tomographic evaluation resulting in a diagnosis of a head fracture at the Department of Medical Imaging and Small Animal Orthopaedics of the Faculty of Veterinary Medicine of

Ghent University, Belgium and the private clinic, Rossdales Equine Hospital & Diagnostic Centre, United Kingdom, between 2009 and 2015 were included in the study.

Radiography

The radiographic studies were acquired using computed radiography systems (Konica Minolta[1] at Ghent University and Agfa ADC .NX[2] at Rossdale & Partners). The radiographic protocols used included a variety of standard and lesion-oriented projections and were at the discretion of the attending veterinarian of the case. All radiographic images available were used for this study.

Computed tomography

Two four-slice, helical CT scanners were used for this study. At Ghent University the horses were scanned under general anaesthesia using a GE Medical Systems Lightspeed QX/I[3] and at Rossdale & Partners sedated, standing horses were scanned using a Siemens Somatom Volume Zoom 4[4]. The in-house protocols for equine head imaging were used (120kV, 160mAs, pitch 1, 1,25-2,5mm slices, 512x512 matrix, scan FOV between 192-403mm, bone and standard algorithm at Ghent University and 120kV, 167-220mAs, pitch 1, 2mm slices, 512x512 matrix, scan FOV between 254-500mm, bone and soft tissue algorithm at Rossdale & Partners).

Data evaluation

The radiographic and computed tomographic examinations were retrieved, reviewed, the patient details removed and collated in a randomised order by one of the authors (C.P.C.). Cases were excluded from the study if the radiographic or CT examination did not include the area of the main fracture. The radiographic and CT examinations were evaluated by two of the authors (R.W. and F.V.). All radiographic images were evaluated first, followed by all CT images to assure that both modalities would not influence each other's diagnosis. A standardised evaluation form was used to describe the different fractures: the visibility of an injury (Yes or No), soft tissue involvement (Yes or No), the location of the injury (the involved bones), the fracture type (single or multiple; simple or comminuted; open or closed), the number of fragments, the involvement of surrounding anatomical structures and

additional remarks (subjective assessment of the quality of the study with regard to the fracture present). To be able to reach a consensus in classification of the fractures between the observers, they were asked to describe the fractures and the size, shape and displacement of the fragments. The observers had no knowledge of the horse's identity, clinical history, clinical presentation, surgical or pathologic findings and final diagnosis.

The radiographic and CT evaluations of the observers were recorded and compared by one of the authors (C.P.C.). In case of disagreement on the classification of the fractures, the written descriptions were compared to reach a consensus on the correct classification of the fractures.

Results

Eighteen cases fulfilled the inclusion criteria for this study. These included 10 stallions, 3 geldings and 5 mares, with a median age of 6 years (range: 2m–16y). There were 11 Warmbloods, 3 Thoroughbreds, 2 ponies, 1 Arabian and 1 French Trotter.

The number of radiographs per case ranged from 1-8 views with a median of 5. From the standard projections (latero-lateral, ventro-dorsal, leftventral-rightdorsal-oblique and rightventral-leftdorsal-oblique), in 7 cases all 4 projections, in 6 cases 3 projections, in 3 cases 2 projections and in 2 cases 1 projection, were available. In 15 cases additional radiographs were included: in 12 cases these were additional standard projections and in 8 cases additional intra-oral or the so-called skyline projections. The observers had no remarks on the quality of the radiographic study in 14 cases. In 4 cases additional ventrodorsal (2 cases) or intra-oral (2 cases) projections were suggested to complement the radiographic examination.

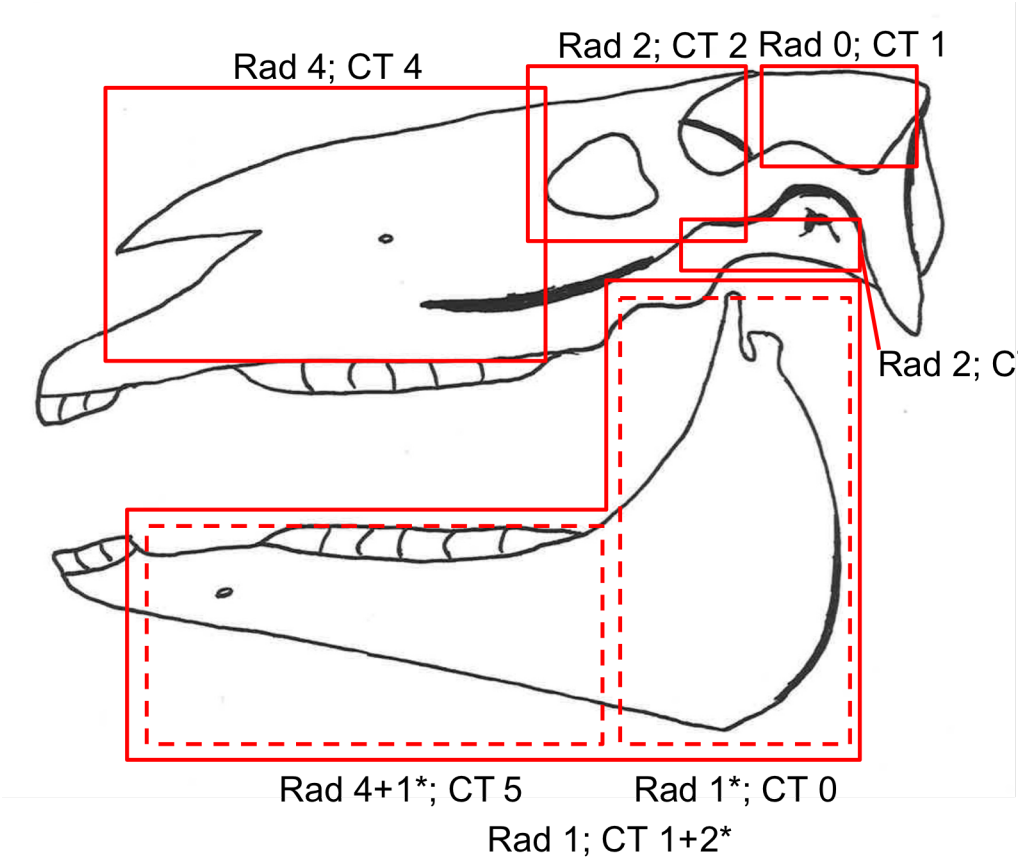

Figure 1: Location of the fractures as detected and diagnosed with radiography and CT. * fracture differently localised between radiography and CT

Fourteen CT studies were performed as part of the clinical work up and 4 studies were performed as part of the research protocol after euthanasia. The CT studies all included a series in bone algorithm and in 14 cases an additional post-processing standard/soft-tissue algorithm was available. In one case performed on a standing horse a motion artefact was present; the artefact however did not obliterate the region of interest.

The radiographic and CT localisation and classification of the fractures is represented in Figure 1 and Table 1.

In 3/18 cases the evaluations of the radiographic examination concluded that no injuries were visible. In contrast, the CT evaluation of these cases showed: a depressed fracture in the temporal and parietal bone with multiple displaced fragments in a 2-month-old colt (case 4), a comminuted fracture of the floor, septum and walls of the sphenopalatinal sinuses in a 2-year-old colt (case 3) and an older

fracture with periosteal reaction of the most apical part of the tooth alveolus of the fractured element 410 in a 6-year-old gelding (case 12).

In the remaining 15/18 cases a fracture was observed radiographically, but the soft tissue involvement (swelling and/or gas) on the radiographs was not detected in 2/15 cases (cases 2 and 5) (Figure 2).

Case, Gender, Age	Modality/ protocol	Injury visible	Soft tissue involvement	Location	Single/ multiple	Type	Open/ closed	Fragments
1, stallion, 6m.	Rad.4+3	Yes	No	15,16	Single	Comm.	Closed	0
	CT B+S	Yes	Yes	15,16	Single	Comm.	Closed	10+
2, mare, 8m.	Rad.3+1	Yes	No	15,16	Single	Comm.	Closed	4
	CT B+S	Yes	No	15,16	Single	Comm.	Open	6+
3, stallion, 2y.	Rad.3+1	No	/	/	/	/	/	/
	CT B+S	Yes	Yes	16	Single	Comm.	Open	3
4, stallion, 2m.	Rad.3	No	/	/	/	/	/	/
	CT B+S	Yes	No	10,11	Single	Depress.	Closed	4
5, stallion, 10y.	Rad.2+3	Yes	No	18	Single	Simple	Closed	2
	CT B+S	Yes	Yes	10,18	Multiple	Comm.	Closed	5+
6, stallion, 2m.	Rad.4+1	Yes	Yes	4,6	Single	Comm.	Open	3+
	CT B	Yes	Yes	4,6,10	Multiple	Comm.	Open	10+
7, stallion, 15y.	Rad.3	Yes	Yes	6	Single	Comm.	Closed	8+
	CT B+S	Yes	Yes	4,6,10	Multiple	Comm.	Closed	10+
8, stallion, 7y.	Rad.4+1	Yes	Yes	2,3	Multiple	Simple	Closed	1
	CT B+S	Yes	Yes	2,3,6	Multiple	Comm.	Open	10+
9, gelding, 4y.	Rad.1	Yes	Yes	2	Multiple	Simple	Open	2+
	CT B	Yes	Yes	2	Multiple	Comm.	Open	5
10, gelding, 14y.	Rad.4	Yes	Yes	3	Single	Simple	Open	0
	CT B+S	Yes	Yes	3	Single	Comm.	Open	4
11, stallion, 6y.	Rad.4+4	Yes	Yes	1,3	Multiple	Comm.	Closed	3
	CT B+S	Yes	Yes	1,3	Multiple	Comm.	Open	3
12, gelding, 6y.	Rad.2+5	No	/	/	/	/	/	/
	CT B	Yes	No	20	Single	Simple*	Closed	3
13, mare, 7y.	Rad.4+1	Yes	Yes	20	Single	Simple*	Closed	0
	CT B+S	Yes	Yes	20	Single	Simple*	Closed	1
14, stallion, 1y.	Rad.3+1	Yes	Yes	20	Multiple	Comm.	Open	4
	CT B+S	Yes	Yes	20	Multiple	Comm.	Open	10+
15, mare, 16y.	Rad.2+2	Yes	Yes	20	Single	Simple*	Open	1
	CT B+S	Yes	Yes	20	Single	Simple*	Open	2
16, mare 6m.	Rad.4+2	Yes	Yes	19	Single	Comm.	Open	6+
	CT B	Yes	Yes	19,20	Multiple	Comm.	Open	10+
17, stallion, 5y.	Rad.3+2	Yes	Yes	20	Multiple	Simple	Open	2
	CT B+S	Yes	Yes	18,19,20	Multiple	Comm.	Open	10+
18, mare, 16y.	Rad.3+6	Yes	Yes	19,20	Multiple	Comm.	Open	6
	CT B+S	Yes	Yes	18,19,20	Multiple	Comm.	Closed	10+

Table 1: Case details, radiographic (included standard projections + additional projections) and CT (included B: bone and S: standard algorithm) protocols, and radiographic and CT fracture evaluation of 18 head fracture cases. *involving the alveolar bone surrounding a cheek tooth.
Legend for the localisation of the fractures: 1=Incisive bone; 2=nasal bone; 3=Maxilla; 4=Zygomatic bone; 5=Lacrimal bone; 6= Frontal bone; 7=Palatine bone; 8= Vomer; 9=Presphenoid bone; 10=Temporal bone; 11=Parietal bone; 12= Interparietal bone; 13= Occipital bone (squamous part); 14= Occipital bone (lateral part); 15= Occipital bone (basilar part); 16= Sphenoid bone; 17= Coronoid process; 18=Condylar process; 19= Ramus mandibula; 20= Body mandibula; 21= Hyoid apparatus

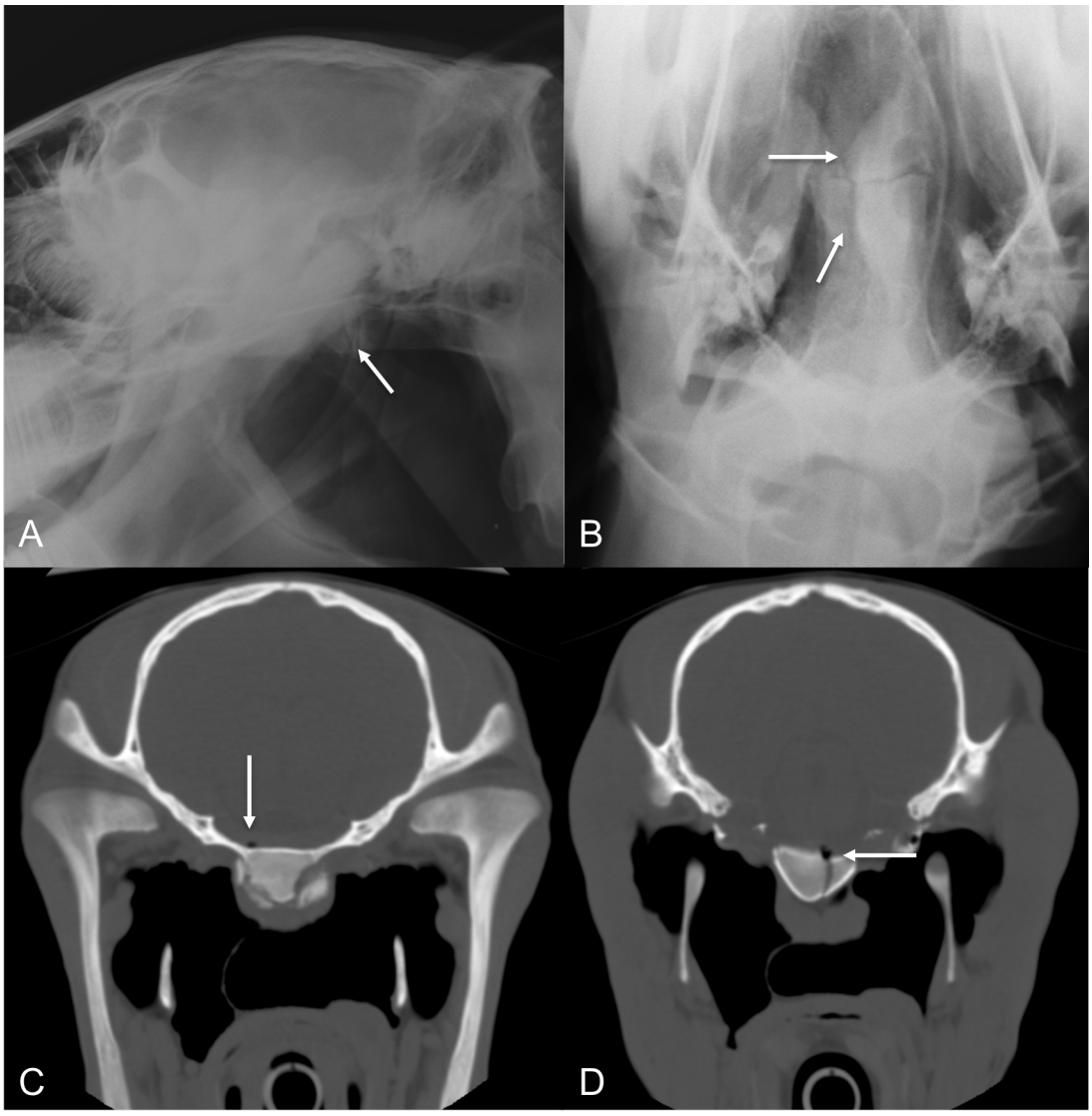

Figure 2: Case 2, laterolateral (A, rostral is to the left) and ventrodorsal (B, rostral is to the top and right is to the left) radiographic projections of the cranium and transverse (C and D, right is to the left) computed tomographic images. On the radiographic images, (A) only a small step just caudal of the spheno-occipital suture line between the basisphenoid and basioccipital bones is detected (A: arrow) and a curved radiolucent line runs in a longitudinally trough the basisphenoid and basioccipital bones (B: arrows). On the CT images, at the level of the TMJ (C) a heavily comminuted fracture of the basisphenoid bone is detected and just cranial to the inner ears (D) only a single fracture line is detected in the basioccipital bone. Note the gas opacities inside the cranium not detected on the radiographs (C and D: arrows).

Locating and determining the fracture extension on radiographs was underestimated in 7/15 cases in which a fracture was detected. In 1 of these cases (case 16) obvious fracture associated changes of the vertical ramus of the mandibula were present, but a none-displaced, simple, fracture of the rostral body which was not included in the radiographic exam was missed. In 6 other cases the fracture extension was hidden due to superimpositions on the radiographs (Figure 3 and 4). In case 8, the fracture extended further caudally to include the frontal bone, in addition to the involvement of the nasal and maxillary bone, which was identified radiographically. In 5 cases (cases 5, 6, 7, 17 and 18), fractures were located in the caudodorsal part of the skull involving the temporal bone (cases 5, 6 and 7) (Figure 3) or the condylar process (cases 17 and 18) (Figure 4). In addition to underestimating the number of bones involved, the involvement of the temporomandibular joint (TMJ) was not detected on radiography in these cases (Figure 3 and 4). In 4/10 cases (cases 5, 6, 7 and 16) diagnosed with multiple fractures on CT the observers diagnosed only a single fracture with radiography. In 5/13 cases (cases 5, 8, 9, 10 and 17) diagnosed with a comminuted fracture on CT the observers diagnosed a simple fracture with radiography. In 3/15 cases (cases 2, 8 and 11) the fractures were scored closed with radiography and open with CT. In 1/15 (case 18) the fractures was scored open with radiography and closed with CT. In 14/15 cases the number of fragments was underestimated with radiography. Only in one case (case 11) involving only large fragments without smaller fragments, the observers were able to determine a similar amount of fragments on both radiographic and CT images.

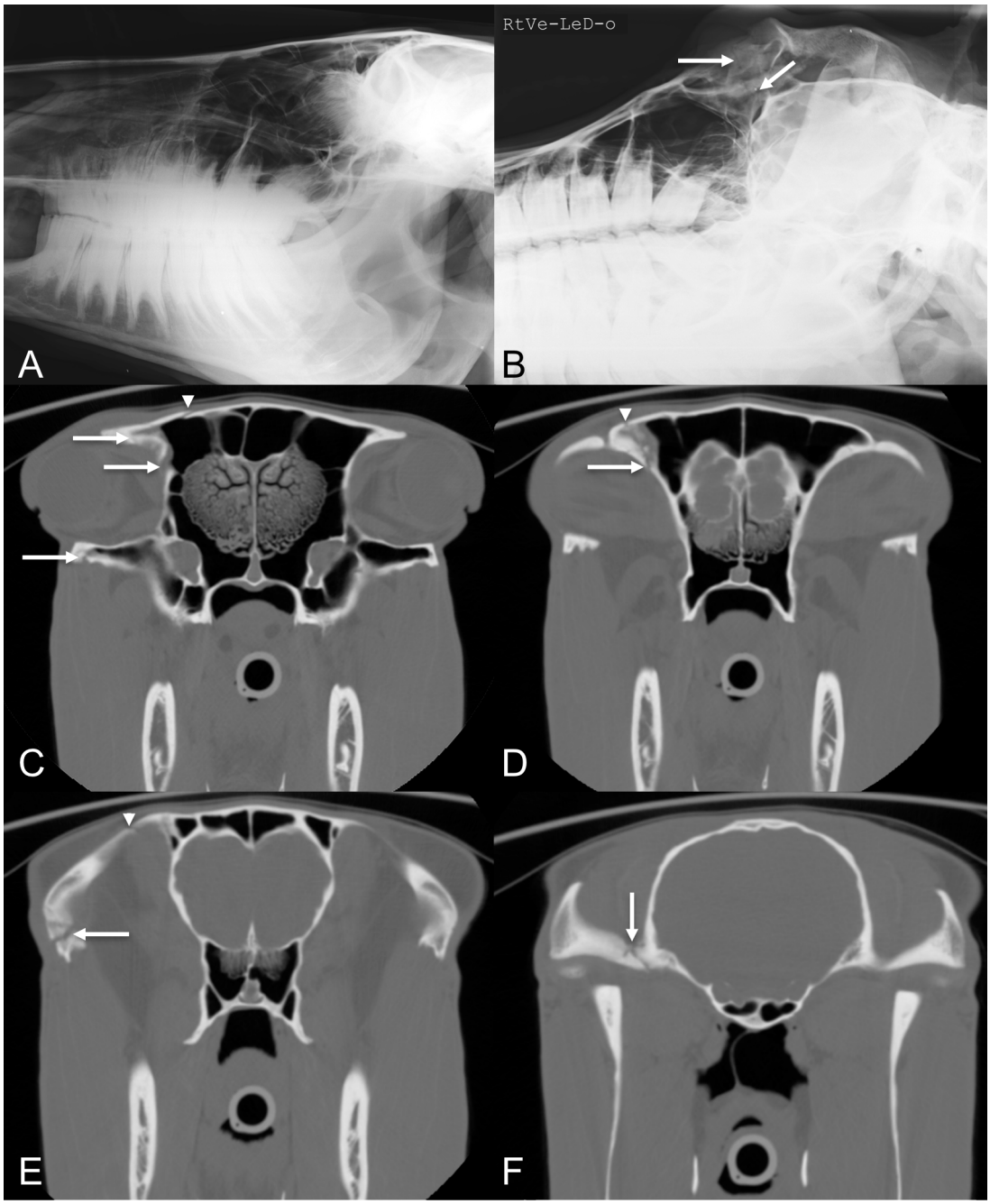

Figure 3: Case 7, laterolateral (A, rostral is to the left) and rightventral-leftdorsal-oblique (B, rostral is to the left) radiographic projections of the nasofrontal region, and transverse (C, D, E and F, right is to the left) CT images. On the laterolateral projection (A) no evidence of a bony injury is detected, on the rightventral-leftdorsal oblique projection (B) only 2 thin radiolucent lines (arrows) are superimposed over the region of the right orbita. The transverse CT images at the level and just caudal of the right showing, multiple and several displaced fracture lines surrounding the right orbita (C, D, and E: arrows), and a singular fracture line in the frontal bone (E: arrowheads). On the transverse CT image at the level of the temperomandibular joints, the temporomandibular joint is involved in the fracture, as multiple fracture lines are present in the temporal bone (F: arrows).

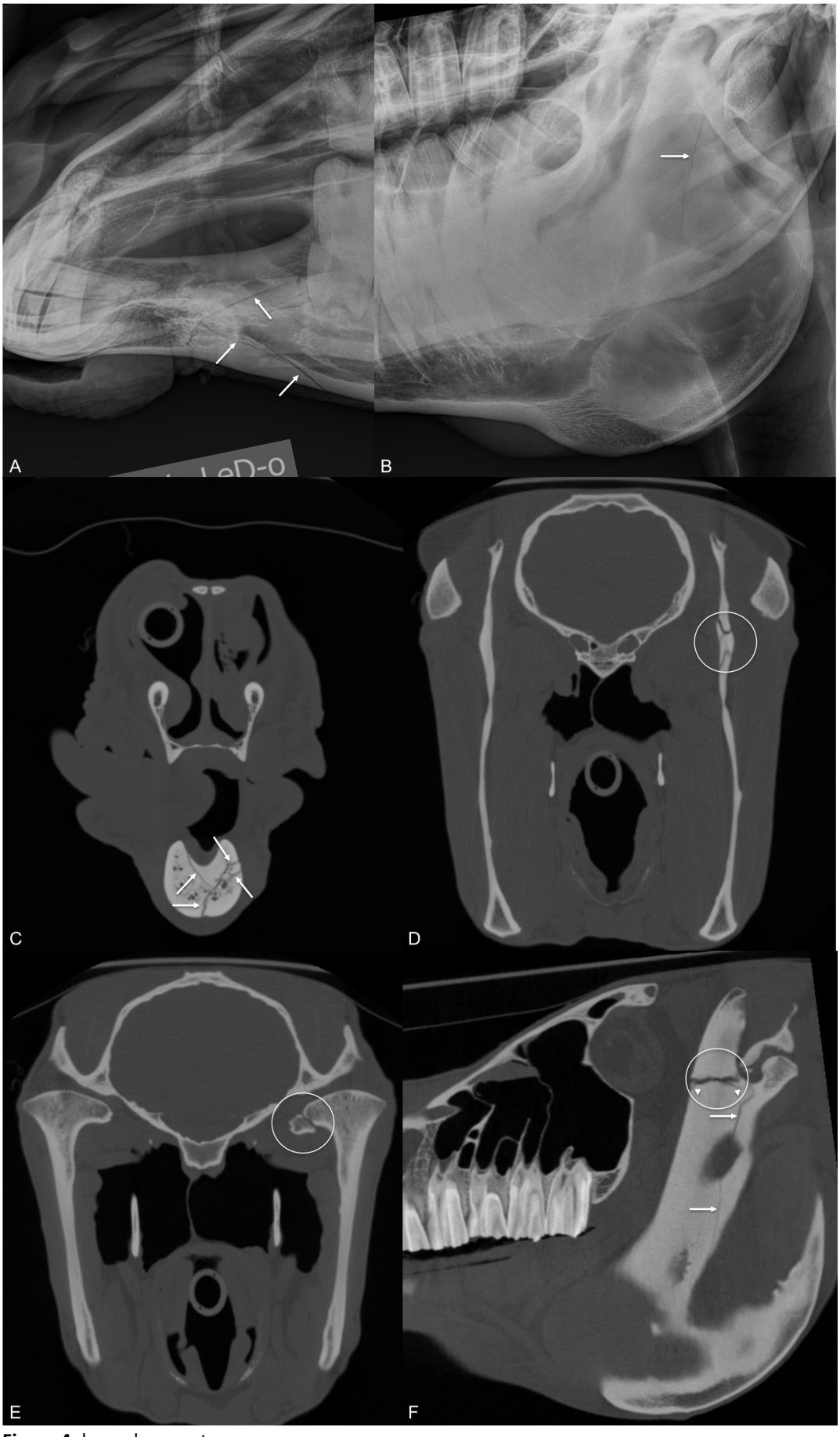

Figure 4: legend on next page

Figure 4: Case 18, rightventral-leftdorsal-oblique radiographic projections (rostral is to the left) of the rostral part of the head (A) and left mandibular ramus (B), and transverse (C, D and E, right is to the left) and sagittal (F, rostral is to the left) CT images. On the radiographic images, several sharp delineated fracture lines are present in the left body of the mandible (A: arrows) and one sharp delineated fracture line is detected in the vertical ramus of the left mandible running in a ventrodorsal direction (B: arrow). On the CT images, several sharp delineated fracture lines are present in both the left and right mandibular body in the caudal part of the mandibular symphysis (C: arrows). In the region of the TMJ an area of comminution is present in the left coronoid process just ventral to the level of the TMJ (D: circle), a separated fragment is present at the axial portion of the left condylar process (E: circle). In (F) at the level of the left TMJ, a sharp delineated thin fracture line is running in a dorsoventral direction in the left mandibular ramus (arrows) and a wider, more irregular fracture line (circle) surrounded by two sharp delineated thin fracture lines (arrowheads) is running in a rostrocaudal direction.

Discussion

In this study we compared the differences between radiography and CT in visualising and diagnosing equine skull fractures. Our purpose was to determine the contribution of both imaging modalities in the final fracture diagnosis. Ideally every fracture should be described individually in detail, as every detail is potentially diagnostically relevant. To allow direct comparison between the two modalities, a simplified classification system was used in line with previous studies in small animals and human medicine [13, 16, 17].

The fractures in the cases considered radiographically normal were subtle and located in anatomically complex areas. As previously described for distal limb fractures, the combination of lesion severity and the degree of superimposition can cause fractures to go unnoticed [18]. However, subtle, previously unnoticed lesions on radiography can retrospectively be suspected if their presence has been demonstrated using CT [18, 19]. Moreover, the general limitations of radiography need to be considered. Firstly, the x-ray beam should be parallel to a fracture line and, secondly, superimposition should not interfere with the interpretation of the radiographs [13, 17, 20]. An additional limitation related to equine patients, is the inability of recording the entire head on a single image as in small animals [17]. Indications of trauma such as malocclusion of the teeth or misalignment of the bone are therefore possibly missed.

In the case of the 2-months-old foal with a single, depressed, comminuted, temporal and parietal bone fracture, retrospectively at least one fracture line is visible on the radiographs. However, considering the foal's age and in the absence of

visible displacement of the fragments on radiography, this fracture line was initially misinterpreted as an open fontanel. The normal radiographic appearance of the fontanels has not been described in horses; further studies describing these normal open fontanels would be interesting and useful in such cases.

In the remaining cases fractures were diagnosed with both modalities. To be able to compare the modalities' capabilities, fracture extension was determined by listing the bones involved. An underestimation of the fracture extension by incompletely listing the involved bones using radiography was seen in 40% of the cases. In most of these cases the fractures were located in the caudodorsal part of the skull, including the complex regions of the TMJ, the orbita and the skull base. The ability of CT to diagnose more extending fractures in this region compared to radiography is in line with previously published case reports and smaller case series [1, 2, 7]. The main limitation of radiography in this complex anatomical region with a broad variety of opacities is, contrary to lesions involving the paranasal sinuses [21] or the mandible [22], the limited reduction in superimposition by complementary oblique radiographic projections, as is illustrated in a study describing a specific projection to visualise the TMJ [23]. Although the TMJ is the most abaxially located structure in this region, the described projection only reduces superimposition of the abaxial portion of the joint.

In line with the inability to correctly determine fracture extent, 44% of the fractures radiographically diagnosed as single with radiography were diagnosed as multiple on CT. In the caudodorsal part of the skull, involvement of the temporal bone forming the TMJ was underestimated in all these cases. In line with the previous statement on the radiographic visibility of the TMJ, fractures of the articular tuberculum of the temporal bone or the condylar process of the mandible were located in the most axial portion of the joint in 80% of the cases included in this study. Only in one case (5) the complete width of the TMJ was involved in the lesion. Although specific projections of the TMJ were included for this case, the radiographic study underestimated this lesion. Trauma is one of the reasons for the development of TMJ disease. An initial correct diagnosis of the involvement of the TMJ is therefore prognostically important to avoid long-term sequelae [13, 24, 25].

Misclassifying the individually detected fractures further by type (simple or comminuted) not only included the caudodorsal part of the skull as seen for the fracture extent but also included the rostral part of the skull. In line with these results, the number of fragments was underestimated on radiography in all but one case. Fragments were missed with radiography in cases classified as simple but also when classified as comminuted. Reviewing specific fragments, two factors led to diagnostic differences between radiography and CT in detecting fragments. Firstly, some fragments (small and large) were not recognised on radiography, and secondly, in the absence of displacement, several smaller fragments identified on CT could appear as one larger fragment on radiography.

Although the final outcome of the individual cases was not included in this study, the decision between a conservative or a surgical treatment and the estimation of a prognosis are mainly influenced by the interpretation and perception of a fracture [3, 8, 12]. Regarding the surgical guidelines for head fractures described in several publications [4, 8, 9, 12], preoperative considerations vary depending on localisation, configuration, degree of comminution, and the involvement of additional structures in a fracture [8, 12]. In line with these guidelines, the differences between the radiographic and CT findings described in this study would influence the preoperative considerations and the estimated prognosis for each fracture.

Contrary to human medicine where CT suits are widely accessible and CT examinations are more routinely used in cases of suspected head trauma [26], the availability and the use of CT in equine medicine are limited. A shortcoming of this study is the inclusion of only a sub selection of cases diagnosed with a head fracture. Only cases that underwent both a radiographic and a CT examination met the inclusion criteria of the study. This inadvertently led to an inclusion bias of cases in which radiographic findings insufficiently explained clinical problems. Thus the head fractures included in the study are partially biased towards subtle or complex lesions. In addition, based on the definitive (CT) diagnosis these patients were treated conservatively, underwent (partial) surgical stabilisation or underwent pathologic examination. Therefore, CT functioned as the reference modality for

radiography in this study. In the absence of a reliable gold standard in all cases, sensitivity and specificity of the modalities were not calculated.

The heterogeneity of the radiographic examinations can also be considered a shortcoming of this retrospective study. However, in a previous study describing the ability to visualise maxillofacial structures in cats and dogs, including only standard views and standardising the radiographic examination was considered to lower the ability to visualise specific structures [17]. In the study of Bar-Am et al. (2008), inclusion of specific projections is suggested to increase the ability to visualise specific structures. Variation of the fracture types included and specific (e.g. unilateral) lesion presentation can therefore justify the lack of standardisation in the radiographic protocol in this study. Furthermore, the observers suggested in 4 cases additional ventrodorsal (2 cases) or intra-oral (2 cases) projections to complement the radiographic examinations. The radiographic examinations however were performed under clinical conditions on standing horses. The inability of producing additional projections is due to uncooperativity or discomfort of the patients. Reviewing the CT examinations for which additional intra-oral radiographic projections were suggested (14 and 17), both cases involved bilateral multiple comminuted (one severely displaced) fractures of the mandibular body. In one of these cases an intra-oral projection of the most rostral part of the mandible, was included in the radiographic study. Although an intra-oral projection would diminish the superimposition of the maxilla over the fractured mandibula, the patient's discomfort most likely prevented these projections to be taken of more caudal structures. Moreover, taking intra-oral projections in the presence of an unstable, (partially) displaced fracture could be contraindicated.

In conclusion, the inability to similarly classify fractures using radiographic or CT modalities causes a difference in interpretation and perception of these fractures. Consequently, diagnosing a fracture can be divided into several levels of detail: simply confirming the presence of a fracture, visualising the fracture extension and finally being able to correctly describe fracture details. Depending on the diagnostic request, radiography can be employed as a first imaging step in suspected traumatic cases to rule in a fracture, but it is not able to rule out a fracture. In cases of subtle

lesions or if a complete impression of a lesion is needed for surgical planning or prognosis, CT is definitely the recommended modality.

Footnotes

[1]Konica Minolta, Zaventem, Belgium.

[2]Agfa-Gevaert NV, Mortsel, Belgium.

[3]GE Medical Systems, Milwaukee, Wisconsin, United States of America.

[4]Siemens, Frimley, Surrey, United Kingdom.

References

1. Beccati, F., Angeli, G., Secco, I., Contini, A., Gialletti, R. and Pepe, M. (2011) Comminuted basilar skull fracture in a colt: use of computed tomography to aid the diagnosis. *Equine Vet Educ* **23**, 327-332.

2. Lischer, C.J., Walliser, U., Witzmann, P., Eser, M.W. and Ohlerth, S. (2005) Fracture of the paracondylar process in four horses: advantages of CT imaging. *Equine Vet J* **37**, 483-487.

3. Schaaf, K.L., Kannegieter, N.J. and Lovell, D.K. (2008) Management of equine skull fractures using fixation with polydioxanone sutures. *Aus Vet J* **86**, 481-485.

4. Tremaine, H. (2004) Management of skull fractures in the horse. *In Pract* **26**, 214-222.

5. Wollanke, B., Gerhards, H. and Cronau, M. (2006) Diagnosis and therapy of periorbital diseases in horses: Indication for computed tomography (CT) or magnetic resonance tomography (MRT). *Pferdeheilkunde* **22**, 431-438.

6. Ramirez, O., Jorgensen, J.S. and Thrall, D.E. (1998) Imaging basilar skull fractures in the horse: a review. *Vet Radiol Ultrasound* **39**, 391-395.

7. Gardelle, O., Feige, K., Geissbuhler, U., Geyer, H., Schmucker, N., Sydler, T. and Kaser-Hotz, B. (1999) The use of computed tomography in two equine patients with basilar skull fractures. *Schweiz Arch Tierh* **141**, 267-272.

8. Auer, J.A. (2012) Craniomaxillofacial Disorders. In: *Equine Surgery*, 4th Edition edn., Eds: J.A. Auer and J.A. Stick, Elsevier Saunders. p 1531.

9. Fürst, A., Jackson, M., Kummerle, J., Bettschart-Wolfensberger, R. and Kummer, M. (2010) Summary of current therapeutic measurements in head fractures of horses. *Pferdeheilkunde* **26**, 503-514.

10. Caldwell, F.J. and Davis, H.A. (2012) Surgical reconstruction of a severely comminuted mandibular fracture in a horse. *Equine Vet Educ* **24**, 217-221.

11. Henninger, R.W., Beard, W.L., Schneider, R.K., Bramlage, L.R. and Burkhardt, H.A. (1999) Fractures of the rostral portion of the mandible and maxilla in horses: 89 cases (1979-1997). *J Am Vet Med Assoc* **214**, 1648-1652.

12. Beard, W. (2009) Fracture repair techniques for the equine mandible and maxilla. *Equine Vet Educ* **21**, 352-357.

13. Chacon, G.E., Dawson, K.H., Myall, R.W. and Beirne, O.R. (2003) A comparative study of 2 imaging techniques for the diagnosis of condylar fractures in children. *J Oral Maxillofac Surg* **61**, 668-672.

14. dos Santos, D.T., Silva, A.P.A.C., Vannier, M.W. and Cavalcanti, M.G.P. (2004) Validity of multislice computerized tomography for diagnosis of maxillofacial fractures using an independent workstation. *Oral Surg Oral Med Oral Pathol* **98**, 715-720.

15. Marinaro, J., Crandall, C.S. and Doezema, D. (2007) Computed tomography of the head as a screening examination for facial fractures. *Am J Emerg Med* **25**, 616-619.

16. Creasman, C.N., Markowitz, B.L., Kawamoto, H.K., Cohen, S., Kioumehr, F., Hanafee, W.N. and Shaw, W.W. (1992) Computed-tomography versus standard radiography in the assessment of fractures of the mandible. *Ann Plas Surg* **29**, 109-113.

17. Bar-Am, Y., Pollard, R.E., Kass, P.H. and Verstraete, F.J.M. (2008) The diagnostic yield of conventional radiographs and computed tomography in dogs and cats with maxillofacial trauma. *Vet Surg* **37**, 294-299.

18. Crijns, C.P., Martens, A., Bergman, H.J., van der Veen, H., Duchateau, L., van Bree, H.J.J. and GIelen, I.M.V.L. (2014) Intra-modality and inter-modality agreement in radiography and computed tomography of equine distal limb fractures. *Equine Vet J* **46**, 92-96.

19. Crijns, C.P., Gielen, I.M.V.L., van Bree, H.J.J. and Bergman, E.H.J. (2010) The use of CT and CT arthrography in diagnosing equine stifle injury in a Rheinlander gelding. *Equine Vet J* **42**, 367-371.

20. Butler, J.S., Colles, C.M., Dyson, S., Kold, S. and Poulos, P. (2008) *Clinical Radiology of the Horse, 3rd Edition*, Wiley-Blackwell, Oxford. p 760.

21. O'Leary, J.M. and Dixon, P.M. (2011) A review of equine paranasal sinusitis. Aetiopathogenesis, clinical signs and ancillary diagnostic techniques. *Equine Vet Educ* **23**, 148-159.

22. Huggons, N.A., Bell, R.J.W. and Puchalski, S.M. (2011) Radiography and computed tomography in the diagnosis of nonneoplastic equine mandibular disease. *Vet Radiol Ultrasound* **52**, 53-60.

23. Ebling, A.J., McKnight, A.L., Seiler, G. and Kircher, P.R. (2009) A complementary radiographic projection of the equine temporomandibular joint. *Vet Radiol Ultrasound* **50**, 385-391.

24. Sanders, R.E., Schumacher, J., Brama, P.A.J., Zarelli, M. and Kearney, C.M. (2014) Mandibular condylectomy in a standing horse for treatment for osteoarthritis of the temporomandibular joint. *Equine Vet Educ* **26**, 624-628.

25. Weller, R., Maierl, J., Bowen, I.M., May, S.A. and Liebich, H.G. (2002) The arthroscopic approach and intra-articular anatomy of the equine temporomandibular joint. *Equine Vet J* **34**, 421-424.

26. Schuknecht, B. and Graetz, K. (2005) Radiologic assessment of maxillofacial, mandibular, and skull base trauma. *Eur Radiol* **15**, 560-568.

CHAPTER FIVE

The Use of CT and CT Arthrography in Diagnosing Equine Stifle Injury in a Rheinlander Gelding

Casper P. Crijns[1], Ingrid M.V.L. Gielen[1], Henri J.J. van Bree[1], Hendrik-Jan Bergman[2]

[1] Department of Medical Imaging of Domestic Animals, Ghent University, 9820 Merelbeke, Belgium
[2]Lingehoeve Diergeneeskunde, 4033 AK Lienden, The Netherlands

Adapted from:

Casper P. Crijns, Ingrid M.V.L. Gielen, Henri J.J. van Bree, Hendrik-Jan Bergman. The use of CT and CT arthrography in diagnosing equine stifle injury in a Rheinlander gelding *(published in Equine Veterinary Journal (2010) **42** (4) 367-371)*

Summary

A 5-year-old Rheinlander gelding was evaluated for left hind limb stifle lameness. The lameness was localised to the stifle, but the source of the lameness was not specifically diagnosed from the physical, radiographic and ultrasonographic examinations. Computed tomography (CT) and CT arthrography were therefore used for further investigation since this imaging technique images bony structures, cartilage and soft tissues. This examination showed multiple lesions in the stifle: a traumatic osteochondrosis (OC)-like lesion of the medial femoral condyle, bony fragments, cartilage trauma and caudal cruciate ligament injury. The prognosis for continuing use as a sports horse was regarded as unfavourable. Therefore, the horse was subjected to euthanasia. All CT findings were confirmed by gross pathology.

In conclusion, the CT and CT arthrography examination in this case provided a diagnosis not achieved with other conventional imaging techniques.

Introduction

The stifle joint is the largest and most complex joint in horses. The joints consist of two articulations with in total three joint compartments and is stabilised by two menisci and 14 ligaments (Figure 1).

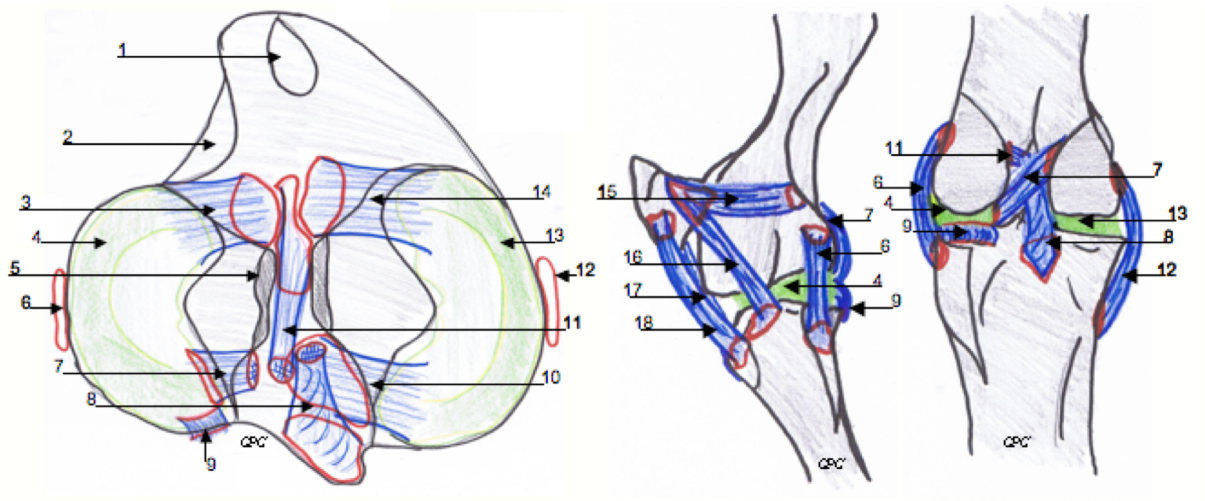

Figure 1: Left image proximal view of the tibial plateau, middle image lateral view and right image caudal view of the stifle joint. The sites of soft-tissue attachments are illustrated in red.
1 groove for the middle patellar ligament; 2 extensor sulcus; 3 cranial tibial ligament of the lateral meniscus; 4 lateral meniscus; 5 eminence of the tibia; 6 lateral collateral ligament; 7 meniscofemoral ligament of the lateral meniscus; 8 caudal cruciate ligament; 9 caudal tibia ligament of the lateral meniscus; 10 caudal tibia ligament of the medial meniscus; 11 cranial cruciate ligament; 12 medial collateral ligament; 13 medial meniscus; 14 cranial tibial ligament of the medial meniscus; 15 lateral femoropatellar ligament; 16 lateral patellar ligament; 17 medial patellar ligament; 18 intermediate patellar ligament

Radiography [1-6] and ultrasonography [3, 5-9] are the most often used diagnostic imaging modalities for visualising stifle joint pathology. However, these techniques have their limitations, because superimposition of the bony structures and surrounding structures restricts visualisation of the ligaments of the stifle. Radiography visualises bony structures only, and ultrasonography visualises bone surfaces and soft tissues only [1, 3, 5]. Because these techniques usually underestimate the pathology, it is difficult to diagnose specific tissue injury and make a proper prognosis [3, 9]. Arthroscopic examination of the joint under general anaesthesia would offer further diagnostic information but computed tomography (CT) and CT arthrography provides a valuable extra perspective for diagnosing stifle injuries without the need for surgical intervention [1].

Case details

History

A 5-year-old Rheinlander gelding used for dressage was presented to Lingehoeve Diergeneeskunde Equine Hospital for evaluation of left hind limb lameness. The horse had become severely lame 2 weeks previously, after it fell and hit a pole with the dorsal surface of the left metatarsus. The lameness improved after several days, training was therefore resumed and the horse was ridden in a competition. However, 5 days later the gelding became severely lame again and was presented to the equine hospital.

Clinical examination

A palpable dilatation of the cranial recess of the left medial femorotibial joint (MFTJ) was identified.

Lameness of the left hind limb was consistently observable, especially when turned on small circles. The lameness was evaluated as 2/5 in a straight line, 2-3/5 on a hard circle on the left rein, and 2/5 on a hard circle on the right rein according to the American Association of Equine Practitioners (AAEP) lameness grading scale [10]. The flexion test of the left stifle was positive.

Radiography

Caudocranial, lateromedial and lateromedial flexed radiographic projections of the left stifle were obtained. The caudocranial radiograph showed a mineralisation in the MFTJ centrally between the femoral condyle and tibia condyle. The lateromedial (Figure 2a) and lateromedial flexed radiographs showed mineralisation cranial to the intercondylar eminences of the tibia.

Ultrasonography

An extensive ultrasonographic examination was carried out according to the protocol described by Hoegaerts et al. (2005) [8], including scanning with the leg in flexion. Ultrasonography[a] showed severe effusion of the medial femorotibial joint and an irregular alignment present on the caudoaxial margin of the medial femoral condyle (Figure 2b).

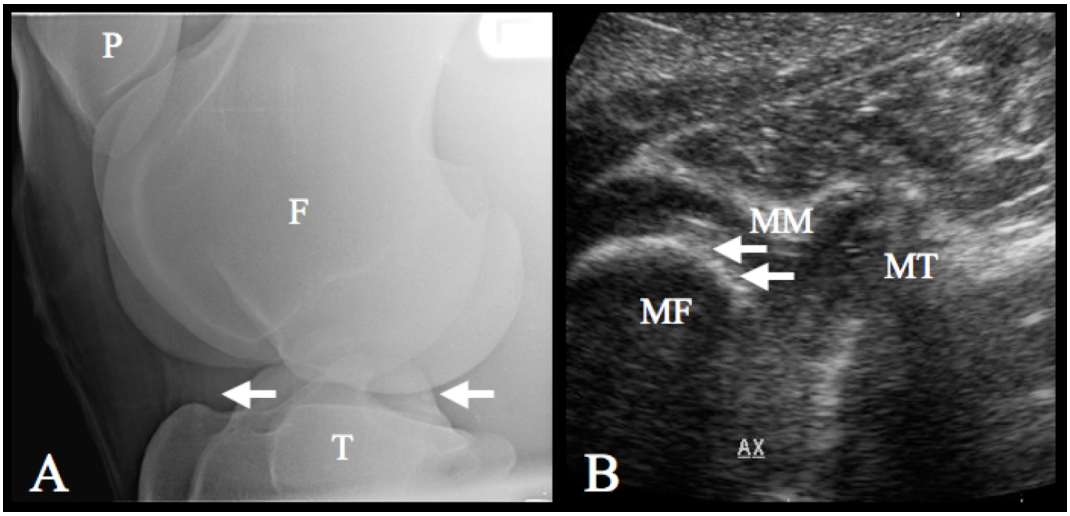

Figure 2: Radiographic and ultrasonographic images. A) This latero-medial radiographic projection, cranial is to the left, shows mineralisation cranial to the intercondylar eminences of the tibia and a fragment present in the femorotibial joint (arrows). B) Ultrasonographic image, caudal view, proximal is to the left, irregular alignment of the axial part of the caudo-medial margin of the medial femoral condyle (arrows). F, femur; MF, medial femur condyle; MM, medial meniscus; MT, medial tibia condyle; P, patella; T, tibia.

The lameness was isolated to the left stifle joint based on the clinical, radiographic and ultrasonographic examinations. Due to the complexity of the stifle joint, it was impossible to complete the diagnosis and provide a reliable prognosis for the future with these imaging modalities. Therefore, further investigation was performed using CT and CT arthrography.

Computed tomographic examination

Computed tomography and CT arthrography examination of the left stifle joint was performed as described by Bergman et al. (2007) [1].

Anaesthesia was induced by ketamine [e] (2mg/kg [0.9mg/lb]) and midazolam [c] (0.1-0.2 mg/kg [0.045-0.09mg/lb]). After tracheal intubation, the horse was laid on a custom-made table and positioned in left dorsolateral recumbency with the lame leg pulled fully extended in the gantry, so that the longitudinal axis of the limb was parallel to the table and perpendicular to the gantry. The right limb, in full flexion, was pulled out of the gantry (Figure 3). Anaesthesia was maintained with an IV drip of 500 ml 5% guaifenesin[d] with 1000 mg ketamine and 10 mg detomidine.

The CT and CT arthrography examination consists firstly of one native series and secondly of 3 contrast series following intra-articular, ultrasound-guided[b] contrast administration in each compartment with ~60 ml iodinated contrast

Figure 3: The position of the horse during the CT examination of the stifle. The lame leg is fully extended and fixated to the CT-table; the overlaying leg is pulled in full flexion out of the gantry (not seen). The red laser indicator visualises where the scanning-plan of the gantry is situated on the leg.

material[f] diluted 1:1 with 0.9% NaCl saline solution. Computed tomographic images were obtained with a four-slice CT scanner[h]. The imaging parameters were 120 kV and 266 mAs, with 0.625 pitch, with a rotation time of 1.5s, 4 overlapping slices ~1.3mm. The display field of view was 20x20 cm, pixel matrix 512x512 and ~90s acquisition time per series. Images were evaluated using Osirix v3.5.1[g] DICOM viewing software.

The native CT series showed the presence of an osseous fragment in the medial femorotibial joint (MFTJ) at the level of the meniscus. Several osseous fragments associated with the caudal and axial margin of the medial femoral condyle were also noted (Figure 4a). A focus of mineralisation was presented cranial to the intercondylar eminences of the tibia, which appeared to be within the cranial aspect of the MFTJ. The CT arthrography series showed that the fragment in the MFTJ was present between the medial femoral condyle and the proximal surface centrally on the caudal horn of the medial meniscus. There was a linear cartilage lesion on the medial femoral condyle (Figure 4b+d). After injection of the lateral femorotibial joint (LFTJ), the CT arthrography series showed contrast present within the caudal cruciate ligament (Figure 4c). No abnormalities were noticed in the CT arthrography study of the femoropatellar joint (FPJ).

Diagnosis and conclusion

During the initial trauma 2 weeks earlier, the caudal cruciate ligament was probably damaged, and a few fragments of the traumatic osteochondrosis (OC)-like lesion on the caudo-axial margin of the medial femoral condyle probably became loose.

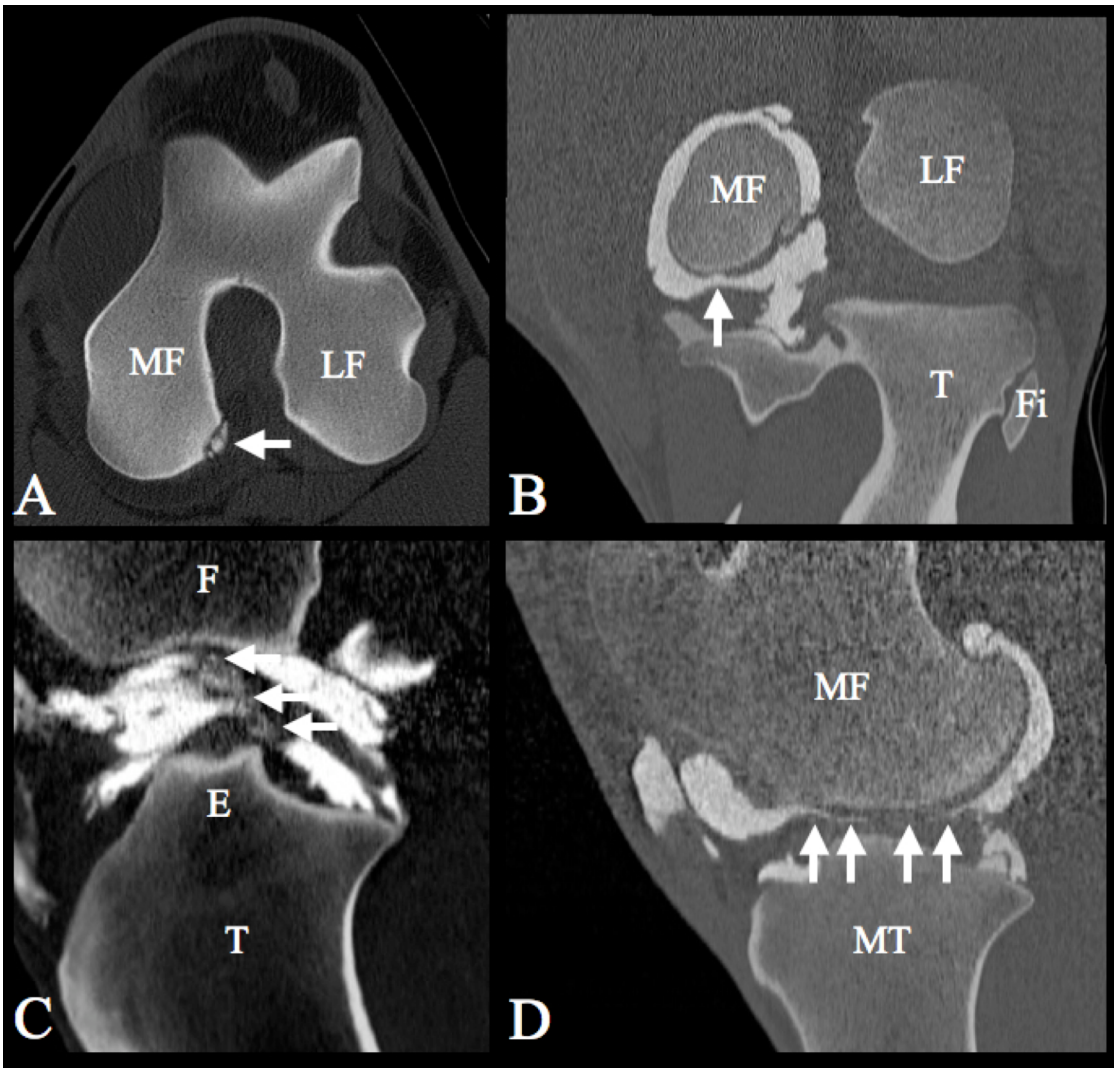

Figure 4: CT and CT arthrographic images of the left stifle. Medial is to the left and cranial is top (A and B). A) Transverse CT image shows a large traumatic OC-like lesion of the axial part of the caudal margin of the medial femoral condyle (arrow). Images B, C and D obtained after use of the multi-planar reformatting tool. B) Dorsal plane arthrographic image of the MFTJ, showing a cartilage defect that is filled-up with contrast (arrow). On images C and D cranial is to the left. C) Sagittal plane arthrographic image of the LFTJ, showing contrast present in the caudal cruciate ligament (arrows) and suggesting an injury of the ligament. D) Sagittal plane arthrographic image of the medial femoral condyle, the cartilage defect shown in Fig 3B seems to be a linear defect in the cartilage (arrows). E, intercondylar eminences of the tibia; F, femur; Fi, fibula; LF, lateral femoral condyle; MF, medial femoral condyle; MT, medial tibial condyle; T, tibia.

After this trauma, the pathology of the caudal cruciate ligament could have led directly to the horse's lameness. The large fragment in the MFTJ probably entered the stifle joint during the training movement, ending between the medial femoral condyle and the medial meniscus. Due to the pressure of the ligaments on the stifle joint and the weight of the horse, the fragment was pushed partially into the medial meniscus and also made a linear deformity in the cartilage of the medial femoral condyle. When the innervated subchondral bone was reached, the horse probably became painfully lame again. The damage in this stifle was untreatable. To our knowledge, there is no procedure for removing a fragment at this site in the medial meniscus and it was considered that the horse would remain permanently lame. The owner was advised of the poor prognosis and euthanasia was recommended and carried out.

Gross pathology

Gross pathology revealed a linear defect in the cartilage of the medial femoral condyle associated with a fragment (0.375 x 0.775 cm) that was partially pressed into the medial meniscus. This fragment appeared to have originated from the severe TRAUMATIC OC-like injury on the caudo-axial margin of the medial femoral condyle. A haemorrhagic tear was visible axially in the distal half of the

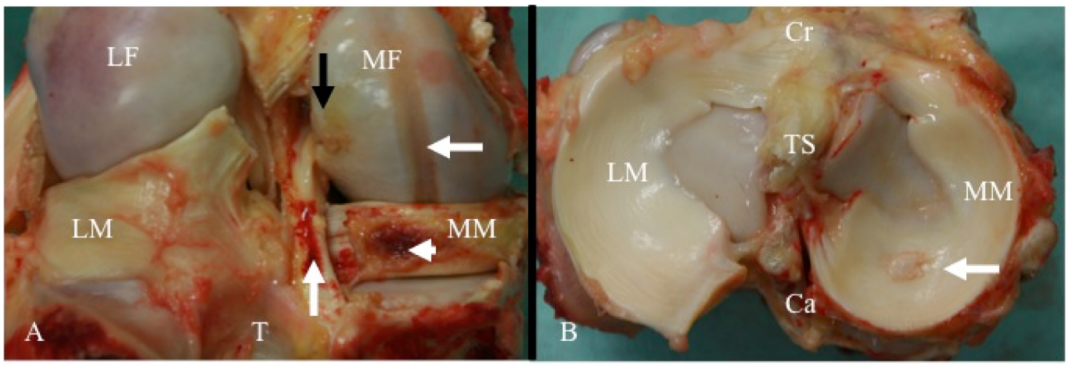

Figure 5: Gross pathology image. On these images, lateral is to the left and proximal or cranial to the top. A) The traumatic OC-like lesion (black arrow), the linear cartilage defect (horizontal arrow), the linear haemorrhagic tear in the caudal cruciate ligament (vertical arrow) and a superficial tear in the caudal tibial ligament of the medial meniscus (arrow point) are visible. B) A large fragment (arrow) is pressed in the caudal horn of the MM, this fragment caused the linear cartilage defect in the MF seen on image A. Ca, caudal; Cr, cranial; LF, lateral femoral condyle; LM, lateral meniscus; MF, medial femoral condyle; MM, medial meniscus; T, tibia; TS. intercondylar eminences of the tibia.

caudal cruciate ligament and the medial meniscus contained a superficial lesion on the caudal part of the meniscal tibial ligament (Figure 5a+b). Cranial to the intercondylar eminences of the tibia, some mineralisation's in the surrounding tissue were visible.

Discussion

The CT and CT arthrography examination in this case provided a diagnosis not achieved with other conventional imaging techniques. Radiography and ultrasonography were performed in this case, but they did not image all the injuries diagnosed with CT and CT arthrography. Arthroscopy was not used in this case, but the limitations of this technique do not allow a complete evaluation of all structures [11, 12].

The injured stifle presented multiple abnormalities diagnosed with CT and CT arthrography. Most important were the caudal cruciate ligament injury, the traumatic OC-like lesion on the caudo-axial margin of the medial femoral condyle, the osseous fragment in the MFTJ between the medial meniscus and the medial femoral condyle, and the injuries this fragment caused to the cartilage of the femoral condyle.

The gross pathology examination allowed the results of the different diagnostic imaging techniques to be compared. There were no indications of a chronic injury known, therefore the mineralisation's in the surrounding tissue cranial to the intercondylar eminences of the tibia probably also originated from the TRAUMATIC OC-like injury. During the gross pathology examination an extra osteochondrosis (OC) lesion was presented on the proximal medial femoral trochlea. This injury could be seen on one of the ultrasonographic images. However, this region was not included in the CT study due to the size of the horse, and since this OC lesion had no influence on the diagnosis, it was considered to be an incidental.

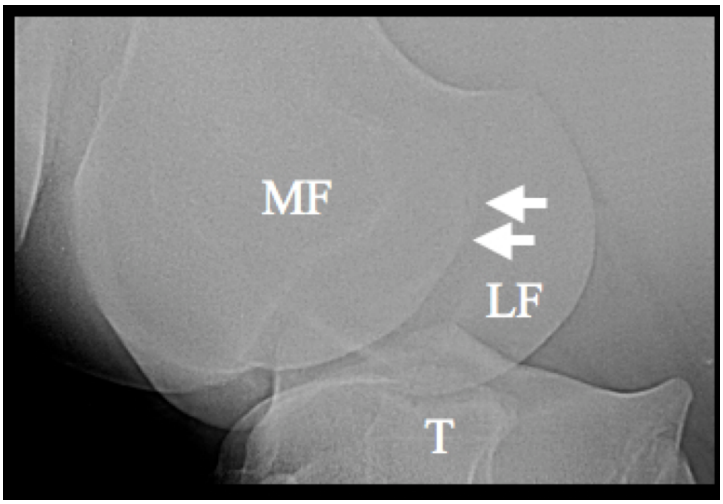

Figure 6: Craniolateral-caudomedial-oblique radiographic projection. On this image, the traumatic OC-like injury diagnosed in the CT examination, see Fig 4A (arrows), is visible. LF, lateral femoral condyle; MF, medial femoral condyle; T, tibia.

The additional injuries seen in the CT examination prompted the veterinarian to take 2 extra radiographs: the craniomedial-caudolateral-oblique and the craniolateral-caudomedial-oblique projections. Several attempts were necessary to image the lesions on the medial femoral condyle on the oblique projections (Figure 6) and it was considered that these lesions might not have been imaged even with an extensive radiographic examination.

Although arthroscopic surgery is used both to diagnose and treat stifle pathology, the limitations of this technique are that some intra-articular structures cannot be visualised and that only injuries starting at the surfaces of structures can be evaluated [6, 11, 12]. Performing a complete stifle arthroscopy is technically quite difficult because of the anatomy of the three compartments. Even with the new techniques only the cranial and caudal parts of the femorotibial joints can be examined, so a complete evaluation of the femorotibial joint is not possible. [11, 12]. Computed tomography and CT arthrography offer a complete view of subchondral and intra-articular pathologies [1, 5] and is less traumatic and risky than arthroscopic surgery on the stifle [11, 12]. Additional merits in comparison with arthroscopic surgery are the shorter examination and general anaesthesia time. The costs for an arthroscopic surgery of the three compartments, is also much higher than a CT examination.

Computed tomography and CT arthrography make it possible to visualise both bony and soft tissue. This technique is available for mature horses. But not all CT gantries are suitable for examinations of the stifle − in this case, the custom-made table made it possible to position the horse correctly [1]. However, the proximal part of the stifle could not be scanned because of the size of the horse in relation to the size of the gantry. However, this area can be well visualised by radiography and ultrasonography. The multi-slice CT provides overlapping cross-sectional images with very thin slices (~1.3 mm), which improves the resolution and quality of the images produced. These hardware improvements, in addition to multi-planar reformatting software improvements, are essential for a correct and complete evaluation of the stifle [1].

Magnetic Resonance Imaging (MRI) visualises soft tissue and cartilage [1]; and, in human medicine, this is the preferred technique for examination of the knee [13]. However, MRI is only experimental available for the stifle of the horse and there are no published or unpublished data available at this moment for a direct comparison.

Gross pathology examination of the stifle confirmed the injuries diagnosed by CT examination. Most interesting is the confirmation that only the caudal cruciate ligament was traumatised. The literature on cruciate ligament injuries in the equine stifle tells us that the cranial cruciate ligament is injured most often and that, if the caudal cruciate ligament is injured, this is usually in combination with the cranial cruciate ligament [14-16]. However, the AAEP Proceedings of Bergman et al. (2007) [1] describe five out of eight cases of cruciate ligament injuries, examined with CT and CT arthrography, with only caudal cruciate ligament injuries [1]. Not yet published data from a larger number of cases support this 50:50 proportion (E. Bergman personal communication: www.vetct.nl). The reason for these different results is not yet clear − over-diagnosis with CT or under-diagnosis with the other imaging techniques are possible causes. Further research on this subject is necessary especially the validation of CT findings at post mortem.

More cases need to be examined and knowledge of image interpretation needs to grow before CT can be fully evaluated and appreciated for its added value in lameness diagnostics. Therefore, CT should be used only as a corollary to clinical

examination and other diagnostic imaging modalities. As is the case in human medicine, the trend for the future in veterinary medicine will be for more precise and thorough diagnosis. Therefore, the use of CT is likely to increase.

Acknowledgement:

We would like to thank Dr J. Walmsley for consulting on this article to prepare it for publication.

Footnotes

[a]Aloka Alpha 10, Germany Aloka GmbH, Meerbusch, Germany.

[b]ATL HDI 3000, Philips, Eindhoven, The Netherlands.

[c]Dormicum, Roche Nederland, Woerden, The Netherlands.

[d]Eurovet, Bladel, The Netherlands.

[e]Ketamine, AST Pharma, Oudewater, The Netherlands.

[f]Optiray 300, 30 mg iodine/ml, Mallinckrodt, Petten, The Netherlands.

[g]OsiriX, Open Source, www.osirix-viewer.com.

[h]Philips Mx8000 Quad multislice CT scanner, Philips, Eindhoven, The Netherlands.

References

1. Bergman, E.H.J. and Puchalski, S.M. (2008) Computed tomography and CT arthrography of the equine stifle. In: *European Veterinary Conference Voorjaarsdagen*. pp 295-297.

2. Bindeus, T., Vrba, S., Gabler, C., Rand, T. and Stanek, C. (2002) Comparison of computed radiography and conventional film-screen radiography of the equine stifle. *Vet Radiol Ultrasound* **43**, 455-460.

3. Latimer, F.G., Pasquini, C. and Kaneps, A.J. (2000) Stifle disease in horses. *Comp Cont Educ Pract* **22**, 381-390.

4. Maulet, B.E.B., Mayhew, I.G., Jones, E. and Booth, T.M. (2005) Radiographic anatomy of the soft tissue attachments of the equine stifle. *Equine Vet J* **37**, 530-535.

5. Tietje, S. (1997) Computed tomography of the stifle region in the horse: a comparison with radiographic, ultrasonographic and arthroscopic evaluation. *Pferdeheilkunde* **13**, 647-658.

6. Walmsley, J.P. (2005) Diagnosis and treatment of ligamentous and meniscal injuries in the equine stifle. *Vet Clin N Am-Equine* **21**, 651-672.

7. De Busscher, V., Verwilghen, D., Bolen, G., Serteyn, D. and Busoni, V. (2006) Meniscal damage diagnosed by ultrasonography in horses: A retrospective study of 74 femorotibial joint ultrasonographic examinations - (2000-2005). *J Equine Vet Sci* **26**, 453-461.

8. Hoegaerts, M., Nicaise, M., van Bree, H. and Saunders, J.H. (2005) Cross-sectional anatomy and comparative ultrasonography of the equine medial femorotibial joint and its related structures. *Equine Vet J* **37**, 520-529.

9. Koneberg, D.G. and Edinger, J. (2007) Three-dimensional ultrasonographic in vitro imaging of lesions of the meniscus and femoral trochlea in the equine stifle. *Vet Radiol Ultrasound* **48**, 350-356.

10. Stashak, T.S. and Adams, O.R. (2002) *Adams' lameness in horses*, 5th edn., Lippincott Williams & Wilkins, Philadelphia. p 1174.

11. Muurlink, T., Walmsley, J., Young, D. and Whitton, C. (2009) A cranial intercondylar arthroscopic approach to the caudal medial femorotibial joint of the horse. *Equine Vet J* **41**, 5-10.

12. Watts, A.E. and Nixon, A.J. (2006) Comparison of arthroscopic approaches and accessible anatomic structures during arthroscopy of the caudal pouches of equine femorotibial joints. *Vet Surg* **35**, 219-226.

13. Vande Berg, B.C., Lecouvet, F.E., Poilvache, P., Maldague, B. and Malghem, J. (2002) Spiral CT arthrography of the knee: technique and value in the assessment of internal derangement of the knee. *Eur Radiol* **12**, 1800-1810.

14. Robinson, N.E. and Sprayberry, K.A. (2009) *Current therapy in equine medicine*, 6th edn., Saunders Elsevier, St. Louis, Mo. p 1066.

15. Rose, P.L., Graham, J.P., Moore, I. and Riley, C.B. (2001) Imaging diagnosis - caudal cruciate ligament avulsion in a horse. *Vet Radiol Ultrasound* **42**, 414-416.

16. Sandersshamis, M., Bukowiecki, C.F. and Biller, D.S. (1988) Cruciate and collateral ligament failure in the equine stifle - 7 cases (1975-1985). *J Am Vet Med Assoc* **193**, 573-576.

CHAPTER SIX

Intra-Arterial Versus Intravenous Contrast-Enhanced Computed Tomography of the Equine Head

Casper P. Crijns[1], Yseult Baeumlin[2], Lieve De Rycke[1], Bart J.G. Broeckx[3], Lieven Vlaminck[4], Erik H.J. Bergman[5], Henri J.J. van Bree[1], Ingrid M.V.L. Gielen[1]

[1] *Department of Medical Imaging and Small Animal Orthopaedics, Ghent University, 9820 Merelbeke, Belgium*
[2] Tierärztliches Überweisungszentrum, Tenniken, Switzerland
[3] *Department of Pharmaceutical Sciences, Ghent University, 9000 Gent, Belgium*
[4] *Department of Surgery and Anaesthesiology of Domestic Animals, Ghent University, 9820 Merelbeke, Belgium*
[5]*Lingehoeve Diergeneeskunde, 4033 AK Lienden, The Netherlands*

Adapted from:

Casper P. Crijns, Yseult Baeumlin, Lieve De Rycke, Bart J.G. Broeckx, Lieven Vlaminck, Erik H.J. Bergman, Henri J.J. van Bree, Ingrid M.V.L. Gielen. Intra-arterial versus intra venous contrast-enhanced computed tomography of the equine head *(published in BMC Veterinary Research (2016)* ***12*** *(6))*

Summary

The anatomical complexity of the horse's head limits the abilities of radiography. Computed tomography (CT) in combination with contrast-enhanced CT is used more often for diagnosing various head pathology in horses. The objective of this study was to compare intravenous (IV) and intra-arterial (IA) contrast-enhancement techniques and describe normal and abnormal contrast enhancement in the horse's head. 24 horses that underwent a diagnostic IV (n=12) or IA (n=12) contrast-enhanced CT of the head were included in the study. All horses recovered without complication from the procedures. Compared to the pre-contrast studies, post-contrast studies showed significant contrast enhancement in the pituitary gland (IA: $p<0.0001$; IV: $p<0.0001$), nose septum (IA: $p=0.002$), nose mucosa (IA: $p<0.0001$; IV: $p=0.02$), parotid salivary gland (IA: $p<0.0001$; IV $p<0.0001$), cerebrum (IA: $p<0.0001$; IV: $p<0.0001$), longus capitis muscle (IA: $p<0.0001$; IV $p=0.001$), temporal muscle (IA: $p<0.0001$), masseter muscle (IA: $p <0.0001$) and brainstem (IV: $p=0.01$). No significant contrast enhancement was seen in the eye (IA: $p=0.23$; IV $p=0.33$), tongue (IA $p=0.2$; IV $p=0.57$), brainstem (IA: $p=0.88$), nose septum (IV: $p=0.26$), temporal muscle (IV: $p=0.09$) and masseter muscle (IV: $p=0.46$). Three different categories of abnormal enhancement were detected: a strong vascularised mass, an enhanced rim surrounding an unenhanced structure and an inflamed anatomical structure with abnormal contrast enhancement.

In conclusion, using the intra-arterial technique, similar contrast enhancement is achieved using less contrast medium compared to the intravenous technique. Using the intravenous technique, a symmetrical and homogenous enhancement is achieved, however timing is more crucial and the contrast dosage is more of influence in the IV protocol. Knowing the different normal contrast enhancement patterns will facilitate the recognition of abnormal contrast enhancements.

Introduction

Radiography is a primary ancillary imaging modality for the evaluation of the horse's head. However, due to anatomical complexity and superimposition of tissues of the head, the interpretation of the radiographs remains difficult [1]. The tomographic ability to produce reconstructed images allows computed tomography (CT) compared to radiography to excel in depicting the complex anatomical structures of the head [2].

Normal CT anatomy of the horse's head has been described in foals [3] and in adult horses [4]. In horses, CT of the head has been used for the diagnosis of sinusitis, alveolitis and apical infection of the cheek teeth [5, 6], mandibular, nasal and paranasal tumours and cysts [7-9], ethmoid hematoma [10], parapharyngeal aneurysm [11], fractures [12-14], temporohyoid osteopathy [12], neurologic [15] and intracranial disorders such as abscesses [16], acute haemorrhage and other space-occupying masses [13, 17], and is routinely performed in such cases. Contrast media are used to perform contrast-enhanced CT examinations to accurately locate masses in the head, fully depict the extension of space occupying diseases in these areas and help plan the surgical approach [7, 18, 19]. Contrast enhancement CT after intravascular contrast medium administration is based on the principle of an increased opacity in (neo-) vascularised structures and extra-vascular structures in comparison to the native CT study [20, 21]. In small animals, contrast-enhanced CT of the head is common practice following an intravenous route of contrast administration [22-25]. Contrast-enhanced CT helps in these cases to differentiate normal soft tissues from lesions in the soft tissues as soft tissue lesions show an alteration in their blood flow and/or have an altered vascular permeability [26].

In horses, two routes of intravascular contrast injection have been reported. The most common is the total body systemic intravenous (IV) route as described in small animals. A systemic bolus of contrast medium is administered intravenously; the contrast medium will pass the heart first and will be diluted before reaching the region of interest. In small animals a protocol of 2 mL/kg body weight (~600 mgI/kg body weight) of intravenous contrast medium injected at a rate of 2mL/s has been established [22, 24, 25]. For horses this protocol is costlier and impractical due to the

large volume that needs to be injected. In the equine literature several protocols with a wide range of volumes and dosages (250-400 mL of 350-370 mgI/mL or about 160-250 mgI/kg body weight) have been described for horses [9, 13, 27]. A second route is intra-arterial (IA) contrast-enhanced CT, which has been described to characterise distal limb conditions [20, 21] and more recently has been presented for the horse's head [28]. The advantage of the direct route of intra-arterially administration of contrast medium is a local high vascular concentration in the region of interest. In the publications a standardised protocol using continuous IA infusion at a rate of 2 mL/s while scanning an entire volume (the distal limb or the head) beginning 3 s before initiation of the CT scan, injecting a volume of less than 200mL is described [20, 21, 28].

The first purpose of the current study is to describe and compare the normal contrast enhancement of the soft tissue structures after systemic IV and direct IA administration of contrast medium. The second purpose is to describe the differences in abnormal contrast enhancement between the two techniques. We hypothesised that 1) after IV or IA contrast administration, post-contrast CT images show significant enhancement of the selected soft tissue structures compared to the pre-contrast CT images, 2) while using less contrast medium with the IA technique, a similar or higher contrast enhancement will be obtained as with the IV technique and 3) both technique would allow to detect some specific abnormal contrast enhancement patterns.

Materials and Methods

Study design

Retrospective comparative clinical study, ethical committee oversight is currently not required for this type of study.

Cases

Case records were reviewed for horses, which underwent for different clinical reasons a diagnostic native CT and intravascular (IV or IA) contrast-enhanced CT evaluation of the head. All horses that underwent IA contrast-enhanced CT were

included. A selection of IV contrast-enhanced cases was made based on the presence of a complete CT evaluation of the head.

Computed tomographic examination

CT scans of the head were acquired with the horses under general anaesthesia. Each horse was sedated using detomidine[a] (0,005 mg/kg IV) as a premedication. Anaesthesia was induced with a combination of ketamine[b] (2,2 mg/kg, IV) and midazolam[c] (0,06 mg/kg, IV). After intubation, anaesthesia was maintained with inhaled isoflurane[d] and oxygen (on effect, ±1,2% expiratory). Vital parameters like heart rate, ECG, respiratory rate and respiratory curve were monitored continuously. The horses were positioned in dorsal recumbency with the head in the gantry. Images were acquired with two fourth generation 4-slices helical CT scanners (Lingehoeve Equine Clinic: Philips Mx8000 Quad multislice CT scanner[e]; Ghent University: GE Medical Systems Prospeed four slice[f]) using the in-house protocols for equine head imaging (Lingehoeve Equine Clinic: 120 kV, 185 mAs, pitch 1, 1,3 mm slices, 512x512 matrix, scan FOV 293-463 mm, sharp algorithm; Ghent University: 120 kV, 160 mAs, pitch 1, 1,25-2,5 mm slices, 512x512 matrix, scan FOV between 192-403 mm, bone and standard algorithm). A pilot study was performed first to assess the symmetric position of the horse's head in the gantry, followed by pre- and post-contrast CT studies in all horses.

IA contrast protocol

IA contrast-enhanced CT studies were performed after aseptic ultrasound guided (7,5mHz linear probe) catheterisation (14-gauge x 80 mm) of one of the common carotid arteries in the mid to caudal cervical region through the skin, with the bevel directed towards the heart. The common carotid artery was located deep to the jugular vein and colour Doppler helped to confirm the arterial nature of the blood vessel. The catheter was introduced through the thick wall of the carotid artery in one fast and strong movement. The catheter was fixed to the skin with polypropylene sutures. A three-way stopcock and an extension set were attached to the catheter to facilitate injection. The extension set was prefilled with contrast medium before attaching to the catheter. A pressure injector containing 250ml of non-ionic iodinated contrast medium was connected to the extension set. A

continuous arterial infusion protocol during scanning was used, with an injection rate of 2 mL/s (total volume injected <180mL) of Ioversol 350 mgI/mL (Optiray®350[g]). The post-contrast scan was initiated with a 3s delay from the start of the contrast medium administration. The intra-arterial catheter was removed at the end of the procedure and a 5-minute manual compression was applied to avoid bleeding and hematoma formation. Then a bandage with moderate compression was placed around the neck at the site of injection for the time of the recovery.

IV contrast protocol

IV contrast-enhanced CT studies were performed after blind catheterisation (18 gauge x 80 mm) of one of the cephalic veins in the thoracic limbs, with the bevel directed away from the heart. The catheter was fixed to the skin with cyanoacrylate adhesive. Two pressure injectors containing 200 ml of non-ionic iodinated contrast medium were connected to an extension set. The extension set was prefilled with contrast medium before attaching to the catheter. A systemic bolus of 400 mL of Iobitridol 350 mgI/mL (Xenetix®350[h]) was injected at a rate of 15 mL/s. The post-contrast scan was initiated about 30 s after the start of the contrast medium administration. After removal of the catheter a bandage with moderate compression was placed around the limb at the site of injection for the time of the recovery.

Image analysis

Image analysis was performed separately by two of the authors on a dedicated diagnostic imaging viewing station with a 2880x1800 pixel flat screen monitor using Osirix[i] DICOM viewer software. Images were reviewed using a soft tissue (window wide (WW): 200-400 Hounsfield Unit (HU); window level (WL): 40-100 HU) and a bone window (WW: 2000 HU; WL: 750 HU). The post-contrast images were evaluated using a soft tissue window to review the normal pattern of contrast enhancement and to describe the abnormal enhancement due to pathology. A semi-quantitative grading scale was used to describe (abnormal-) contrast enhancement in the different soft tissue structures: none (no enhancement), mild (minimal enhancement), moderate (apparent enhancement) and severe (obvious enhancement).

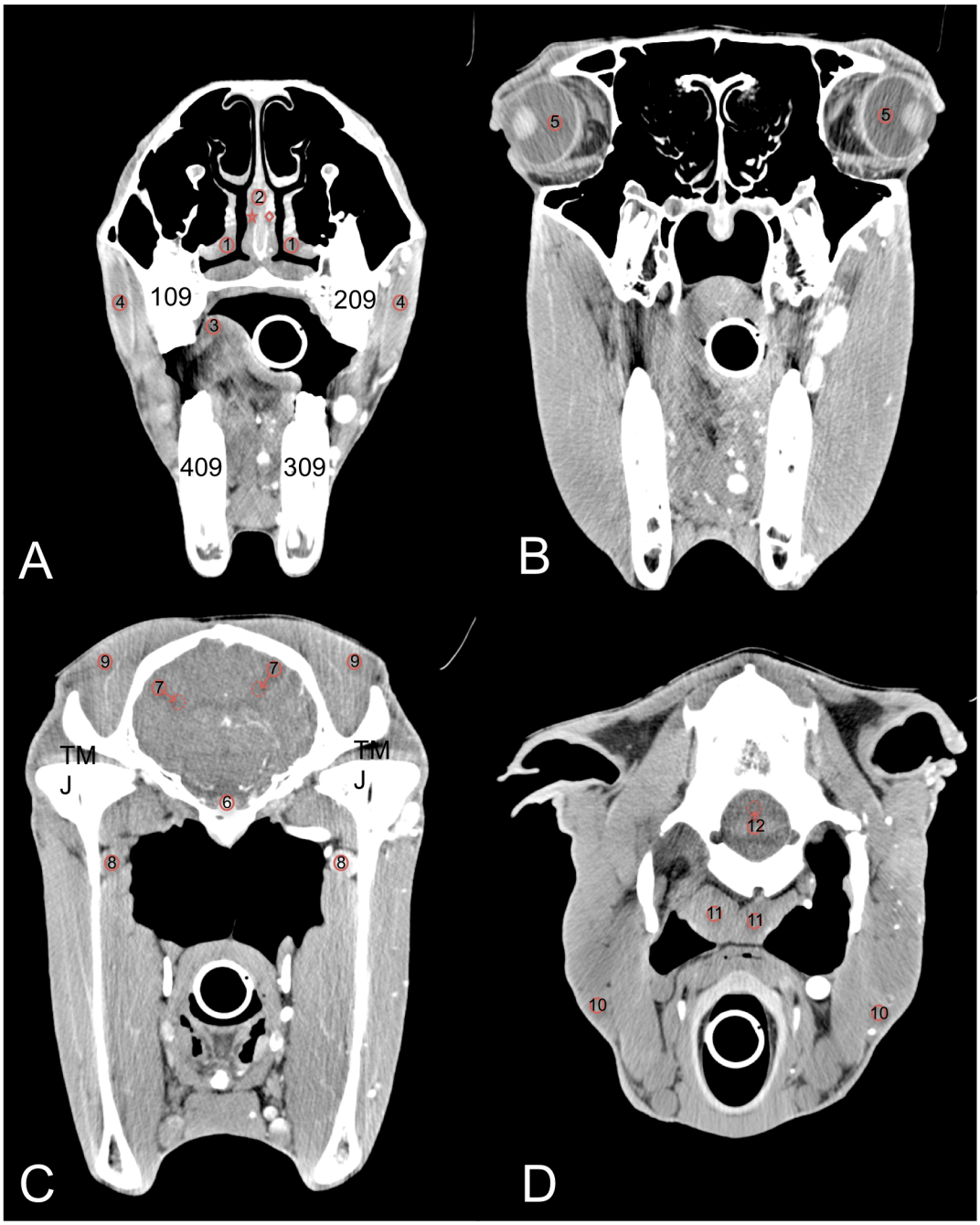

Figure 1: Transverse IA contrast-enhanced CT images of the equine head (right is to the left and dorsal is to the top). A) At the level of the 09's, ROI's are placed on the epithelial lining of the ventral nasal conchae (1), the nasal septum (2), the tongue (3) and the masseter muscles (4). Note the homogeneous (star) and inhomogeneous and patchy (diamond) enhancement pattern in the nasal septum. B) At the level of the eyes, ROI's are placed on the corpora vitrea (5). C) At the level of the temporo-mandibular joints, ROI's are placed on the pituitary gland (6), the cerebral cortex (7), the maxillary veins (8) and the temporal muscles (9). D) At the level of foramen magnum, ROI's are placed on the parotid salivary gland (10), the longus capitis muscles (11) and the brainstem (12). Note the different ROI's placed on the grey matter (circle) and white matter (doted circle) of the cerebrum and brainstem in figures C and D.

Figure 2: Transverse IV contrast enhanced CT images of the equine head (right is to the left and dorsal is to the top). A) At the level of the 09's, ROI's are placed on the epithelial lining of the ventral nasal conchae (1), the nasal septum (2), the tongue (3) and the masseter muscles (4). Note the air opacities (star) in the mild enhancing and swollen right masseter muscles. B) At the level of the eyes, ROI's are placed on the corpora vitrea (5). C) At the level of the temporo-mandibular joints, ROI's are placed on the pituitary gland (6), the cerebral cortex (7), the maxillary veins (8) and the temporal muscles (9). D) At the level of foramen magnum, ROI's are placed on the parotid salivary gland (10), the longus capitis muscles (11) and the brainstem (12). Note the rim enhancement (arrows) surrounding a hypodense retropharyngeal abscess (diamond).
Note the different ROI's placed on the grey matter (circle) and white matter (doted circle) of the cerebrum and brainstem in figures C and D.

Circular semi-automatic regions-of-interest (ROI's) (size: ~0,5 cm^2) were manually placed on predefined normal soft tissue structures on the contrast-enhanced images, as illustrated in Figure 1 and Figure 2 using the sharp (IA studies) and standard (IV studies) algorithm. To increase to repeatability of the ROI placement, only easily identifiable soft tissue structures were reviewed in this study, on which the ROI's could be placed completely isolated from adjacent structures. To ensure that the ROIs contained mainly the parenchyma of the soft tissue structures, we avoided inclusion of macroscopic vessels visible in the structures. The areas of interest in the soft tissue structures were selected on 4 different transverse slides. The most rostral selected slide at the level of the first molars (Figure 1a and Figure 2a), allowed reviewing the epithelial lining of the nasal conchae, the nasal septum and the tongue as well as the body of the masseter muscle. On the second slide, at the mid-level of the orbita the corpus vitreum of the eyes was reviewed (Figure 1b and Figure 2b). The third slide was selected at the level of the temporomandibular joint (Figure 1c and Figure 2c), as at this level the pituitary gland is anatomically situated, allowing the review of the pituitary gland, the cerebral cortex, the maxillary vein and the body of the temporal muscle. The most caudal slide was selected at the level of foramen magnum: the brainstem, the parotid salivary gland and the body of the longus capitis muscle are easily identified at this level (Figure 1d and Figure 2d). To assure the ROI's on the pre- and post contrast images were incorporating the same tissue, the ROI's were copied and pasted to the pre-contrast images. The mean value registered in each ROI separately was recorded and used for the quantification of contrast enhancement in the selected normal soft structures. If structures were not incorporated in the CT study due to a partial study of the head or if a structure was obliterated by pathology e.g. due to a mass effect, ROI's were not placed on these structures.

Statistical analysis

A mixed model analysis was conducted for each separate anatomical structure (dependent variable)[j]. Independent fixed effects were the effect of observer (one or two), contrast medium (yes or no), route of contrast medium administration (IV or IA) and, if the structure was measured bilaterally, asymmetry (side of the catheter or contralateral side). The patients were included in the analysis as random effect. Homoscedasticity and normality of residuals were visually checked using residuals versus fitted plots and QQ plots. If necessary, power transformations were applied, using a Box-Cox plot for guidance. A P-value <0,05 (linear mixed model) was considered significant.

Results

Eleven Warmblood horses and 1 Arabian horse that underwent IA contrast-enhanced CT of the head at Lingehoeve Equine Clinic were identified, 7 geldings, 3 mares and 2 stallions, median age of 8,5 years (range between 1 and 18 years). A group of 12 horses (10 Warmblood horses, 1 trotter and 1 pony) that underwent IV contrast-enhanced CT evaluation of the complete head at the Department of Medical Imaging of the Faculty of Veterinary Medicine of Ghent University were selected for the study. Four geldings, 7 mares and 1 stallion, median age 14 years (range between 4 and 25 years), median weight 540 kg (range between 375 and 695 kg).

The CT diagnoses of the included cases were: apical infections in combination with secondary sinusitis (n=6), ethmoid hematoma (n=4), sinus cyst (n=3), mass/neoplasm (n=2), inflammatory/infectious disease (n=2), traumata (n=1) bilateral temporohyoid osteoarthropathy (n=1) and no diagnosis (n=5) (Table 1).

The first attempt of catheterisation of the common carotid artery, in the first patient included in the study, was not fully successful leading to hematoma formation. The reason of the hematoma formation was a hesitant introduction of the catheter through the thick arterial wall and probably dissection of the wall with leakage of blood from the arterial lumen. The procedure was still pursued and no harmful side effects were observed for the patient.

Case	Breed	Age	Sex	Reason to perform the scan	IV / IA	Diagnosis	Enhancement
1	WB	17	G	Intermittent unilateral epistaxis	IA 2mL/s	No significant abnormalities	x
2	WB	8	M	Headshaking	IA 2mL/s	Widened infraorbital canal, remaining tooth fragments	x
3	WB	4	G	Unilateral nasal discharge	IA 2mL/s	Ectopic tooth, apical infection	x
4	WB	1	M	Facial swelling, difficulty breathing	IA 2mL/s	Sinus cyst	Mild enhancement of the capsule
5	WB	4	G	Facial swelling, unilateral nasal discharge	IA 2mL/s	Inflammatory/infectious disease with intra-cranial extension	Irregular enhancement of the trigeminal nerve and soft tissue enhancements surrounding the osteolysis
6	Arabian	11	S	Soft tissue mass soft palate	IA 2mL/s	Squamous cell carcinoma	Heterogeneous enhancement of the mass
7	WB	14	G	Swelling behind left mandible	IA 2mL/s	Soft tissue mineralisation's, bilateral TMJ disease,	x
8	WB	18	S	Bilateral sinusitis	IA 2mL/s	Progressive ethmoidal hematoma	Very mild enhancement
9	WB	8	M	Infectious process	IA 2mL/s	Fractured right external acoustic meatus	x
10	WB	9	G	Opacity in the frontal sinus	IA 2mL/s	Sinus cyst	x
11	WB	6	G	Unilateral nasal discharge	IA 2mL/s	Apical infection, tooth fracture and secondary sinusitis	x
12	WB	1	G	Facial swelling, unilateral nasal discharge	IA 2mL/s	ameloblastoma	x
13	WB	10	M	Epistaxis after surgery	IV 241 mgI/kg	Subcutaneous emphysema	x
14	WB	19	M	Study	IV 305 mgI/kg	No significant abnormalities	x
15	Trotter	22	G	Unilateral nasal discharge with decreased air passage	IV 281 mgI/kg	Progressive ethmoidal hematoma with secondary sinusitis	Adjacent mucosal enhancement
16	WB	8	M	Unilateral nasal discharge	IV 216 mgI/kg	Apical infection with abscess	Mild enhancement of the capsule
17	WB	16	M	Intermitted unilateral epistaxis	IV 311 mgI/kg	Progressive ethmoidal hematoma	Very mild enhancement
18	WB	9	G	Difficulty breathing	IV 252 mgI/kg	Sinus cyst	Mild enhancement of the capsule
19	Pony	4	S	Facial swelling	IV 373 mgI/kg	Alveolitis	x
20	WB	25	G	Intermitted unilateral epistaxis	IV 201 mgI/kg	Progressive ethmoidal hematoma	Rim enhancement
21	WB	10	M	Unilateral nasal discharge	IV 219 mgI/kg	Alveolitis with secondary sinusitis	x
22	WB	16	M	Epilepsy	IV 257 mgI/kg	No significant abnormalities	x
23	WB	9	M	Epilepsy	IV 260 mgI/kg	No significant abnormalities	x
24	WB	22	G	Maxillary swelling	IV 279 mgI/kg	Inflammation of the right masseter musc. With abcess	Mild homogeneous enhancement of the musc and rim enhancement surrounding an abcess

Table 1: Anamnesis of the horses included in the study, contrast administration protocol used and final (CT) diagnosis.

All horses recovered without complications, no adverse reactions on the contrast medium administrated or administration technique were observed in the included patients.

Normal contrast enhancement

IA protocol

During the IA injection of contrast medium, there was moderate to severe contrast enhancement of the maxillary veins (Table 2). In this group, the contrast enhancement was asymmetrical between injection side and the contralateral side in all cases (Figure 1 and 3). In the maxillary veins ipsilateral to the side of intra-arterial injection, part of the contrast medium was seen pooling along the dependant wall of the vein creating a layered and partial severe contrast enhancement in the lumen of the vein in 7 of the 12 cases. In 4 of these patients this layer of non-mixed contrast medium occupied about 50% of the lumen. In the other 3 patients the layer of contrast medium occupied about 25% of the lumen of the vein. In the maxillary vein contralateral to the side of injection, no such dependant contrast medium layer was detected in any case. Enhancement in this vein was considered moderate and homogeneous (Table 2, Figure 3).

Mild to moderate contrast enhancement was seen and measured for the pituitary gland ($p<0.0001$), nose septum ($p=0.002$), nose mucosa ($p<0.0001$) and parotid salivary gland ($p<0.0001$) (Table 2). Two different enhancement patterns of the nose septum and nose mucosa were observed in the included cases. In 7 cases the enhancement was mild, homogeneous and symmetrical. In 2 cases the enhancement was inhomogeneous, patchy and not always symmetrical (Figure 1).

On the post-contrast scans the cerebral arteries became asymmetrical and more clearly visible on the ipsilateral side of injection during IA contrast administration (Figure 1). The cerebrum showed only none to mild contrast enhancement ($p<0.0001$) (Table 2). None to mild contrast enhancement was also only measured, but not detected while visually reviewing the cases for the longus capitis muscles ($p<0.0001$), temporal muscles ($p<0.0001$) and masseter muscles ($p=0.001$) (Table 2).

No significant contrast enhancement was detected in the corpus vitreum (p=0.23), the brainstem (p=0.88) and the tongue (p=0.12) (Table 2).

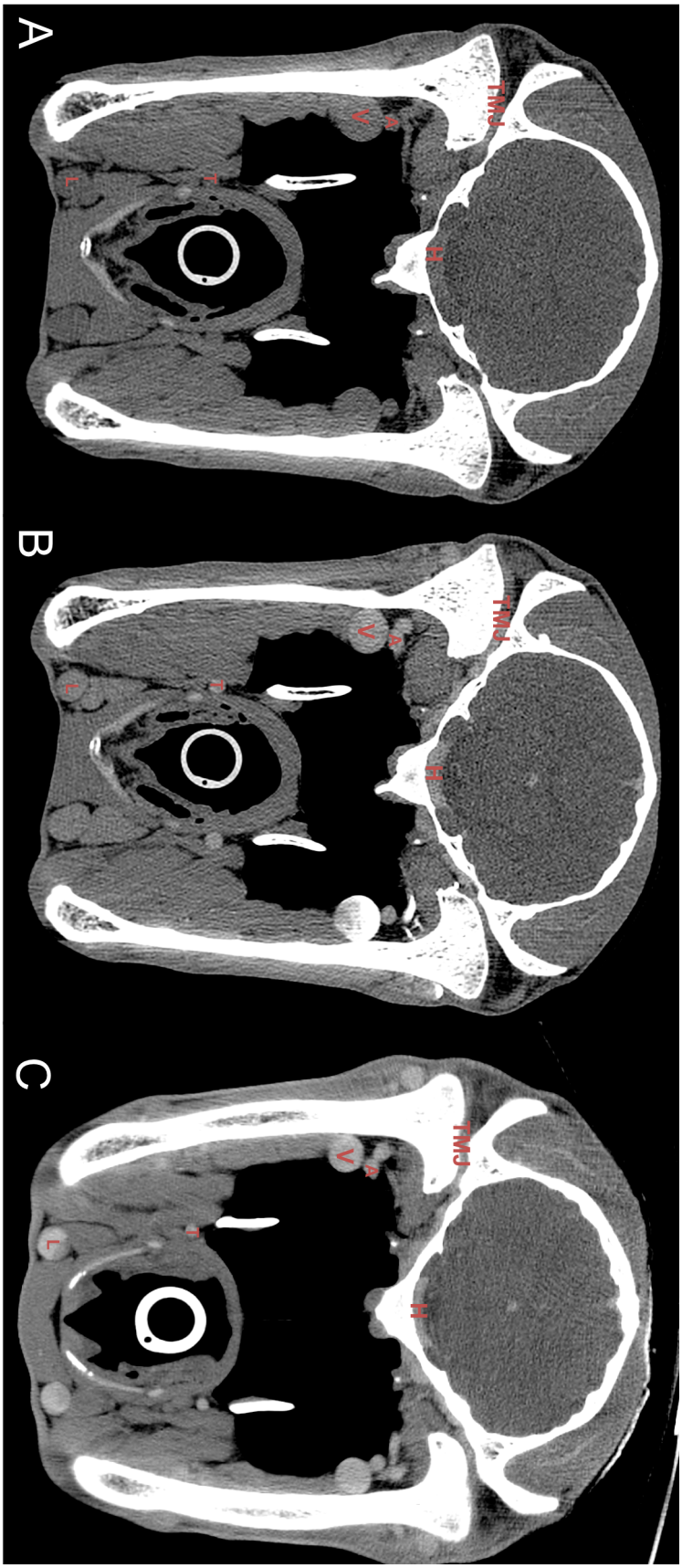

Figure 3: Transverse pre-contrast (A), IA post-contrast (B) and IV post-contrast (C) CT images at the level of the temporo-mandibular joints (right is to the left and dorsal is to the top). A) The visibility of the vascular structures are less clear defined compared to the post-contrast images, especially the smaller arterial structures (A and T) are more difficult to distinguish from the surround soft tissue. B) Bilateral contrast-enhancement after unilateral left-sided intra-arterial contrast injection is clearly delineating the vascular structures; contrast streaming is seen in the left maxillary vein. C) Homogenous, bilateral contrast-enhancement of the arterial and venous vascular structures after intra-venous contrast injection. TMJ: temporomandibular joint; H: pituitary gland; A: maxillary artery; V: maxillary vein; T: truncus linguofacialis; L: linguofacial vein.

Structure	Injection Side	Intravenous Protocol			Intra-arterial Protocol		
		n	Pre-Contrast (HU)	Post-Contrast (HU)	n	Pre-Contrast (HU)	Post-Contrast (HU)
Maxillary vein	Ipsilat.	12	63.8(34.9-90.7)	109.7(81.3-146.5)	12	62.3(43.2-97.1)	307.9(91.8-2587.6)
	Contralat.	12	63.0(36.7-97.8)	104.3(67.9-151.4)	12	61.0(48.7-80.7)	112.6(66.6-241.4)
Pituitary gland	N/A	12	47.5(38.5-66.6)	78.7(58.6-100.0)*	12	57.2(34.7-108.0)	83.8(56.5-182.2)*
Nose septum	N/A	9	68.5(32.5-115.0)	81.9(61.9-120.9)	11	67.6(50.5-108.1)	97.3(63.2-142.4)*
Nose mucosa	Ipsilat.	9	64.0(24.8-134.5)	83.7(23,3-142.5)*	10	48.2(40.0-92.4)	77.7(40.9-125.5)*
	Contralat.	8	63.2(14.4-128.6)	89.8(36.3-127.3)*	10	56.6(27.3-98.6)	86.1(30.3-148.0)*
Parotis salivary gland	Ipsilat.	12	44.7(24.3-61.1)	62.0(37.6-97.7)*	8	42.0(32.4-55.5)	62.9(37.2-95.6)*
	Contralat.	12	47.7(32.9-61.7)	66.3(37.8-110.5)*	8	43.7(33.7-53.8)	65.5(32.3-93.7)*
Cerebrum	Ipsilat.	12	40.0(30.5-55.0)	41.4(29.8-56.4)*	12	38.2(31.4-53.8)	45.7(33.2-64.4)*
	Contralat.	12	40.5(30.2-53.0)	44.8(31.4-56.1)*	12	38.7(30.4-67.0)	45.8(35.2-91.1)*
Longus capitis musc.	Ipsilat.	12	46.3(19.6-59.8)	52.1(23.6-65.1)*	8	52.2(30.7-58.9)	57.3(43.5-95.3)*
	Contralat.	12	50.8(32.9-66.4)	54.6(36.0-67.1)*	8	51.1(35.7-57.8)	62.0(50.3-83.9)*
Temporal musc.	Ipsilat.	12	66.5(47.7-87.7)	69.3(50.0-91.8)	12	68.4(46.9-81.7)	73.7(59.4-91.0)*
	Contralat.	12	66.1(44.6-79.6)	67.8(49.8-97.0)	12	67.3(47.3-76.6)	75.3(55.2-92.0)*
Masseter musc.	Ipsilat.	9	79.4(50.8-125.8)	85.3(53.5-140.0)	11	85.5(55.6-98.6)	91.0(67.8-154.5)*
	Contralat.	9	79.3(55.5-128.6)	83.0(59.8-129.0)	11	84.7(52.4-105.4)	84.9(59.7-149.6)*
Corpus vitreum	Ipsilateral	11	14.9(4.2-25.9)	15.7(8.3-25.8)	11	9.7(2.7-20.9)	11.2(3.3-24.8)
	Contralat.	12	15.3(4.6-28.8)	14.8(5.6-23.4)	11	8.7(2.8-21.0)	8.5(1.5-39.8)
Brainstem	N/A	12	44.7(31.6-64.4)	48.3(33.6-67.4)*	8	39.8(23.0-68.0)	40.0(21.5-75.2)
Tongue	N/A	9	55.7(23.2-103.2)	62.2(24.4-107.4)	11	48.4(17.8-78.4)	56.3(27.7-81.2)

Table 2: The median and range of the HU measurements of the different structures, ipsilateral and contralateral of the injection site, on the pre- and post-contrast CT images for the intravenous and intra-arterial protocols. n = amount of structures measured; HU = Hounsfield Unit; * = Significant increase in contrast enhancement between pre- and post contrast scans

IV protocol

After IV injection of contrast medium, moderate, homogeneous and symmetric enhancement between the right and left maxillary veins in all cases, independently of the catheter side was detected (Figure 2 and 3) and measured (Table 2).

Mild to moderate contrast enhancement was seen and measured for the pituitary gland ($p<0.0001$), nose mucosa ($p=0.02$) and parotid salivary gland ($p<0.0001$) (Table 2). In most horses' mild to moderate contrast enhancement was only seen and measured in the nose septum, but this enhancement was not significant ($p=0,26$) in the entire group. Two different enhancement patterns of the nose septum and nose mucosa were also observed in this group. In 7 cases the nose mucosa and in 5 cases the nose septum showed mild, homogeneous and symmetrical enhancement (Figure 2). In 4 cases the enhancement was inhomogeneous, patchy and not always symmetrical. And in 2 cases the nose septum showed no clear enhancement.

On the post-contrast scans the cerebral arteries became mild and symmetrical visible after IV injection of contrast medium (Figure 2). The cerebrum was only none to mild contrast enhancing ($p<0.0001$) (Table 2). None to mild contrast enhancement was also only measured, but not detected while visually reviewing the cases for the longus capitis muscles ($p=0.001$) and the brainstem ($p=0.01$) (Table 2).

No significant contrast enhancement was detected in the corpus vitreum ($p=0.33$), temporal muscles ($p=0.09$), masseter muscles ($p=0.46$) and the tongue ($p=0.57$) (Table 2).

Comparing the ipsilateral and contralateral enhancement to the side of the catheter

A visual obvious difference in contrast enhancement was detected for the maxillary vein ipsilateral compared to the contralateral side of the side of the contrast injection, in the IA group, but no statistical analysis was performed due to the outliers. Only the longus capitis muscles showed a significant asymmetric

enhancement (p=0,001). The other structures showed no significant asymmetry in contrast enhancement (parotis salivary gland p=0.07; temporal muscles p=0.26; cerebrum p=0.08; corpora vitrea p=0.07; nose mucosa p=0.2; masseter muscles p=0.26).

Comparing the IA and IV protocol

The eye (p=0.02), the pituitary gland (p=0.05), longus capitis muscles (p=0.02) showed a significant higher increase in attenuation for the IA protocol compared to the IV protocol.

Comparing the two observers

A significant difference in measurements between the two observers was detected for the cerebrum (p<0.0001) and brainstem (p<0.0001) only (Figure 1 and Figure 2).

Abnormal contrast enhancements

Abnormal contrast enhancement was reported in 4 cases after IA contrast medium administration and in 6 cases after IV contrast medium administration (Table 1). In these reported cases, the detected abnormal contrast enhancements could be divided in three categories: a strong vascularised mass (Figure 4), an enhanced rim surrounding an unenhanced structure (Figure 2d and Figure 5) and a normal but inflamed anatomical structure highlighted as a region with increased vascular perfusion and permeability (Figure 6). No differences in these abnormal contrast enhancement patterns were identified between the IV and IA protocols.

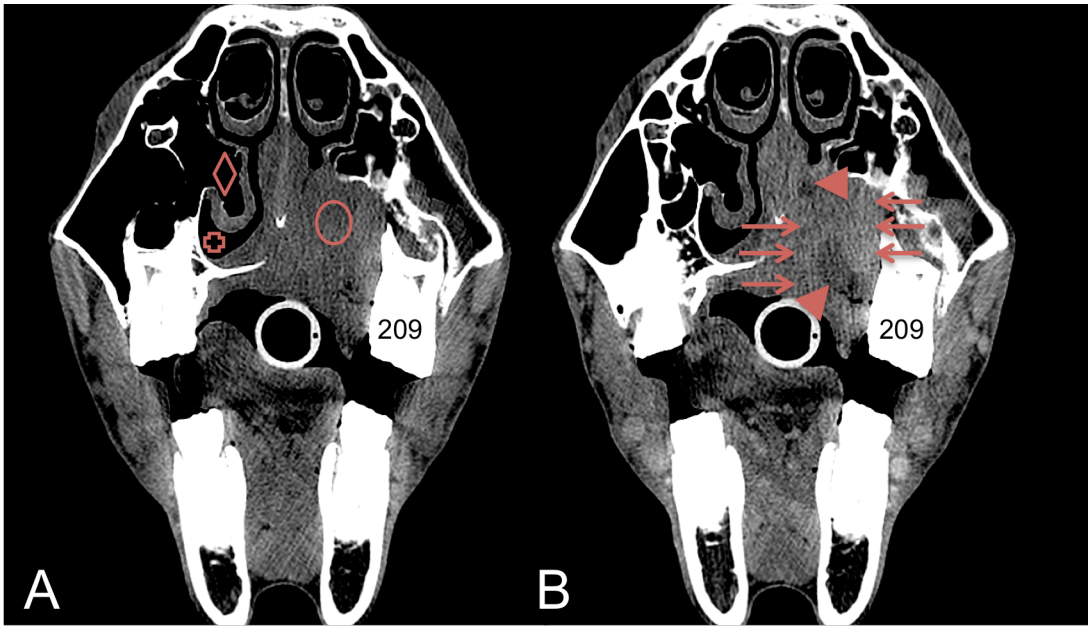

Figure 4: Transverse CT and IA contrast enhanced CT images of case 6 (right is to the left and dorsal is to the top). A) Squamous cell carcinoma in the hard palate causing a mass effect in the left ventral nasal meatus and suppressing the left ventral conchal sinus. The hard palate and the alveolar bone of elements 209 and 210 are destructed. B) Heterogeneous contrast enhancement of the mass, enhancement of the mass is indicated by the arrows and non-enhancing portion of the mass are indicated by arrowhead.

Discussion

In this study the use of IA and IV contrast-enhanced CT of the equine head was described using clinical cases. Several studies have described the use of contrast medium in horses [9, 13, 20-22, 26, 27], however the different routes of contrast administration have not been compared. As we used two different scanners in this study, interscanner variability needed to be considered [29].

The absolute attenuation values of the studied structures were only used to determine the structures enhancement and are not directly compared between the two scanners. The contrast medium administration protocols and scanners were consistent pairs. In the presence of interscanner or intrascanner variability, significant differences in enhancement can therefore not be explained without considering differences between the two protocols.

It was hypothesized that, the IA contrast medium administration technique would result in a similar or higher contrast enhancement using a lower volume of contrast medium compared to the IV technique. Contrast enhancement of a structure is intrinsically depending on its specific anatomy and vascular supply,

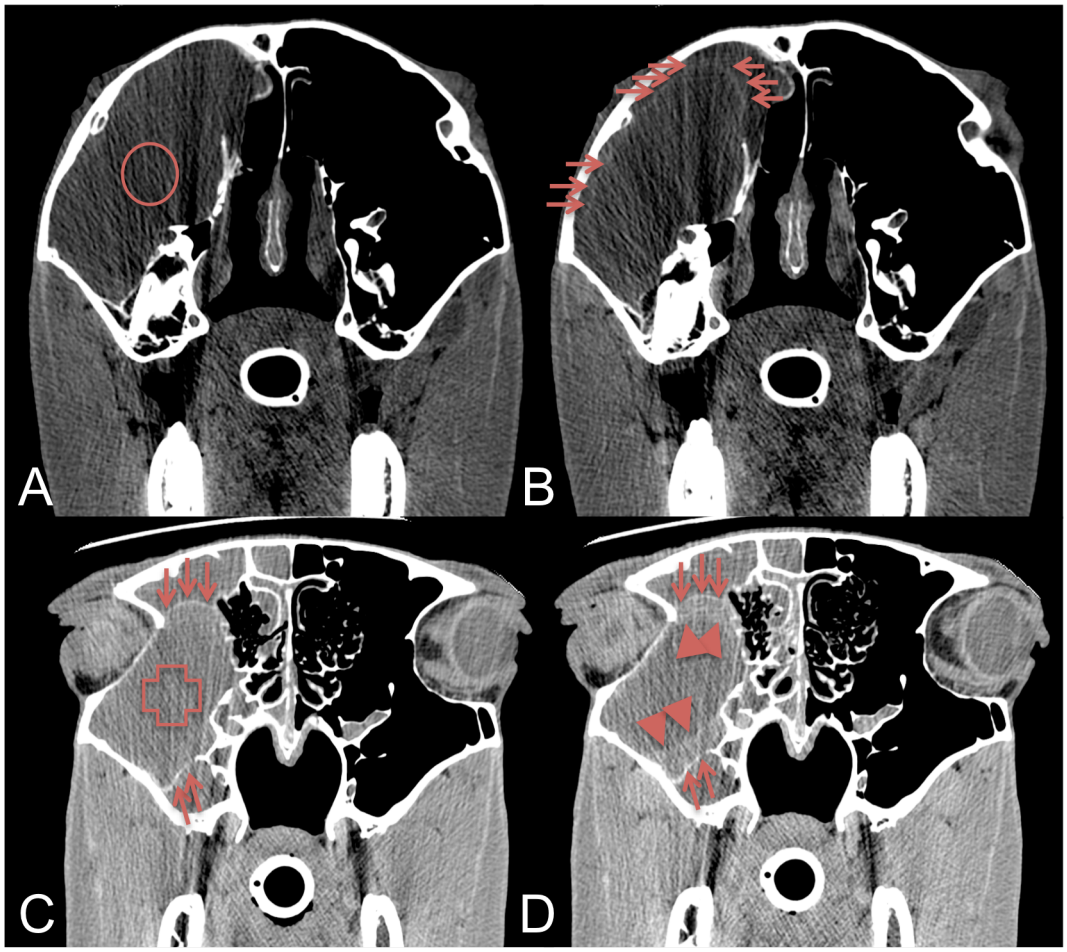

Figure 5: Transverse CT and IV contrast enhanced CT images of two cases with a sinus cyst (right is to the left and dorsal is to the top). A) Native CT image showing a fluid filled right caudal maxillary and conchofrontal sinus. B) Contrast enhanced CT image at the same level as image A, showing a thin mild contrast enhancement of the capsule (arrows). C) Native CT image showing a fluid filled right caudal maxillary and frontal sinus, a partial mineralised capsule is detected (arrows). D) Contrast enhanced CT image at the same level as image C, showing the partial mineralised capsule (arrows) with an adjacent moderate contrast enhancement (arrowheads) revealing a much thicker capsule.

extrinsically on the local dose of contrast medium and the timing of injection relative to the scan protocol. In the described study no controls were performed to exclude the influence of the individual case's intrinsic properties on contrast enhancement of the different structures. Recognising this shortcoming, we assume differences in contrast enhancement was only influenced by the extrinsic properties.

The local contrast medium dose compared to the total dose administered and the influence of timing are different for the two techniques. The local contrast medium dose in the IV technique is influenced by the amount of contrast medium injected as a bolus and the systemic dilution (influenced mainly by the size of the

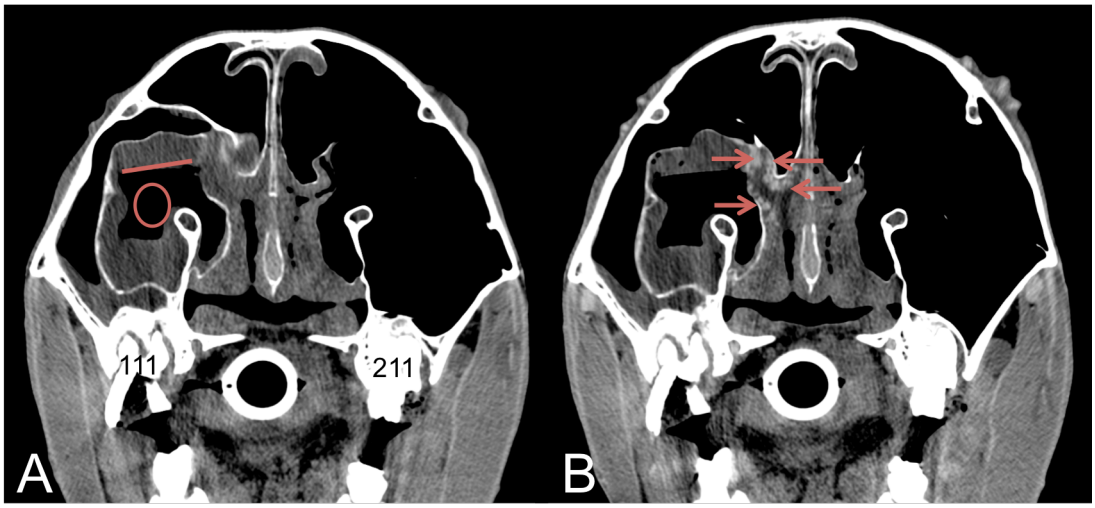

Figure 6: Transverse CT and IV contrast enhanced CT images of case 15 (right is to the left and dorsal is to the top). A) Secondary sinusitis in the right ventral conchal sinus characterised by mucosal thickening and free fluid. B) Adjacent mucosal contrast enhancement (arrowheads) is detected

individual in combination with blood pressure) of this bolus. In the IA technique the dose of contrast medium in the common carotid artery is only influenced by the local dilution with the blood in the common carotid artery at the moment of injection.

Timing of injection relative to the scan protocol for the IV technique is crucial as selective arterial enhancement, the so called “first pass”, is only seen for a relative short period. In human a 10 second time-window of selective arterial enhancement of the carotid arteries was identified 20 seconds after the start of the intravenous contrast medium bolus administration [30]. The results of the present study showed semi-quantitative moderate to severe enhancement of both the arterial and the venous system in all IV cases. The continuous injection of the IA protocol is assuring the visibility of contrast medium in the arterial lumen. As previously seen for the distal limb, the short delay before initiation of the scan and the time needed to scan the entire head is assuring contrast enhancement of the vascular bed, possible extravascular structures [20, 21] and (as shown in the results) the venous system. Based on these findings, both techniques represent a mixed (arterial and delayed)-phase CT angiography.

Our results showed for both techniques a similar semi-quantitative ranking from highest to least enhancing structures. Highest enhancement and extreme

outliers were seen in the maxillary veins. Due to these extreme outliers, statistical analysis was not considered useful. Pooling was the cause of these outliers in the maxillary veins. Pooling is visible as the layered appearance of highly attenuating contrast medium and blood in the vasculature due to the lack of optimal mixing. This phenomenon was detected in both the arterial and venous systems in the IA group. In the arterial system, streaming has previously been reported after intra-arterial drug administration and depends on the rate of infusion, the type of catheter used and the position of the catheter in relation to the arterial branching [31]. Streaming in the venous system has previously been reported to occur in the portal vein following direct injection of contrast medium in the splenic parenchyma in dogs [32]. However, in several cases streaming was present in the venous system and absent in the arterial system after intra-arterial contrast administration. An explanation is lacking for this observation.

The major arteries that supply blood to the head are both common carotid arteries (left and right side of the head) and the basilar artery (brainstem, cerebellum and caudal cerebrum) [33-35]. Both protocols differ based on the arterial supply of contrast rich blood to the head. The intravenous protocol is non-selective, using both common carotid arteries and the basilar artery, compared to selective intra-arterial protocol, using only one common carotid artery. As only in the IV group a small statistical significant difference in enhancement of the brainstem was measured in this study, the inability of the IA protocol to supply contrast rich blood to the brainstem, cerebellum and caudal cerebrum should be considered a potential limitation of the protocol. Anatomically however the common carotid artery is supplying blood to the basilar artery in the domestic animals and humans [33-35], by forming the cerebrospinal artery, which is fusing with the vertebral artery to form the basilar artery. Interestingly, the occipital arteries in horses are relatively large compared to other domestic animals and humans. As in contrast to other domestic animals and humans, in horses the common carotid arteries are divided into three arteries (the external and internal carotid arteries and also the occipital artery). Further research will be needed to determine to amount of contrast medium reaching the basilar artery through this connection.

Interestingly, homogenous contrast enhancement of the nose mucosa,

parotid salivary gland, cerebrum, temporal muscles and masseter muscles was seen and/or measured in the IA group at the contralateral side following unilateral contrast medium injection. This simultaneous opacification is most likely the result of communications between the right and left arterial systems, through the caudal intercarotid artery and via the arterial circle of Willis [33-36]. Regardless of the side of injection, the nasal mucosa showed a significant enhancement bilaterally. As such, horses with bilateral sinonasal disorders could possibly be scanned following a single arterial injection.

The pituitary gland, the nose septum and mucosa and the parotid salivary gland are highly vascularised structures, which showed marked enhancement on most post-contrast images. Previous reports described the accuracy of delineating the pituitary gland of adult horses, using 250mL MD-76 (370mgI/mL) [27]. The higher dose of IV contrast medium used in this study, 400mL Iobitridol (350mgI/mL), will probably not improve one's ability to detect the pituitary gland and the other marked enhanced structures. However, for the nose septum and mucosa, two patterns of contrast enhancement were observed. In our experience the patchy pattern is more often visible with an increasing dose of contrast medium. Due to a local higher contrast medium concentration, this pattern of enhancement is most likely highlighting the small calibre blood vessels running in these structures. Interestingly, no significant enhancement of the nose septum in the IV group was detected, review of the data showed almost no enhancement in several cases and moderate enhancement in the other cases. Similar results were seen for the temporal and masseter muscles. The absence of significant enhancement in these structures is most likely caused by the variation in contrast dosage (due to the differences in bodyweight) between the individuals included in this group.

The remaining structures had none to very mild significant contrast enhancement. In none of these structures, the enhancement was appreciated while reviewing the cases. Increasing the local dose of contrast medium would theoretically result in higher enhancements in these structures. Based on our results the absence of visible contrast enhancement in these structures after contrast medium administration using one of the above-described protocols has to be considered normal.

A conspicuous finding in these un-enhancing structures is several higher attenuation measurements on pre-contrast images compared to post-contrast images. This is most likely due to small movements of the horses in between scans. The copied ROI's incorporated therefore not exactly the same tissue samples of the structures. This intra-patient variability has to be considered if abnormal contrast enhancement is diagnosed.

Comparing both techniques, the results display different enhancements in three structures: the eye, pituitary gland and longus capitis muscle. Although all three structures show a significant difference, for the eye and pituitary gland, the median difference was very small (1.1 and 0.4HU respectively). For the longus capitis muscle the difference was higher (6.9HU). This muscle receives its blood supply directly from the common carotid arteries. A possible explanation for the detected difference and the significant asymmetric enhancement could be the streaming causing a local exceptionally high concentration of the contrast medium in the blood supplied to the longus capitis muscles.

Significant interobserver differences were only detected for the measurements performed on the brain and brainstem. Placement of the ROI's on these structures differed between the two observers. Reviewing the ROI's placed on the brain did not allow to detect a difference in attenuation (median interobserver difference of 4.5HU), this in accordance with previous reports [4]. In contrary depending on the WW and WL setting used to review the brainstem, the grey and white matter could clearly be distinguished (median interobserver difference of 9.2HU). Depending on the distance to the cranium for the brain and the central or peripheral localisation for the brainstem, an attenuation measurement is made of the more attenuating grey matter (observer 2) or less attenuating white matter (observer 1).

In this study, mild or marked abnormal contrast enhancement was seen in several cases. Three different abnormal enhancement patterns were detected in the included cases: enhancement due to the strong vascularisation of a soft tissue mass, rim enhancement of an encapsulated structure and increased enhancement due to inflammation of an anatomical structure. Diagnostically these findings help in the characterisation of a lesion and in the delineation of the margins between normal

soft tissue and soft tissue lesions that are not always evident on pre-contrast images [7, 13, 19]. Especially contrast enhancement in structures, that are normally not or only very mild enhancing, as previously described for cerebral lesions [13, 15] and seen in case 5 and 24, have to be considered abnormal. In none of the cases with abnormal contrast enhancement the IA and IV techniques were simultaneously performed. Direct comparing and determining differences between the two protocols in demonstrating specific lesions is therefore not possible based on this study.

Some concerns may be raised for both techniques. In the first case in which catheterisation of the common carotid artery was attempted this lead to hematoma formation. The wall of the common carotid artery is thick and the introduction of the catheter should therefore be done with a fast and strong movement to penetrate the vessel wall. This procedure had a steep learning curve considering the fact that only the first catheterisation was followed by the formation of a hematoma. A specific concern for intra-carotid drug administration in humans is cerebral embolism due to air emboli [31]. Carefully removing air from the pressure injector and prefilling the extension set prior to attaching to the catheter are provisions to prevent air emboli. In human, a transient but clinically tolerable increase in intra-arterial pressure of the internal carotid and vertebral artery has also been observed, following prolonged intra-arterial injection of contrast medium [37]. In horses, an elevated mean arterial blood pressure or heart rate were seen in 5% of the cases after intra-arterial iodinated contrast medium administration without requiring intervention [38]. Intra-arterial pressure was not monitored quantitatively in any of the horses included in the study. However, volatile agent-induced hypotension is well known and a concern during inhalation anaesthesia in horses [39]. Our main consideration not to monitor intra-arterial pressure was to keep the total anaesthesia time as short as possible.

A second concern is the contrast medium induced anaphylactic reactions, reported for several species including horses [38, 40-42]. Mild reactions as an elevated heart rate, changes in blood pressure, urticarial and oedema are the most often seen symptoms. Excluding these reactions in the study population solely based on the clinical records is difficult, as for these conditions no treatment or

intervention is considered necessary [38, 42] and blood pressure is not standardly recorded in our institutes during CT studies. Moderate and severe anaphylactic reactions require treatment or intervention [38, 42]. No such reactions have been described in the anaesthesia and clinical records of the included cases.

In conclusion, either protocol used in this study showed similar marked, mild or none obvious contrast enhancement depending on the reviewed structure. The major advantage of IA contrast medium administration during CT studies is that a similar contrast enhancement is achieved with less contrast medium compared to IV contrast administration, with the disadvantage of the presence of contrast streaming and pooling. The major advantage of the IV contrast medium administration in the cephalic vein is the symmetrical and homogenous enhancement, however timing is more crucial and the contrast dosage is more of influence in this protocol. Knowing the different normal contrast enhancement patterns of the soft tissues will facilitate the recognition of abnormal contrast enhancements in the horse's head. Further research will be needed to identify indications specifically profiting from either technique.

Footnotes

[a] Domidine, Eurovet, Belgium.

[b] Anesketin, Eurovet, Belgium.

[c] Dormicum, Roche, Belgium.

[d] Isoflo, Abbolt Laboratories Ltd, United Kingdom.

[e] Philips Medical Systems, Eindhoven, The Netherlands.

[f] GE Medical Systems, Milwaukee, Wisconsin, United States of America.

[g] Optiray 350, Covidien AG, Hazelwood, Missouri, United States of America.

[h] Xenetix 350, Guerbet, Roissy, France.

[i] OsiriX, Open Source, http://www.osirix-viewer.com.

[j] Bates D., Maechler M., Bolker B. And Walker S. (2014). lme4: linear mixed-effects models using Eigen and S4. R package version 1.1.6. http://CRAN.R-project.org/package=lme4.

References

1. Tremaine, W.H. and Dixon, P.M. (2001) A long-term study of 277 cases of equine sinonasal disease. Part 1: Details of horses, historical, clinical and ancillary diagnostic findings. *Equine Vet J* **33**, 274-282.

2. Tucker, R.L. and Farrell, E. (2001) Computed tomography and magnetic resonance imaging of the equine head. *Vet Clin N Am-Equine* **17**, 131-144.

3. Smallwood, J.E., Wood, B.C., Taylor, E. and Tate, L.P. (2002) Anatomic reference for computed tomography of the head of the foal. *Vet Radiol Ultrasound* **43**, 99-117.

4. Morrow, K.L., Park, R.D., Spurgeon, T.L., Stashak, T.S. and Arceneaux, B. (2000) Computed tomographic imaging of the equine head. *Vet Radiol Ultrasound* **41**, 491-497.

5. Henninger, W., Frame, E.M., Willmann, M., Simhofer, H., Malleczek, D., Kneissl, S.M. and Mayrhofer, E. (2003) CT features of alveolitis and sinusitis in horses. *Vet Radiol Ultrasound* **44**, 269-276.

6. Veraa, S., Voorhout, G. and Klein, W.R. (2009) Computed tomography of the upper cheek teeth in horses with infundibular changes and apical infection. *Equine Vet J* **41**, 872-876.

7. Cissell, D.D., Wisner, E.R., Textor, J., Mohr, F.C., Scrivani, P.V. and Theon, A.P. (2012) Computed tomographic appearance of equine sinonasal neoplasia. *Vet Radiol Ultrasound* **53**, 245-251.

8. Veraa, S., Dijkman, R., Klein, W.R. and van den Belt, A.J.M. (2009) Computed tomography in the diagnosis of malignant sinonasal tumours in three horses. *Equine Vet Educ* **21**, 284-288.

9. Crijns, C.P., Vlaminck, L., Verschooten, F., van Bergen, T., de Cock, H.E., Huylebroek, F., Pool, R. and Gielen, I. (2015) Multiple mandibular ossifying fibroma in a yearling Belgian Draught horse filly. *Equine Vet Educ* **27**, 11-15.

10. Tietje, S., Becker, M. and Bockenhoff, G. (1996) Computed tomographic evaluation of head diseases in the horse: 15 cases. *Equine Vet J* **28**, 98-105.

11. Powell, S.E. (2010) Use of multi-detector computed tomographic angiography in the diagnosis of a parapharyngeal aneurysm in a 6-week-old foal. *Equine Vet J* **42**, 270-273.

12. Hilton, H., Puchalski, S.M. and Aleman, M. (2009) The computed tomographic appearance of equine temporohyoid osteoarthropathy. *Vet Radiol Ultrasound* **50**, 151-156.

13. Lacombe, V.A., Sogaro-Robinson, C. and Reed, S.M. (2010) Diagnostic utility of computed tomography imaging in equine intracranial conditions. *Equine Vet J* **42**, 393-399.

14. Pownder, S., Scrivani, P.V., Bezuidenhout, A., Divers, T.J. and Ducharme, N.G. (2010) Computed tomography of temporal bone fractures and temporal region anatomy in horses. *J Vet Intern Med* **24**, 398-406.

15. Sogaro-Robinson, C., Lacombe, V.A., Reed, S.M. and Balkrishnan, R. (2009) Factors predictive of abnormal results for computed tomography of the head in horses affected by neurologic disorders: 57 cases (2001-2007). *J Am Vet Med Assoc* **235**, 176-183.

16. Allen, J.R., Barbee, D.D., Boulton, C.R., Major, M.D., Crisman, M.V. and Murnane, R.D. (1987) Brain abscess in a horse: diagnosis by computed tomography and successful surgical treatment. *Equine Vet J* **19**, 552-555.

17. Vink-Nooteboom, M., Junker, K., van den Ingh, T.S.G.A.M. and Dik, K.J. (1998) Computed tomography of cholesterinic granulomas in the choroid plexus of horses. *Vet Radiol Ultrasound* **39**, 512-516.

18. Baum, U., Greess, H., Lell, M., Nomayr, A. and Lenz, M. (2000) Imaging of head and neck tumors--methods: CT, spiral-CT, multislice-spiral-CT. *Eur J Radiol* **33**, 153-160.

19. Vanschandevijl, K., Gielen, I., Nollet, H., Vlaminck, L., Deprez, P. and van Bree, H. (2008) Computed tomography-guided brain biopsy for in vivo diagnosis of a cholesterinic granuloma in a horse. *J Am Vet Med Assoc* **233**, 950-954.

20. Puchalski, S.M., Galuppo, L.D., Hornof, W.J. and Wisner, E.R. (2007) Intraarterial contrast-enhanced computed tomography of the equine distal extremity. *Vet Radiol Ultrasound* **48**, 21-29.

21. Puchalski, S.M., Galuppo, L.D., Drew, C.P. and Wisner, E.R. (2009) Use of contrast-enhanced computed tomography to assess angiogenesis in deep digital flexor tendonopathy in a horse. *Vet Radiol Ultrasound* **50**, 292-297.

22. Collins, S.P., Matheson, J.S., Hamor, R.E., Mitchell, M.A., Labelle, A.L. and O'Brien, R.T. (2013) Comparison of the diagnostic quality of computed tomography images of normal ocular and orbital structures acquired with and without the use of general anesthesia in the cat. *Vet Ophthalmol* **16**, 352-358.

23. Kishimoto, M., Yamada, K., Seok, J.S., Shimizu, J., Kobayashi, Y., Akiba, Y., Morishita, Y., Iwasa, A., Iwasaki, T. and Miyake, Y. (2008) Analysis of blood

flow in a third ventricular ependymoma and an olfactory bulb meningioma by using perfusion computed tomography. *J Vet Med Sci* **70**, 981-983.

24. Kromhout, K., Gielen, I., De Cock, H.E., Van Dyck, K. and van Bree, H. (2012) Magnetic resonance and computed tomography imaging of a carotid body tumor in a dog. *Acta Vet Scand* **54**, 24.

25. Paul, A.E., Lenard, Z. and Mansfield, C.S. (2010) Computed tomography diagnosis of eight dogs with brain infarction. *Aust Vet J* **88**, 374-380.

26. Puchalski, S.M. (2012) Advances in equine computed tomography and use of contrast media. *Vet Clin N Am-Equine* **28**, 563-581.

27. Pease, A.P., Schott, H.C., Howey, E.B. and Patterson, J.S. (2011) Computed tomographic findings in the pituitary gland and brain of horses with pituitary pars intermedia dysfunction. *J Vet Intern Med* **25**, 1144-1151.

28. Bergman, H.J., Puchalski, S.M. and Saunders, J. (2012) Intracarotid contrast-enhanced computed tomography of the equine head. In: *16th congress of the international veterinary radiology association* Bursa, Turkey.

29. Birnbaum, B.A., Hindman, N., Lee, J. and Babb, J.S. (2007) Multi-detector row CT attenuation measurements: assessment of intra- and interscanner variability with an anthropomorphic body CT phantom. *Radiology* **242**, 109-119.

30. Levy, R.A. and Prince, M.R. (1996) Arterial-phase three-dimensional contrast-enhanced MR angiography of the carotid arteries. *Am J Roentgenol* **167**, 211-215.

31. Joshi, S., Meyers, P.M. and Ornstein, E. (2008) Intracarotid delivery of drugs: the potential and the pitfalls. *Anesthesiology* **109**, 543-564.

32. Echandi, R.L., Morandi, F., Daniel, W.T., Paquette, J.L. and Daniel, G.B. (2007) Comparison of transplenic multidetector CT portography to multidetector CT-angiography in normal dogs. *Vet Radiol Ultrasound* **48**, 38-44.

33. Barone, R. (1996) *Anatomie comparée des mammifères domestiques*, 4 edn., Vigot, Paris. p 904.

34. Nickel, R., Schummer, A. and Seiferle, E. (2004) *Lehrbuch der Anatomie der Haustiere*, 4 edn., Parey, Berlin,. p 664.

35. Sisson, S. and Grossman, J.D. (1953) *Anatomy of the Domestic Animals*, 4th edn., W.B. Saunders Company, Philadelphia. p 972.

36. Macdonald, D.G., Fretz, P.B., Baptiste, K.E. and Hamilton, D.L. (1999) Anatomic, radiographic and physiologic comparisons of the internal carotid and maxillary artery in the horse. *Vet J* **158**, 182-189.

37. Waldenberger, P., Chemelli, A. and Mallouhi, A. (2009) Intra-arterial haemodynamic changes during cerebral three-dimensional rotational angiography. *Eur Radiol* **19**, 503-508.

38. Pollard, R.E. and Puchalski, S.M. (2011) Reaction to intraarterial ionic iodinated contrast medium administration in anesthetized horses. *Vet Radiol Ultrasound* **52**, 441-443.

39. de Vries, A., Brearley, J.C. and Taylor, P.M. (2009) Effects of dobutamine on cardiac index and arterial blood pressure in isoflurane-anaesthetized horses under clinical conditions. *J Vet Pharmacol Ther* **32**, 353-358.

40. Gunkel, C.I., Valverde, A., Robertson, S.A., Thompson, M.S., Keoughan, C.G. and Ferrell, E.A. (2004) Treatment for a severe reaction to intravenous administration of diatrizoate in an anesthetized horse. *J Am Vet Med Assoc* **224**, 1143-1146.

41. Pollard, R.E., Puchalski, S.M. and Pascoe, P.J. (2008) Hemodynamic and serum biochemical alterations associated with intravenous administration of three types of contrast media in anesthetized cats. *Am J Vet Res* **69**, 1274-1278.

42. Vance, A., Nelson, M. and Hofmeister, E.H. (2012) Adverse reactions following administration of an ionic iodinated contrast media in anesthetized dogs. *J Am Anim Hosp Assoc* **48**, 172-175.

CHAPTER SEVEN

Computed Tomographic Findings on the Size, Age and Sex Influencing the Size of the Pituitary Gland in Normal Horses

Casper P. Crijns[1], Henri J.J. van Bree[1], Bart J.G. Broeckx[2], Stijn Schauvliege[3], Gunther Van Loon[4], Ann Martens[3], Katrien Vanderperren[1], Walter B. Dingemanse[1], Ingrid M.V.L. Gielen[1]

[1] Department of Medical Imaging and Small Animal Orthopaedics, Ghent University, 9820 Merelbeke, Belgium
[2] Department of Pharmaceutical Sciences, Ghent University, 9000 Gent, Belgium
[3] Department of Surgery and Anaesthesiology of Domestic Animals, Ghent University, 9820 Merelbeke, Belgium
[4]Department of Internal Medicine and Clinical Biology of Large Animals, Ghent University, 9820 Merelbeke, Belgium

Adapted from:

Casper P. Crijns, Henri J.J. van Bree, Bart J.G. Broeckx, Stijn Schauvliege, Gunther Van Loon, Ann Martens, Katrien Vanderperren, Walter B. Dingemanse, Ingrid M.V.L. Gielen. Computed tomographic findings on the size, age and sex influencing the size of the pituitary gland in normal horses *(submitted to Anatomia, Histologia, Embryologia)*

Summary

The objective of this study was to examine the influence of the size, age and sex of the horse on the size of the pituitary gland and determine the possibility of using the pituitary gland height-to-brain area ratio (P:B ratio) to allow comparison of different sized and aged horses. 32 horses without pituitary pars intermedia dysfunction that underwent a contrast-enhanced computed tomographic (CT) examination were included in a cross-sectional study. On the CT images, the pituitary gland height was measured and the P:B ratio was calculated. These measurements were correlated to the size, age and sex of the horses. The pituitary gland height was significantly associated with the size ($p<0.001$) and the age ($p<0.001$), but not with the sex ($p=0.40$), of the horses. No significant association was found between the P:B ratio and the size ($p=0.25$), the age ($p=0.06$) or the sex ($p=0.25$) of the horses.

In conclusion, the pituitary gland size varies between different sized and aged horses. The use of the P:B ratio is a valuable metric for making comparisons between the pituitary glands of these horses.

Introduction

Pituitary pars intermedia dysfunction (PPID) is the most common endocrinologic disorder in horses, characterised by an increase in plasma concentration of adrenocorticotropin hormone (ACTH) and α-melanocyte stimulating hormone [1-4]. Pathophysiologically, PPID results from the slow progressive loss of dopaminergic (inhibitory) input to the melanotropes of the pars intermedia (PI) of the pituitary gland [4]. PPID is thus a progressive neurodegenerative syndrome in horses. A presumptive diagnosis is often based on typical changes in blood parameters. However, an increase in size of the pituitary gland is considered to be associated with PPID [3-7]. Based upon histologic examination the pituitary gland can be divided into 5 grades (grade 1 till 5): grade 1 is considered normal, grade 2 has focal or multifocal areas of PI hypertrophy or hyperplasia which are considered to be normal aging changes. Grade 3 (diffuse PI adenomatous hyperplasia), grade 4 (PI adenomatous hyperplasia with micro-adenomas) and grade 5 (PI or pars anterior containing a macro-adenoma) are considered to be abnormal changes in the ptuitary gland suggesting PPID.

Computed tomography (CT) in combination with contrast-enhanced CT has been used to visualise the pituitary gland in human and veterinary medicine [3, 6-10]. In canine veterinary literature the pituitary gland height-to-brain area ratio (P:B ratio) was introduced to allow the comparison of the pituitary gland size of small and large dog breeds [9, 10]. Based on cadaver studies, variables such as age, size and sex seem to influence the pituitary gland size in horses [5, 6, 8]. Reference values of the normal or abnormal size of the pituitary gland have been published [6, 7], but in these reports the age, size and sex of the individuals have not been taken into account.

The aims of this study were to document the potential effect of several parameters on the size of the pituitary gland in horses without PPID. We first hypothesised that while using CT the use of the pituitary gland height-to-brain area ratio, instead of the pituitary gland height measurement, would allow direct comparison of horses of different sizes. Secondly, we hypothesised that the pituitary

gland size would be positively correlated with the age and size of the horse. The third hypothesis was that the size would vary between the two sexes.

Materials and methods

Animals

This study was performed after receiving approval from the ethical committee of Ghent University's Faculty of Veterinary Medicine. Horses were selected from the patients admitted to the University clinic between 2009 and 2015 that underwent a CT and contrast-enhanced CT examination for reasons unrelated to this study, without intra-cranial lesions and from horses belonging to the Faculty's research herd. Only horses with normal ACTH values (Aug-Nov: <47 pg/mL or <10.3 pmol/L; Nov-Jul <29 pg/mL or <6.4 pmol/L [11]) were included and owner consent was obtained prior to inclusion in the study. For all included horses, age, sex, and weight were recorded.

Computed tomographic examination

CT scans of the head were acquired with the horses under general anaesthesia. Each horse was sedated using romifidine[a] (0.08 mg/kg, IV). Anaesthesia was induced with a combination of ketamine[b] (2.2 mg/kg, IV) and midazolam[c] (0.06 mg/kg, IV). After orotracheal intubation, anaesthesia was maintained with inhaled isoflurane[d] in oxygen (on effect, ±1.2% expiratory). Routine monitoring was performed throughout anaesthesia.

The horses were positioned in dorsal recumbency with the head in the gantry. The earliest horses were examined using a single slice, helical CT scanner[e]. For the subsequent horses, images were acquired with a fourth generation 4-slice helical CT scanner[f]. The in-house protocols for equine head imaging were used (120 kV, 160 mAs, pitch 0.75-1, 1.25-5 mm slices, 512x512 matrix, scan FOV between 192-403 mm, bone and standard algorithm).

First, a pilot study was performed to assess the symmetric position of the horse's head in the gantry, followed by pre- and post-contrast CT studies in all horses. Post-contrast CT was performed after catheterisation (18 gauge x 80 mm) of one of the cephalic veins in the thoracic limbs, with the bevel directed away from

the heart. The catheter was fixed to the skin with cyanoacrylate adhesive. Two pressure injectors containing 200 ml of non-ionic iodinated contrast medium were connected to an extension set. The extension set was prefilled with contrast medium before being attached to the catheter. A bolus of 400 mL of Iobitridol[g] (350 mgI/mL) was injected intra-venous at a rate of 15 mL/s. The post-contrast scan was initiated about 30 s after the start of the administration of the contrast medium. After the catheter was removed, a bandage with moderate compression was placed around the limb at the site of injection for the time of the recovery.

Image analysis

A sub-selection of the post-contrast CT studies, including the entire sella turcica, was selected from each case, anonymised and randomly numbered. Unaware of the status of the cases, two observers (CC, IG) performed the measurements of the pituitary gland height and brain area on two separate occasions. Measurements were performed using a DICOM viewer[h] and according to the protocol previously described for dogs [9]. The transverse slice (WL 80; WW 250) with the largest cross-section height of the pituitary gland was visually selected. On the selected slice, the pituitary gland height was measured in the midline, and the brain area on the same slice was semi-automatically calculated using the segmentation tool (-2000; 150) (Figure 1). Using these two measurements, the P:B ratio was calculated using the following formula:

$$\text{P:B ratio} = (\text{pituitary gland height (mm)}/\text{brain area (mm}^2)) \times 100$$

Statistical analysis

First of all, the intra- and inter-observer agreements of the three measurements (pituitary gland height, brain area and P:B ratio) were assessed using Bland-Altman curves. To determine the presence of a systematic bias between measurements and between observers, a paired T-test was performed. The 95% limits of agreement were calculated to determine the random variation. In addition, the coefficient of variation was calculated to allow a direct comparison of the three measurements. The relation between age or weight as independent variables and

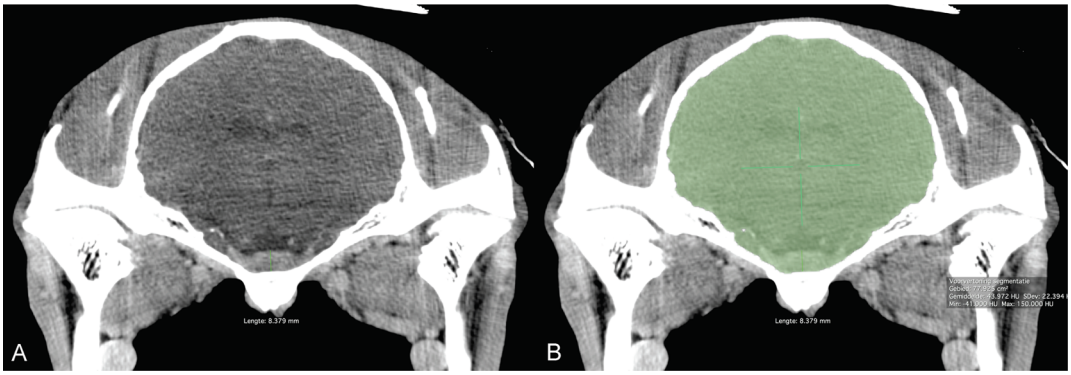

Figure 1: Transverse contrast-enhanced CT images of a 16.5 year old Warmblood gelding of 615kg. A: the pituitary gland height is measured in the midline on the visually selected transverse-slice with the largest cross-sectional height (0.838 cm). B: on the same slices the brain-area is semi-automatically calculated using the segmentation tool (77.925). This horse has a P:B ratio of 0.11 mm^{-1}.

the first principal component of the four measurements of pituitary gland size, or the P:B ratio on the other hand, (dependent variables) was investigated using simple regression. A two sample T-test was performed to determine whether the height of the pituitary gland or P:B ratio differed between the two sexes. P-values < 0.05 were considered significant [12]. All analyses were conducted in R^i.

Results

A cross-sectional study of a total of 32 horses, 30 patients and 2 horses of the Faculty's research herd, was performed. There were 22 Warmbloods, 4 ponies, 2 miniature horses and 1 Andalusian, 1 Arabian, 1 Belgian draft horse and 1 polo pony. This included 18 mares, 2 stallions and 12 geldings with a median age of 9.5 years (range 0.5 - 23.5) (Figure 2) and a median weight of 454 kg (range 60 – 675) (Figure 2). The sub-selection of the post-contrast CT studies included median of 66 slices (range 21 - 151), with slice thicknesses of 1.25 mm (n=7), 2.5 mm (n=24), 3.75 mm (n=1) and 5 mm (n=2).

The mean difference, the 95% limits of agreement, the standard deviation, the statistical significance of the mean difference and the coefficient of variation for the intra-observer and intra-modality agreement of the pituitary gland height measurements, the brain area determination and the P:B ratio calculations are represented in Table 1.

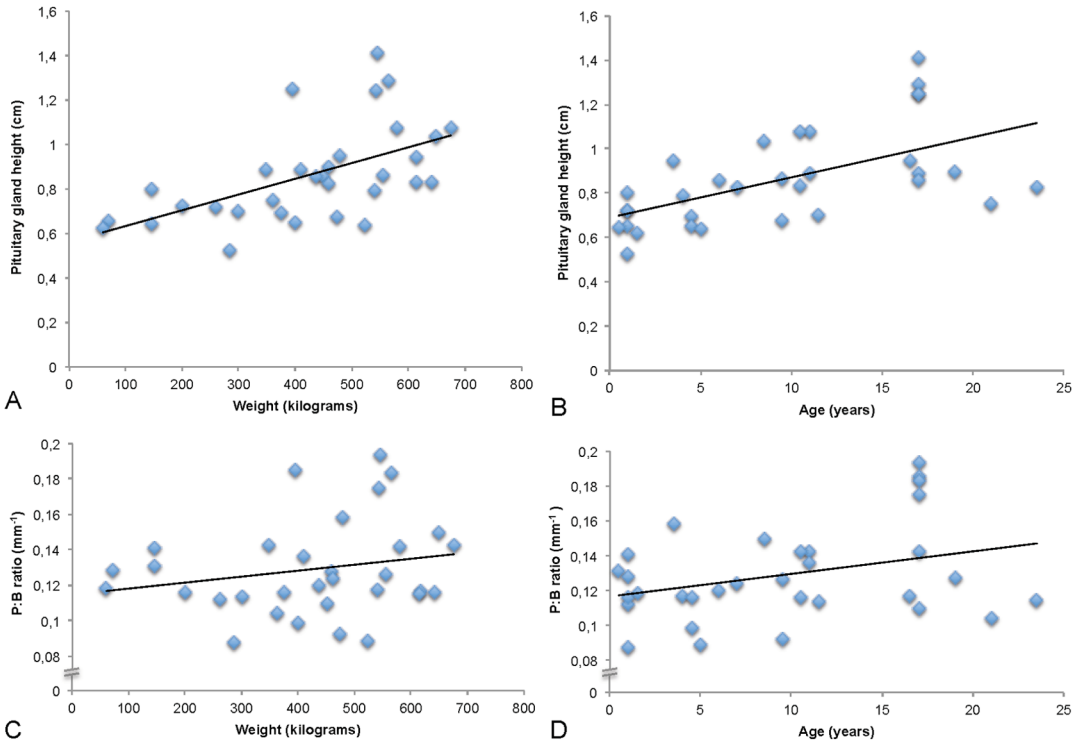

Figure 2: Simple scatter plots showing the CT pituitary gland height measurements and P:B ratio calculations of 32 horses of different ages and weights with normal ACTH. Plots include a linear trend line of best fit of the association between: a) the pituitary gland height and the weight of the horses (R^2=0.31418, p=<0.001); b) the pituitary gland height and the age of the horses (R^2=0.34118, p=<0.001); c) the P:B ratio and the weight of the horses (R^2=0.04455, p=0.25); d) the P:B ratio and the age of the horses (R^2=0.10901, p=0.06).

The first principal component of both the P:B ratio and the height of the pituitary gland explained 98% of the variation. There was a significant association between the pituitary gland height measurements and the weight of the horses (p<0.001) and between the pituitary gland height measurements and the age of the horses (p<0.001) (Figure 2 and Figure 3). There was no significant difference in the pituitary gland height measurements between the sexes (p=0.40).

However, there was no significant association between the P:B ratio and the weight of the horses (p=0.25), the P:B ratio and the sex of the horses (p=0.25) and only a positive, though non-significant (p=0.06), association between the P:B ratio and the age of the horses (Figure 2).

		Mean (bias)	95% limits of agreement	SD	P-value	Coefficient of variance
Height (cm)	Intra 1	-0.014	-0.13-0.1	0.056	0.18	0.065
	Intra 2	0.01	-0.041-0.066	0.027	0.01*	0.031
	Inter 1st	-0.001	-0.15-0.13	0.07	0.43	0.079
	Inter 2nd	0.016	-0.064-0.097	0.04	0.03*	0.047
Area (cm^2)	Intra 1	0.12	-1.106-1.344	0.61	0.28	0.009
	Intra 2	0.06	-0.511-0.641	0.3	0.21	0.004
	Inter 1st	0.04	-0.614-0.695	0.33	0.49	0.005
	Inter 2nd	-0.01	-1.322-1.295	0.65	0.9	0.01
P:B ratio (mm^{-1})	Intra 1	-0.001	-0.009-0.007	0.004	0.13	0.031
	Intra 2	0.002	-0.007-0.010	0.004	0.03*	0.033
	Inter 1st	0.000	-0.001-0.001	0.000	0.94	0.053
	Inter 2nd	0.003	-0.01-0.015	0.006	0.02*	0.049

Table 1: Agreement between observers for the pituitary gland height and brain area measurements, and the P:B ratio calculations (total n = 32 included cases) SD = standard deviation; * = significant difference; Intra 1 = between the measurements of observer 1; intra 2 = between the measurements of observer 2; Inter 1st = between the first measurement of observer 1 and 2; Inter 2nd = between the second measurement of observer 1 and 2.

Discussion

In our study, we evaluated the repeatability of the pituitary gland height measurement and the P:B ratio in a group of 32 PPID-free horses of different sizes, ages, genders and breeds. The main finding in this study was the presence of a significant association between the pituitary gland height and the size or age of the horses and the absence of a significant association between the P:B ratio and the size or age of the horses.

The use of the P:B ratio in this study was introduced to provide information about the pituitary gland that can be used irrespective of the size or weight of the horses, as previously seen in dogs [9, 10]. In a previous cadaver study, the 'relative

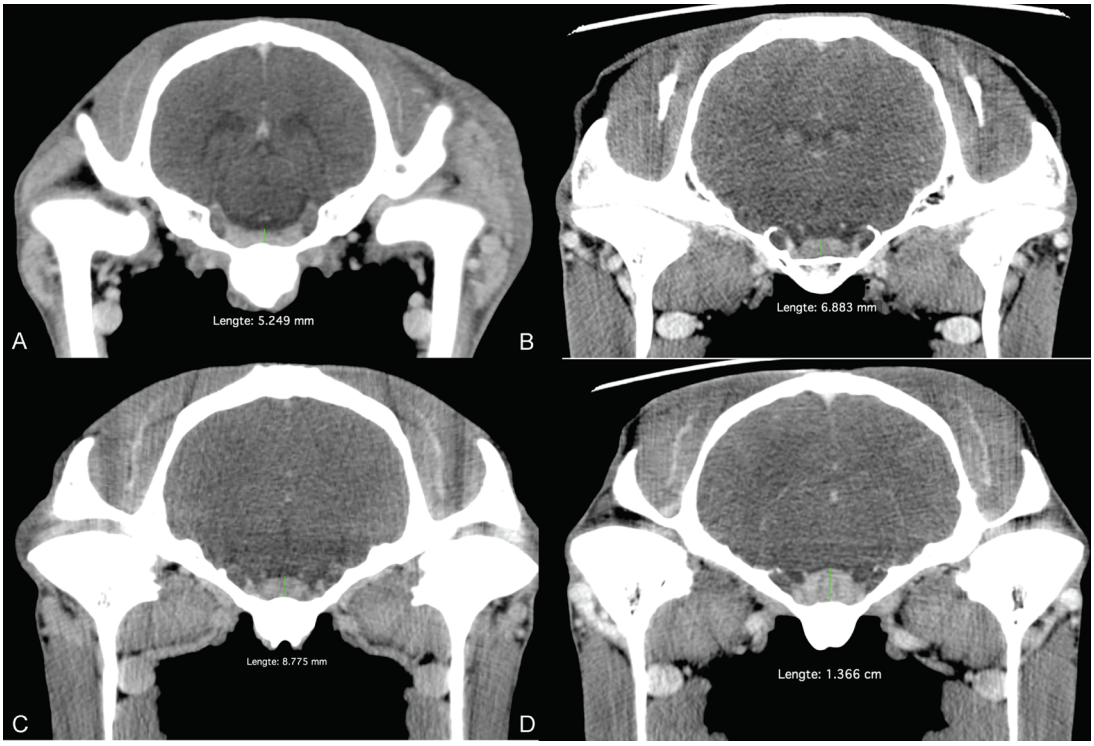

Figure 3: Transverse contrast-enhanced CT images of a foal, an adult pony, an adult Warmblood and an aged Warmblood showing the variation in pituitary gland size of horses with normal ACTH values. A: a 9 month old Warmblood stallion of 285 kg (Height: 0.525 cm, P:B ratio: 0.09 mm^{-1}); B: an 11 year old pony mare of 300kg (Height: 0.688 cm, P:B ratio: 0.11 mm^{-1}); C: a 10,5 year old Warmblood gelding of 640 kg (Height: 0.878 cm, P:B ratio 0.12 mm^{-1}); D: a 17 year old Warmblood mare of 544 kg (Height: 1.366 cm, P:B ratio 0.19 mm^{-1}).

pituitary gland weight' (pituitary gland weight (g)/body weight (g)) was not significantly different between horses and ponies with clinical signs of PPID [8]. Similarly, but in horses without PPID, no association was found in the present study between the P:B ratio and the size of the horses. It was therefore possible to directly compare pituitary glands of horses of different weights. This direct comparison was not possible when the absolute results of the pituitary gland height measurements were used.

Several studies have suggested an age-related increase in the size of the pituitary gland [3, 8]. In the present study a positive, though non-significant (p=0.06), association was found between the P:B ratio and age. It must be remembered that the pituitary gland is undergoing the normal growth of an individual and an additional disproportional growth. The normal growth of an individual links the age of the horse to the size of the pituitary gland, as the P:B ratio of a foal is smaller than the P:B ratio of a pony and an adult Warmblood, although the size of the pituitary

gland of a foal and a pony are both smaller compared to the size of the pituitary gland of an adult Warmblood. The disproportional growth of the pituitary gland has previously been described histologically as focal or multifocal hypertrophy and hyperplasia of the PI [3]. In this histological pituitary gland grade 2, the PI can increase up to twofold in size without abnormal plasma ACTH concentration and these are considered normal aging changes [3, 8]. Although CT is not able to distinguish between the different parts of the pituitary gland, the highest ratios were observed in the aged horses of this study. The inability to statistically demonstrate the age-associated disproportional growth in this study is most likely due to the large individual variation in the pituitary gland size as previously described [5, 8] and seen in this study. In the study population the largest pituitary glands were seen in four 16-year-old horses and not in the older horses included. The inclusion criterion of this study (normal plasma ACTH concentration) most likely selected horses with little (histologically grade 1 [3, 8]) disproportional growth in the aged group. With PPID being a progressive degenerative syndrome, a horse with a disproportional growth (histologically grade 2 [3, 8]) of the pituitary gland (which is considered normal) could transit over time into a clinical case of PPID. In a larger study population, the age-related increase in size of the pituitary gland could become more evident. Interestingly, the highest measurements of the pituitary gland height in this study were close to the average measurements of the pituitary gland height of horses with PPID described by Pease et al. 2011 [7]. The large pituitary glands seen in aged horses with and without PPID illustrate the presence of a grey zone between a normal and abnormal pituitary gland. This grey zone makes it more difficult to distinguish between individuals with and without PPID based on CT.

Gender-related differences in pituitary gland size and histologic grade have been described, with pregnant and lactating mares having larger pituitary glands with more pituitary PI lesions compared to mares in other reproductive states, stallions or geldings [5, 8]. As our study population included only non-pregnant and non-lactating mares, the absence of gender-associated differences in pituitary gland height or P:B ratios is in line with the results of these previous studies.

A significant consistent bias was found when the measurements of the pituitary gland height and P:B ratio of observer 2 were compared. However, the

mean (bias), 95% limits of agreement and the SD of observer 2 are smaller compared to the intraobserver results of observer 1. This significant consistent bias originated from a systematic difference in measuring the pituitary gland height by observer 2 between the first and second series of measurements. As pituitary gland height is used to calculate the P:B ratio and no significant differences were observed in the area measurements, we expected to observe the same trend for both. Review of the cases did not allow the identification of a specific change in measurement protocol between the first and second case series of observer 2. A bigger issue would be a large SD (and consequently large limits of agreement), as this indicates a non-systematic difference. However, the results in this study showed less random variation in measurements of the pituitary gland height (smaller SDs) compared to previous studies in dogs and horses [6, 10]. Possible explanations are the improved contrast-enhanced CT protocols (higher contrast dose, increased injection rate and better scan timing in comparison to previous studies [7]) and post-processing algorithms, which allows to increase the contrast between the very mildly contrast-enhancing normal brain tissue and the moderate to severe contrast-enhancing of the pituitary gland. The zoom function improved the possibilities of image analysis, enabling more precise cursor placement for the measurements. Using the segmentation tool is especially accurate in cases were the boundaries between two tissues (brain-bone) are highly contrasting. Semi-automatic calculation instead of manual delineation [10] of the brain area eliminated human error from the determination of the brain area.

A limitation of this study was that the individuals included were mainly Warmbloods, as this is the primary population of our CT patients. Previous studies have shown the absence of breed influence on the pituitary gland size [5]. The number of ponies or horses in the other breed groups was too small to compare the different breeds and perform reliable statistical analysis. Another limitation of this study was the inability to compare the CT results with histologic findings of the pituitary glands in this mainly patient-based population. In a recent study however, following contrast administration (intravenous or intra-arterial) measurements were not significantly different from those obtained during post-mortem examination ($p>0.13$) [13].

In conclusion, the pituitary gland size is influenced by the size and age of the horses. The use of the P:B ratio is a valuable method for reducing the differences in absolute pituitary gland height measurements and allows a comparison between the pituitary glands of variable sized and aged horses.

Footnotes

[a] Sedivet, Boehringer Ingelheim, Brussel, Belgium.

[b] Anesketine, Eurovet, Lille, Belgium.

[c] Dormicum, Abbott Laboratories Ltd, Kent, United Kingdom.

[d] Isoflo, Zoetis, Louvain-la-Neuve, Belgium.

[e] Prospeed single slice, GE Medical Systems, Milwaukee, Wisconsin, United States of America.

[f] Lightspeed QX/I, GE Medical Systems, Milwaukee, Wisconsin, United States of America.

[g] Xenetix®,Guerbet, Roissy, France.

[h] OsiriX, Open Source, http://www.osirix-viewer.com

[i] R version 3.1.2, Open Source, https://cran.r-project.org

References

1. McGowan, T.W., Pinchbeck, G.P. and McGowan, C.M. (2013) Prevalence, risk factors and clinical signs predictive for equine pituitary pars intermedia dysfunction in aged horses. *Equine Vet J* **45**, 74-79.

2. McGowan, T.W., Pinchbeck, G.P. and McGowan, C.M. (2013) Evaluation of basal plasma alpha-melanocyte-stimulating hormone and adrenocorticotrophic hormone concentrations for the diagnosis of pituitary pars intermedia dysfunction from a population of aged horses. *Equine Vet J* **45**, 66-73.

3. Miller, M.A., Pardo, I.D., Jackson, L.P., Moore, G.E. and Sojka, J.E. (2008) Correlation of pituitary histomorphometry with adrenocorticotrophic hormone response to domperidone administration in the diagnosis of equine pituitary pars intermedia dysfunction. *Vet Pathol* **45**, 26-38.

4. McFarlane, D. (2011) Equine pituitary pars intermedia dysfunction. *Vet Clin N Am-Equine* **27**, 93-113.

5. Cordero, M., McFarlane, D., Breshears, M.A., Miller, L.M., Miller, M.A. and Duckett, W.M. (2012) The effect of season on the histologic and histomorphometric appearance of the equine pituitary gland. *J Equine Vet Sci* **32**, 75-79.

6. McKlveen, T.L., Jones, J.C., Sponenberg, D.P., Scarratt, K., Ward, D.L. and Aardema, C.H. (2003) Assessment of the accuracy of computed tomography for measurement of normal equine pituitary glands. *Am J Vet Res* **64**, 1387-1394.

7. Pease, A.P., Schott, H.C., Howey, E.B. and Patterson, J.S. (2011) Computed tomographic findings in the pituitary gland and brain of horses with pituitary pars intermedia dysfunction. *J Vet Intern Med* **25**, 1144-1151.

8. van der Kolk, J.H., Heinrichs, M., van Amerongen, J.D., Stooker, R.C.J., Jansen, L., de Wal, L.J.I. and van den Ingh, T.S.G.A.M. (2004) Evaluation of pituitary gland anatomy and histopathologic findings in clinically normal horses and horses and ponies with pituitary pars intermedia adenoma. *Am J Vet Res* **65**, 1701-1707.

9. van der Vlugt-Meijer, R.H., Meij, B.P., van den Ingh, T.S., Rijnberk, A. and Voorhout, G. (2003) Dynamic computed tomography of the pituitary gland in dogs with pituitary-dependent hyperadrenocorticism. *J Vet Intern Med* **17**, 773-780.

10. van der Vlugt-Meijer, R.H., Meij, B.P. and Voorhout, G. (2006) Intraobserver and interobserver agreement, reproducibility, and accuracy of computed

tomographic measurements of pituitary gland dimensions in healthy dogs. *Am J Vet Res* **67**, 1750-1755.

11. Copas, V. E. N. and Durham, A. E. (2012) Circannual variation in plasma adrenocorticotropic hormone concentrations in the UK in normal horses and ponies, and those with pituitary pars intermedia dysfunction. *Equine Vet J* **44**, 440-443.

12. Bland, J.M. and Altman, D.G. (1999) Measuring agreement in method comparison studies. *Stat Methods Med Res* **8**, 135-160.

13. Carmalt, J.L. and Montgomery, J. (2015) Intraarterial injection of iodinated contrast medium for contrast enhanced computed tomography of the equine head. *Vet Radiol Ultrasound* **56**, 384-390.

CHAPTER EIGHT

General Discussion

Equine diagnostic imaging has significantly progressed over the last 20 years. Radiography and/or ultrasonography are still the first imaging techniques applied. However inconclusive findings obtained via radiography and ultrasonography create the necessity for more advanced imaging techniques such as CT, MRI and scintigraphy which are used for evaluation of a great variety of lesions. Depending on the expected type of lesion and structures involved, the clinician will have to choose an appropriate imaging modality. In order to do so, knowledge of the capabilities and maybe even more importantly, the limitations of each imaging modality is necessary.

In textbooks the difference between radiography and CT is thoroughly described [1, 2]. The knowledge of the value of these techniques for specific lesions is however not yet complete. In the first part of this thesis the advantages and limitations of radiography and CT to detect, describe and diagnose distal limb fractures (chapter 3) and head fractures (chapter 4) are evaluated.

The first two studies are based on the fundamental clinical principle that a complete and correct diagnosis should precede treatment. If some fractures and fracture characteristics remain undiagnosed, they are not taken into account in the treatment plan, which can result in inappropriate therapy and consequently poor outcome. Thus, in order to improve fracture treatment in horses, fracture diagnostics has to improve as well.

In both studies (chapter 3 and 4) only a subgroup of the fracture cases was included. Case selection was based on a positive fracture diagnosis on CT. However, calculating sensitivity and specificity of radiography and CT was not possible in the absence of gross pathology (or surgery) as the gold standard. This study limitation is important because sensitivity and specificity of CT is not 100% for all fracture types as shown in human literature for fractures of the mandibular condyle, orbital and maxillary sinus [3, 4].

In both studies several fractures went completely undetected on radiography. These fractures can/could be categorised as (1) subtle fractures or (2) fractures masked by surrounding anatomical complexity. Although both categories were detected in both studies, the subtle lesions most likely have a different aetiology in the head versus the distal limbs. The trauma severity most likely

influences the severity of the lesion detected in the head, whereas prodromal pathology has to be considered as an aetiology for subtle distal limb lesion. Prodromal pathology in the form of stress fractures in the distal limb is considered to be a precursor of catastrophic fractures. Not recognizing these lesions carries an important risk for fracture propagation [5]. Beside CT, both MRI [6-9] and scintigraphy [5, 10, 11] have proven their diagnostic capabilities in horses without radiographic bone abnormalities.

In contrast to CT, MRI studies mainly describe radiographically undetected fractures with a focus on the distal limbs of racehorses [6-8, 12, 13]. Hence MRI research is mainly concentrated on uncovering imaging characteristics of adaptive changes considered to be prodromal pathology [6-8, 14, 15]. In two cross-sectional cadaver studies, the presence of a fissure line resulted in altered signal intensity on STIR and T2*GRE sequences (bone-marrow oedema type signal), heterogeneous hypointense signal on T1- and T2*-weighted images (bone densification), or a combination of these patterns [15, 16]. Depending on the fracture type, bone-marrow oedema type signal in the distal condyles of the third metacarpus [16] or bone densification in proximal sesamoid bones [15] was detected more often in ipsi- and contralateral limbs of horses sustaining a fatal fracture. In a case series on unicortical condylar fractures, various severities of STIR hyperintensity in one or both metacarpal/tarsal condyles were detected [7]. The biomechanical forces involved in these different fracture types explain the variation in signal pattern. Compressive forces cause more bone marrow oedema, compared to tensile forces by which the bone marrow space becomes more fibrotic from repetitive injuries [15]. To our knowledge, no comparative studies between CT and MRI exist on the topic of prodromal fracture pathology. The advantage of MRI over CT would be the ability to detect bone marrow oedema surrounding a fissure. This allows MRI to differentiate between active and benign or developmental defects [7]. However, the sensitivity of both modalities to detect fissure lines and bone densification is unknown. A (comparative) longitudinal study of a group of horses would be interesting to further uncover the aetiology of these fractures.

In contrast to CT and MRI, scintigraphy is not representing specific anatomical structures but is reflecting physiological function of tissue [10]. Equine scintigraphy is best suited for detecting acute soft tissue and osseous abnormalities because radiopharmaceutical uptake often precedes radiographic detection. However, scintigraphy can also be used to locate potential areas of abnormal osseous turnover in horses with chronic, vague lameness. Technetium 99m linked to the radiopharmaceutical methylene diphosphonate is the most commonly used radionuclide in equine imaging [10]. The quantity of the radiopharmaceutical binding to hydroxyapatite in bone is a relative indication of osteoblastic activity, bone metabolism and blood flow to the bone in a specific region [10]. As subtle structural bone changes are preceded by functional changes [5, 17], scintigraphy is maybe able to detect pathologic processes in an earlier stage. However, in a study exclusively including horses with increased radionuclide uptake in the lateral metatarsal condyle, differentiation between cartilage damage, osteoarthritis or subchondral bone pathology could not be made [11]. Similar results of increased radiopharmaceutical uptake in the proximal part of the third metacarpal or –tarsal bone has been shown to indicate desmitis of the proximal suspensory ligament or a cortical stress fracture [10]. A comparative study between CT, MRI and scintigraphy would be interesting to compare their capabilities in detecting subtle insertion desmopathies and prodromal fracture lesions.

Beside some subtle fractures and those masked by complex anatomy, the majority of fractures included in chapter 3 and 4 were initially detected with radiography. Fracture details however were substantial misdiagnosed or underdiagnosed. Knowledge of these fracture details can however be very important in successful fracture repair. Indeed, due to the high weight of the animals, their temperament and the limitations in the use of external immobilisation to support internal fixation, good results can often only be obtained by maximizing apposition and alignment of the fracture fragments and minimizing the number of mechanical “errors” [18]. The limited ability to determine fracture length, complexity and orientation on radiographs has been observed during surgery [19]. Detecting additional fracture lines during surgery complicated and lengthened the procedure and general anaesthesia time. Moreover, complications due to affected local

vascularity, infection, and delayed healing are reported during aggressive open fracture repairs [18]. To minimize these complications during and after surgery, surgical procedures have evolved to be less invasive. Performing these techniques however necessitates (prior to surgery) accurate imaging diagnosis of the fracture complexity and orientation [18, 20]. The use of CT for surgical planning has therefore been suggested [21-25]. To determine the additional value of CT in these cases, the ability to visualise specific fracture characteristics with radiography and CT were compared. In chapter 3 the intermodality agreements for identifying articular involvement, comminution and displacement of the fracture were only fair. The intermodality agreements between radiography and CT for fracture orientation, number of fragments and fracture width were even poor. In line with these findings on the distal limbs, the fracture extension was also underestimated with radiography compared to CT in fractures of the head (chapter 4). Furthermore head fractures were more often classified simple on radiography opposed to comminuted on CT, and the amount of fragments present was almost always underestimated with radiography.

More accurate knowledge of the fracture configuration prior to surgery allows more reliable and accurate surgical planning. The advantage of pre- or intra-operative CT in such cases has shown to limit the time needed to visualise the fracture [20, 26, 27], compared to the intra-operative use of arthroscopy and fluoroscopy only. This development is considered to increase the efficiency during surgery [20]. In addition, general anaesthesia time seems to decrease if CT is used, although this has not been evaluated objectively.

The major disadvantage of CT has always been the necessity of general anaesthesia, especially in cases where a treatment would be performed on the standing horse. Indeed, general anaesthesia for purely diagnostic purposes is expensive and has an inherent risk related to the recovery of the horses [28, 29]. Introduction of standing CT to image the head [30] and standing CT and MRI to image distal limbs [31, 32] on sedated horses has overcome this limitation. The increased number of scientific publications, with around 60 published reports prior to 2006 and about 250 published reports after 2006, on these technologies reflects the rise of their popularity. Moreover as discussed previously, these setups make CT

and MRI more accessible for preventive screening in cases where radiography and ultrasonography are inconclusive [6-8].

The horizontal orientation of the head and neck in horses was advantageous in the development of standing CT, as no changes in vertical scan plan of existing systems were needed to scan the head. Adaptations were focused on levelling the head to the CT table and allowing the equine platform to move simultaneously and smoothly during scanning [30]. However, to be able to scan the distal limbs a horizontal scan plan is needed. As human systems do not allow an alteration of the scan plan by 90 degrees, specifically designed modalities are required. At the moment only a modality using a translate-rotate multidetector system, used for peripheral quantitative computerised tomography (pQCT) in human medicine, is available [32]. Compared to conventional CT, pQCT has several limitations. First, the relatively low x-ray energy used (60 kVp vs 120-140 kVp in conventional CT) favours bone and limits soft tissue definition [33]. Secondly, pQCT is an axial scanning modality with a long acquisition time per slice (90 s vs 0,6-0,8 s in conventional CT). Thirdly, quality of reformatted images is poor due to the very limited number of slices per study (average 6 slices) [32]. Fracture details in between the slices therefore remain unknown.

In equine literature, an increasing range of orthopaedic procedures performed on standing patients is described [34-37]. It is to be expected that, following the development of standing CT to image the equine head; new techniques will be developed to avoid (also for distal limbs) general anaesthesia for diagnostic procedures alone.

The aim of the second part of this thesis was to establish and/or evaluate contrast–enhanced CT protocols and applications used for the equine head. The main goal of contrast-enhanced CT is to improve soft tissue contrast in an attempt to avoid the need of an MRI examination. While MRI is considered to visualise soft tissue with superior contrast compared to CT [1], the limited availability of MRI and the longer examination time under general anaesthesia are disadvantageous. Two comparative studies between CT and MRI about imaging the head have been published [38, 39]. Although several differences between the two modalities were described, both studies did not favour one modality over the other. Furthermore, a wide range of

intra- and extracranial lesions is described both with CT [39-56] and MRI [13, 39, 57-63] further illustrating the broad overlap in capabilities of these imaging modalities. In a selection of cases with intra- and extracranial lesions the use of contrast-enhanced CT in addition to a native CT has shown to have an additional value [41-45, 49, 55]. To extend the knowledge on contrast-enhanced CT, two different contrast-enhanced CT protocols of the head were evaluated in chapter 6.

In equine medicine two routes of contrast administration, intravenous and intra-arterial, are used for contrast-enhanced CT of the head. The intravenous route is most commonly used in horses [41-44, 64], as well as in small animals [65-67]. The intra-arterial route, adapted from the standardized protocol, has been well described for the evaluation of distal extremities in horses [68-71]. The main purpose for the development of the intra-arterial protocol was to increase the local contrast enhancement, while simultaneously lowering the amount of contrast medium needed [64, 72].

For contrast-enhanced CT of the head no standardized systemic dosage of contrast medium or injection protocol have been determined in equine medicine. Normally the protocol used in small animals would be extrapolated and used in horses (600 mgI/kg injected at a rate of 2 ml/s) [65-67]. However, administering a comparable amount of contrast in horses is considered unworkable, as is illustrated by the various lower dosages of iodine used in equine literature (160-280 mgI/kg bodyweight) [41-44, 64].

The enhancement of normal and abnormal anatomical structures, after intravenous contrast administration, have been described for small animals [73]. In contrast, the enhancement values of the head described in chapter 6 can only be compared to the results described in the study of Carmalt and Montgomery (2015) [64]. That study is unfortunately limited to the structures surrounding the cranium and enhancements are only reported for a limited amount of structures. However, the evaluation of the results of both studies allows us to compare the different contrast injection protocols used. The IV protocol used by Carmalt and Montgomery (2015) consisted of 240 mL iohexol (350 mgI/mL) manually injected into the jugular vein with a 1 minute scan delay after the start of injection. In comparison, the IV protocol in chapter 6 consisted of 400 mL iobitridol (350 mgI/mL) injected with the

use of 2 power injectors (15 mL/s) into the cephalic vein with a 30 s scan delay after the start of injection. The pituitary gland showed an average of 14,2% enhancement over baseline in the study of Carmalt and Montgomery, compared to an average of 65% enhancement over baseline in chapter 6. Considering that the administered dosage and tissue enhancement are proportionally correlated [74], the substantial difference in enhancement cannot only be accredited to the difference in contrast dosage administered. Other factors such as the difference in injection rate, injection duration and scan delay have to be considered as well [74].

Comparing the results of the intra-arterial (IA) protocols used in these studies showed an average enhancement of 12% over baseline in the study of Carmalt and Montgomery and of 46.5% over baseline in chapter 6. The IA protocols used in these studies were however almost identical. Carmalt and Montgomery injected continuously 240 mgI/mL into the carotid artery with an injection rate of 4 mL/s and a scan delay of 5 s. In chapter 6, 350 mgI/mL was injected continuously into the carotid artery with an injection rate of 2 mL/s and a scan delay of 5 s. Carmalt and Montgomery injected a higher equivalent iodine dosage per second (960 mgI/s) compared to our study (700 mgI/s). In contrast to arterial enhancement, parenchymal enhancement is less influenced by injection rate and equivalent iodine dosage per second, but is more determined by the total iodine dose administered [74]. As a result of the different CT scanners used (16 slice vs. 4 slice), scanned object size (cranium vs. complete head) and scan duration (6 s vs. 90 s), the total iodine injected dosage was different between the two studies. The total iodine dosage injected by Carmalt and Montgomery (10.560 mg) was substantially lower compared to the dosage injected in chapter 6 (63.000 mg) explaining the difference in enhancement (respectively 12% versus 46.5% over baseline). Interestingly, no significant difference in parenchymal enhancement of the pituitary gland was detected between the two protocols (IV vs. IA) either in our study and the study of Carmalt and Montgomery, despite the substantially lower total iodine dosage injected IA (respectively 10.560 mg and 63.000 mg) compared to the dosages injected IV (respectively 84.000 mg and 140.000 mg) in both studies.

Taking into account that the limits of injection rate and injection duration are reached for the IV protocol using a single injection site, and that the possibilities to

increase the total iodine dosage administered using an IV protocol are limited. A potential major advantage of the IV technique is the ability to evaluate lesions that are characterised by increased vascular permeability due to the increased scan delay of the IV technique compared to the IA technique. A potential major advantage of the IA technique is the ability to evaluate lesions that are characterised by increased blood flow, as the protocol assures the presence of an intra-arterial phase while scanning. Further research to improve the IA protocol, to assure the visibility of vascular permeability is therefore the best option to further ameliorate contrast-enhanced CT in horses.

The aim of the last study (chapter 7) was to determine a pituitary gland height-to-brain area ratio using contrast-enhanced CT in healthy horses without PPID. Several studies have previously described the appearance and size of the pituitary gland using CT [41, 75] or histopathology [76-79] on healthy and PPID affected horses. In the studies describing the histopathologic appearance of the pituitary gland, several factors (age [77, 78], gender [77, 79] and season [78, 79]) influencing the pituitary gland size in healthy horses were taken into account. The size of the horse however was not included or considered in these studies, although it has been described in dogs [80, 81].

The results in chapter 7 show that both age and size of the horses were significantly associated with the pituitary gland height. A previous CT study [41] showed a significant difference in pituitary gland height between PPID affected and non-PPID affected aged horses. However, several non-PPID affected horses in chapter 7 showed pituitary gland heights approaching the pituitary gland sizes described for the PPID affected horses. In line with the lack of consensus in interpretation of pituitary glands from aged horses between veterinary pathologists [76, 78], the pituitary gland height should also be interpreted cautiously.

The gender of the horses was not of/had no influence on the pituitary gland height. The influence of the season was not included in chapter 7, as unfortunately only 2/8 horses of the faculty's research herd met the inclusion criteria of normal ACTH values. To determine the seasonal effect on the pituitary gland size, a longitudinal study of more than 2 horses is necessary to allow statistical analysis.

However, the reported increase in histomorphometric values of the PI and higher histological grades of the pituitary gland in the fall months suggests seasonal changes in the pituitary gland tissue [79]. In line with this finding the results of the 2 horses with normal ACTH values showed that all measurements of the scans performed in the autumn were higher compared to the scans subsequently performed out of season. This is in line with the 2 cases represented in the study of Pease et al. (2011). These results seem to suggest an association between season and pituitary gland size. This would be in agreement with the well-described seasonal increase in plasma ACTH [82-84] and the dynamic ability of the pituitary gland to adapt to physiological stimulation. Further research on a larger number of horses however will have to confirm these results.

In the study of Pease et al. (2011), dynamic imaging showed that CT was not able to distinguish between the different parts of the pituitary gland. In this study a similar contrast enhancement protocol (250 mL contrast medium injected into the vena jugularis) was used as described by Carmalt and Montgomery (2015). The limited enhancement of the pituitary gland using this protocol compared to the protocol used in dogs could explain the inability to detect the distinct pituitary flush (the distinct contrast enhancement of the pituitary pars nervosa) described in dogs. Further dynamic imaging studies using more enhancing protocols as described in chapters 6 and 7 could contradict the statement made by Pease et al. (2011).

In conclusion, the results of this research work have provided new insights into the capabilities and advantages of CT compared to other imaging modalities (mainly radiography). Further research on contrast-enhanced CT, for example using double intra-arterial contrast enhancement protocols [72] could provide more homogenously distributed contrast enhancement in the equine head and increase the ability to detect subtle abnormalities. In addition, the development of new technological concepts (increasing the gantry opening or making the gantry redundant) specifically for (standing) horses will further increase the indications for CT in equine medicine.

References

1. Thrall, D.E. (2013) *Textbook of veterinary diagnostic radiology*, 6th edn., Saunders Elsevier, St. Louis. p 847.

2. Schwarz, T. and Saunders, J. (2011) *Veterinary computed tomography*, Wiley-Blackwell, Chichester, West Sussex, UK ; Ames, Iowa. p 557.

3. Chacon, G.E., Dawson, K.H., Myall, R.W. and Beirne, O.R. (2003) A comparative study of 2 imaging techniques for the diagnosis of condylar fractures in children. *J. Oral Maxillofac Surg* **61**, 668-672.

4. Marinaro, J., Crandall, C.S. and Doezema, D. (2007) Computed tomography of the head as a screening examination for facial fractures. *Am J Emerg Med* **25**, 616-619.

5. Kuemmerle, J.M., Auer, J.A., Rademacher, N., Lischer, C.J., Bettschart-Wolfensberger, R. and Furst, A.E. (2008) Short incomplete sagittal fractures of the proximal phalanx in ten horses not used for racing. *Vet Surg* **37**, 193-200.

6. Ramzan, P.H. and Powell, S.E. (2010) Clinical and imaging features of suspected prodromal fracture of the proximal phalanx in three Thoroughbred racehorses. *Equine Vet J* **42**, 164-169.

7. Ramzan, P.H.L., Palmer, L. and Powell, S.E. (2015) Unicortical condylar fracture of the Thoroughbred fetlock: 45 cases (2006-2013). *Equine Vet J* **47**, 680-683.

8. Selberg, K. and Werpy, N. (2011) Fractures of the distal phalanx and associated soft tissue and osseous abnormalities in 22 horses with ossified sclerotic ungual cartilages diagnosed with magnetic resonance imaging. *Vet Radiol Ultrasound* **52**, 394-401.

9. Bolt, D.M., Williams, J. and Burba, D.J. (2003) Fracture of the small tarsal bones and luxation of the tarsal joints in horses. *Comp Cont Educ Pract* **25**, 310-316.

10. Archer, D.C., Boswell, J.C., Voute, L.C. and Clegg, P.D. (2007) Skeletal scintigraphy in the horse: current indications and validity as a diagnostic test. *Vet J* **173**, 31-44.

11. Parker, R.A., Bladon, B.M., Parkin, T.D. and Fraser, B.S. (2010) Quantitative evaluation of subchondral bone injury of the plantaro-lateral condyles of the third metatarsal bone in Thoroughbred horses identified using nuclear scintigraphy: 48 cases. *Equine Vet J* **42**, 552-557.

12. Bolt, D.M., Read, R.M., Weller, R., Sinclair, C. and David, F.H. (2013) Standing low-field magnetic resonance imaging of a comminuted central tarsal bone fracture in a horse. *Equine Vet Educ* **25**, 618-623.

13. Tessier, C., Bruhschwein, A., Lang, J., Konar, M., Wilke, M., Brehm, W. and Kircher, P. (2013) Magnetic resonance imaging features of sinonasal disorders in horses. *Vet Radiol Ultrasound* **54**, 54-60.

14. Tranquille, C.A., Parkin, T.D. and Murray, R.C. (2012) Magnetic resonance imaging-detected adaptation and pathology in the distal condyles of the third metacarpus, associated with lateral condylar fracture in Thoroughbred racehorses. *Equine Vet J* **44**, 699-706.

15. Peloso, J.G., Vogler Iii, J.B., Cohen, N.D., Marquis, P. and Hilt, L. (2015) Association of catastrophic biaxial fracture of the proximal sesamoid bones with bony changes of the metacarpophalangeal joint identified by standing magnetic resonance imaging in cadaveric forelimbs of Thoroughbred racehorses. *J Am Vet Med Assoc* **246**, 661-673.

16. Tranquille, C.A., Parkin, T.D.H. and Murray, R.C. (2012) Magnetic resonance imaging-detected adaptation and pathology in the distal condyles of the third metacarpus, associated with lateral condylar fracture in Thoroughbred racehorses. *Equine Vet J* **44**, 699-706.

17. Smith, M.R. and Wright, I.M. (2014) Are there radiologically identifiable prodromal changes in Thoroughbred racehorses with parasagittal fractures of the proximal phalanx? *Equine Vet J* **46**, 88-91.

18. Richardson, D.W. (2008) Less invasive techniques for equine fracture repair and arthrodesis. *Vet Clin N Am-Equine* **24**, 177-189.

19. Smith, M.R. and Wright, I.M. (2014) Radiographic configuration and healing of 121 fractures of the proximal phalanx in 120 Thoroughbred racehorses (2007-2011). *Equine Vet J* **46**, 81-87.

20. Gasiorowski, J.C. and Richardson, D.W. (2015) Clinical use of computed tomography and surface markers to assist internal fixation within the equine hoof. *Vet Surg* **44**, 214-222.

21. Kelmer, G., Wilson, D.A. and Essman, S.C. (2008) Computed tomography assisted repair of a central tarsal bone slab fracture in a horse. *Equine Vet Educ* **20**, 284-287.

22. Martens, P., Ihler, C.F. and Rennesund, J. (1999) Detection of a radiographically occult fracture of the lateral palmar process of the distal phalanx in a horse using computed tomography. *Vet Radiol Ultrasound* **40**, 346-349.

23. Rose, P.L., Seeherman, H. and OCallaghan, M. (1997) Computed tomographic evaluation of comminuted middle phalangeal fractures in the horse. *Vet Radiol Ultrasound* **38**, 424-429.

24. Waselau, M., Bertone, A.L. and Green, E.M. (2006) Computed tomographic documentation of a comminuted fourth carpal bone fracture associated with carpal instability treated by partial carpal arthrodesis in an Arabian filly. *Vet Surg* **35**, 618-625.

25. Whitton, R.C., Buckley, C., Donovan, T., Wales, A.D. and Dennis, R. (1998) The diagnosis of lameness associated with distal limb pathology in a horse: A comparison of radiography, computed tomography and magnetic resonance imaging. *Vet J* **155**, 223-229.

26. Perrin, R., Launois, T., Brogniez, L., Desbrosse, F.G., Coomer, R.P., Clegg, P.D., Reda, A.A., Gehin, S.G. and Vandeweerd, J.M. (2009) Computed tomography to identify preoperative guidelines for internal fixation of the distal sesamoid bone in horses: an in vitro study. *Vet Surg* **39**, 1030-1036.

27. Perrin, R.A.R., Launois, M.T., Brogniez, L., Clegg, P.D., Coomer, R.P.C., Desbrosse, F.G. and Vandeweerd, J.M.E.F. (2011) The use of computed tomography to assist orthopaedic surgery in 86 horses (2002-2010). *Equine Vet Educ* **23**, 306-313.

28. Mark, J. (2013) Morbidity, mortality, and risk of general anesthesia in horses. *Vet Clin N Am-Equine* **29**, 1-18.

29. Czupalla, I. and Gerhards, H. (2013) Risk of general anesthesia in horses - A retrospective study on 1.989 cases. *Pferdeheilkunde* **29**, 729-738.

30. Dakin, S.G., Lam, R., Rees, E., Mumby, C., West, C. and Weller, R. (2014) Technical set-up and radiation exposure for standing computed tomography of the equine head. *Equine Vet Educ* **26**, 208-215.

31. Mair, T.S., Kinns, J., Jones, R.D. and Bolas, N.M. (2005) Magnetic resonance imaging of the distal limb of the standing horse. *Equine Vet Educ* **17**, 74-78.

32. Debrosse, F.G., Vandeweerd, J.-M.E.F., Perrin, R.A.R., Clegg, P.D., Launois, M.T., Brogniez, L. and Gehin, S.P. (2008) A technique for computed tomography (CT) of the foot in the standing horse. *Equine Vet Educ* **20**, 93-98.

33. Puchalski, S.M. (2008) Principles of digital x-ray imaging: computed tomography and digital radiography. *Equine Vet Educ* **20**, 99-102.

34. Compston, P.C. and Payne, R.J. (2013) Standing fracture repair - a new chapter. *Equine Vet Educ* **25**, 386-388.

35. Hawkins, J.F. (2014) Osteoarthritis of the temporomandibular joint and what is possible with standing surgery of the horse? *Equine Vet Educ* **26**, 629-631.

36. Gasiorowski, J.C. and Richardson, D.W. (2014) Diagnostic and therapeutic arthroscopy in the standing horse. *Vet Clin N Am-Equine* **30**, 211-220.

37. O'Brien, T. and Hunt, R.J. (2014) Recent advances in standing equine orthopedic surgery. *Vet Clin N Am-Equine* **30**, 221-237.

38. Tucker, R.L. and Farrell, E. (2001) Computed tomography and magnetic resonance imaging of the equine head. *Vet Clin N Am-Equine* **17**, 131-144.

39. Wollanke, B., Gerhards, H. and Cronau, M. (2006) Diagnosis and therapy of periorbital diseases in horses: Indication for computed tomography (CT) or magnetic resonance tomography (MRT). *Pferdeheilkunde* **22**, 431-438.

40. Tietje, S., Becker, M. and Bockenhoff, G. (1996) Computed tomographic evaluation of head diseases in the horse: 15 cases. *Equine Vet J* **28**, 98-105.

41. Pease, A.P., Schott, H.C., Howey, E.B. and Patterson, J.S. (2011) Computed tomographic findings in the pituitary gland and brain of horses with pituitary pars intermedia dysfunction. *J Vet Intern Med* **25**, 1144-1151.

42. Lacombe, V.A., Sogaro-Robinson, C. and Reed, S.M. (2010) Diagnostic utility of computed tomography imaging in equine intracranial conditions. *Equine Vet J* **42**, 393-399.

43. Sogaro-Robinson, C., Lacombe, V.A., Reed, S.M. and Balkrishnan, R. (2009) Factors predictive of abnormal results for computed tomography of the head in horses affected by neurologic disorders: 57 cases (2001-2007). *J Am Vet Med Assoc* **235**, 176-183.

44. Manso-Diaz, G., Garcia-Lopez, J.M., Maranda, L. and Taeymans, O. (2015) The role of head computed tomography in equine practice. *Equine Vet Educ* **27**, 136-145.

45. Henninger, W., Frame, E.M., Willmann, M., Simhofer, H., Malleczek, D., Kneissl, S.M. and Mayrhofer, E. (2003) CT features of alveolitis and sinusitis in horses. *Vet Radiol Ultrasound* **44**, 269-276.

46. Hilton, H., Puchalski, S.M. and Aleman, M. (2009) The computed tomographic appearance of equine temporohyoid osteoarthropathy. *Vet Radiol Ultrasound* **50**, 151-156.

47. Pownder, S., Scrivani, P.V., Bezuidenhout, A., Divers, T.J. and Ducharme, N.G. (2010) Computed tomography of temporal bone fractures and temporal region anatomy in horses. *J Vet Intern Med* **24**, 398-406.

48. Huggons, N.A., Bell, R.J.W. and Puchalski, S.M. (2011) Radiography and computed tomography in the diagnosis of nonneoplastic equine mandibular disease. *Vet Radiol Ultrasound* **52**, 53-60.

49. Cissell, D.D., Wisner, E.R., Textor, J., Mohr, F.C., Scrivani, P.V. and Theon, A.P. (2012) Computed tomographic appearance of equine sinonasal neoplasia. *Vet Radiol Ultrasound* **53**, 245-251.

50. Textor, J.A., Puchalski, S.M., Affolter, V.K., MacDonald, M.H., Galuppo, L.D. and Wisner, E.R. (2012) Results of computed tomography in horses with ethmoid hematoma: 16 cases (1993-2005). *J Am Vet Med Assoc* **240**, 1338-1344.

51. Allen, J.R., Barbee, D.D., Boulton, C.R., Major, M.D., Crisman, M.V. and Murnane, R.D. (1987) Brain abscess in a horse: diagnosis by computed tomography and successful surgical treatment. *Equine Vet J* **19**, 552-555.

52. Vink-Nooteboom, M., Junker, K., van den Ingh, T.S.G.A.M. and Dik, K.J. (1998) Computed tomography of cholesterinic granulomas in the choroid plexus of horses. *Vet Radiol Ultrasound* **39**, 512-516.

53. Veraa, S., Dijkman, R., Klein, W.R. and van den Belt, A.J.M. (2009) Computed tomography in the diagnosis of malignant sinonasal tumours in three horses. *Equine Vet Educ* **21**, 284-288.

54. Veraa, S., Voorhout, G. and Klein, W.R. (2009) Computed tomography of the upper cheek teeth in horses with infundibular changes and apical infection. *Equine Vet J* **41**, 872-876.

55. Vanschandevijl, K., Gielen, I., Nollet, H., Vlaminck, L., Deprez, P. and van Bree, H. (2008) Computed tomography-guided brain biopsy for in vivo diagnosis of a cholesterinic granuloma in a horse. *J Am Vet Med Assoc* **233**, 950-954.

56. Solano, M. and Brawer, R.S. (2004) CT of the equine head: technical considerations, anatomical guide, and selected diseases. *Clin Tech equine Pract* **3**, 374-388.

57. Manso-Diaz, G., Dyson, S.J., Dennis, R., Garcia-Lopez, J.M., Biggi, M., Garcia-Real, M.I., San Roman, F. and Taeymans, O. (2015) Magnetic resonance imaging characteristics of equine head disorders: 84 cases (2000-2013). *Vet Radiol Ultrasound* **56**, 176-187.

58. Ferrell, E.A., Gavin, P.R., Tucker, R.L., Sellon, D.C. and Hines, M.T. (2002) Magnetic resonance for evaluation of neurologic disease in 12 horses. *Vet Radiol Ultrasound* **43**, 510-516.

59. Gerlach, K., Brehm, W., Gerhards, H. and Ludewig, E. (2011) Diagnostic of equine cheek tooth diseases with magnetic resonance imaging. *Pferdeheilkunde* **27**, 711-718.

60. Gerlach, K., Scharner, D., Muller, K., Lempe, A., Ludewig, E. and Brehm, W. (2012) Magnetic resonance imaging features of progressive ethmoid hematomas in three horses. *Prakt Tierarzt* **93**, 1012-1017.

61. Gerlach, K., Ludewig, E., Brehm, W., Gerhards, H. and Delling, U. (2013) Magnetic resonance imaging of pulp in normal and diseased equine cheek Teeth. *Vet Radiol Ultrasound* **54**, 48-53.

62. Audigie, F., Tapprest, J., George, C., Didierlaurent, D., Foucher, N., Faurie, F., Houssin, M. and Denoix, J.M. (2004) Magnetic resonance imaging of a brain abscess in a 10-month-old filly. *Vet Radiol Ultrasound* **45**, 210-215.

63. Hoppe, C.T., Horstmann, W. and Gerhards, H. (2003) Examination of disorders of the equine head with magnetic resonance imaging - three case reports. *Pferdeheilkunde* **19**, 143-150.

64. Carmalt, J.L. and Montgomery, J. (2015) Intraarterial injection of iodinated contrast medium for contrast enhanced computed tomography of the equine head. *Vet Radiol Ultrasound* **56**, 384-390.

65. Collins, S.P., Matheson, J.S., Hamor, R.E., Mitchell, M.A., Labelle, A.L. and O'Brien, R.T. (2013) Comparison of the diagnostic quality of computed tomography images of normal ocular and orbital structures acquired with and without the use of general anesthesia in the cat. *Vet Ophthalmol* **16**, 352-358.

66. Kromhout, K., Gielen, I., De Cock, H.E., Van Dyck, K. and van Bree, H. (2012) Magnetic resonance and computed tomography imaging of a carotid body tumor in a dog. *Acta Vet Scand* **54**.

67. Paul, A.E., Lenard, Z. and Mansfield, C.S. (2010) Computed tomography diagnosis of eight dogs with brain infarction. *Aust Vet J* **88**, 374-380.

68. Puchalski, S.M., Galuppo, L.D., Drew, C.P. and Wisner, E.R. (2009) Use of contrast-enhanced computed tomography to assess angiogenesis in deep digital flexor tendonopathy in a horse. *Vet Radiol Ultrasound* **50**, 292-297.

69. Puchalski, S.M., Galuppo, L.D., Hornof, W.J. and Wisner, E.R. (2007) Intraarterial contrast-enhanced computed tomography of the equine distal extremity. *Vet Radiol Ultrasound* **48**, 21-29.

70. Vallance, S.A., Bell, R.J.W., Spriet, M., Kass, P.H. and Puchalski, S.M. (2012) Comparisons of computed tomography, contrast enhanced computed tomography and standing low-field magnetic resonance imaging in horses with lameness localised to the foot. Part 1: Anatomic visualisation scores. *Equine Vet J* **44**, 51-56.

71. Vallance, S.A., Bell, R.J.W., Spriet, M., Kass, P.H. and Puchalski, S.M. (2012) Comparisons of computed tomography, contrast-enhanced computed tomography and standing low-field magnetic resonance imaging in horses with lameness localised to the foot. Part 2: Lesion identification. *Equine Vet J* **44**, 149-156.

72. Bergman, H.J., Puchalski, S.M. and Saunders, J. (2012) Intracarotid contrast-enhanced computed tomography of the equine head. In: *16th congress of the international veterinary radiology association* Bursa, Turkey.

73. Wisner, E.R. and Zwingenberger, A.L. Atlas of small animal CT and MRI. p 693.

74. Bae, K.T. (2010) Intravenous contrast medium administration and scan timing at CT: considerations and approaches. *Radiology* **256**, 32-61.

75. McKlveen, T.L., Jones, J.C., Sponenberg, D.P., Scarratt, K., Ward, D.L. and Aardema, C.H. (2003) Assessment of the accuracy of computed tomography for measurement of normal equine pituitary glands. *Am J Vet Res* **64**, 1387-1394.

76. Miller, M.A., Pardo, I.D., Jackson, L.P., Moore, G.E. and Sojka, J.E. (2008) Correlation of pituitary histomorphometry with adrenocorticotrophic hormone response to domperidone administration in the diagnosis of equine pituitary pars intermedia dysfunction. *Vet Pathol* **45**, 26-38.

77. van der Kolk, J.H., Heinrichs, M., van Amerongen, J.D., Stooker, R.C.J., Jansen, L., de Wal, L.J.I. and van den Ingh, T.S.G.A.M. (2004) Evaluation of pituitary gland anatomy and histopathologic findings in clinically normal horses and horses and ponies with pituitary pars intermedia adenoma. *Am J Vet Res* **65**, 1701-1707.

78. McFarlane, D., Miller, L.M., Craig, L.E., Dybdal, N.O., Habecker, P.L., Miller, M.A., Patterson, J.S. and Cribb, A.E. (2005) Agreement in histologic assessments of the pituitary pars intermedia in aged horses. *Am J Vet Res* **66**, 2055-2059.

79. Cordero, M., McFarlane, D., Breshears, M.A., Miller, L.M., Miller, M.A. and Duckett, W.M. (2012) The effect of season on the histologic and histomorphometric appearance of the equine pituitary gland. *J Equine Vet Sci* **32**, 75-79.

80. van der Vlugt-Meijer, R.H., Meij, B.P., van den Ingh, T.S., Rijnberk, A. and Voorhout, G. (2003) Dynamic computed tomography of the pituitary gland in dogs with pituitary-dependent hyperadrenocorticism. *J Vet Intern Med* **17**, 773-780.

81. van der Vlugt-Meijer, R.H., Meij, B.P. and Voorhout, G. (2006) Intraobserver and interobserver agreement, reproducibility, and accuracy of computed tomographic measurements of pituitary gland dimensions in healthy dogs. *Am J Vet Res* **67**, 1750-1755.

82. Copas, V.E.N. and Durham, A.E. (2012) Circannual variation in plasma adrenocorticotropic hormone concentrations in the UK in normal horses and ponies, and those with pituitary pars intermedia dysfunction. *Equine Vet J* **44**, 440-443.

83. Donaldson, M.T., McDonnell, S.M., Schanbacher, B.J., Lamb, S.V., McFarlane, D. and Beech, J. (2005) Variation in plasma adrenocorticotropic hormone concentration and dexamethasone suppression test results with season, age, and sex in healthy ponies and horses. *J Vet Intern Med* **19**, 217-222.

84. McGowan, T.W., Pinchbeck, G.P. and McGowan, C.M. (2013) Evaluation of basal plasma alpha-melanocyte-stimulating hormone and adrenocorticotrophic hormone concentrations for the diagnosis of pituitary pars intermedia dysfunction from a population of aged horses. *Equine Vet J* **45**, 66-73.

SUMMARY

There have been tremendous advances in the veterinary diagnostic imaging field over the last decades. Beside the primary imaging modalities, radiography and ultrasonography, which are widely available to equine practitioners, more advanced cross-sectional imaging modalities, such as computed tomography (CT) and magnetic resonance imaging (MRI) have become more available in equine medicine. In order to properly choose between the different imaging modalities, practitioners need a general understanding of the possibilities and shortcomings of each modality. The general aim of this research is to evaluate the use, capabilities and limitations of CT in equine medicine.

The **first chapter** describes the general concept of CT in equine medicine. An overview of the existing literature regarding the main indications for CT in horses i.e. musculoskeletal injuries of the limbs, head and cranial neck, dental pathology, and sinonasal disease is presented.

The **second chapter** states the scientific aims of this work. The aim of the first part of this thesis is to compare radiography and CT in their ability to detect, describe and diagnose bony lesions occurring in horses. The aim of the second part of this thesis is to establish and/or evaluate contrast–enhanced CT protocols and applications used for the equine head.

In the **third chapter** the differences between radiography and CT in visualising equine distal limb fractures and their anatomic characteristics is described. Four observers retrospectively reviewed the radiographic and CT images of 27 horses with a distal limb fracture and 3 negative controls. The level of agreement among the observers for a predefined set of radiological characteristics for radiography and CT separately, as well as between the two imaging modalities, were documented using Cohen's kappa and weighted kappa analysis. Both CT and radiography had very good intramodality agreement in identifying fractures, but intermodality agreement was lower. There was good intermodality and intramodality agreement for anatomical localisation and the identification of fracture displacement. Agreement for articular involvement, fracture comminution

and fracture fragment number was towards the lower limit of good agreement. There was poor to fair intermodality agreement regarding fracture orientation, fracture width and coalescing cracks; intramodality agreement was higher for CT than for radiography for these features.

In conclusion, CT offers added value in diagnosing distal limb fractures in horses. Relative to radiography, CT is better capable in detecting the presence of a fracture; there is more agreement over the fracture orientation and the other fracture characteristics.

In the **fourth chapter** the differences between radiography and CT in visualising equine head fractures and their anatomic characteristics are described. Two observers retrospectively reviewed the radiographic and CT images of 18 horses with a head fracture. To allow direct comparison between the two modalities, a simplified fracture classification system was used. In 3/18 cases, radiographic examination revealed no abnormalities. In 2/15 cases soft tissue involvement was not detected and in 7/15 cases the extension of the fracture was underestimated with radiography in comparison to CT. Radiography classified 4/10 multiple fractures incorrectly as single fractures and 5/15 comminuted fractures on CT were diagnosed as simple fractures with radiography. In line with this last finding, the number of fragments was underestimated with radiography in 14/15 cases.

In conclusion, radiography is able to diagnose a head fracture in most cases. Head fractures however are not similarly classified after radiographic and CT evaluation, which causes a difference in interpretation and perception of the fractures.

In the **fifth chapter** the diagnostic advantages of CT in combination with CT arthrography of a stifle joint, in an adult Warmblood horse, compared to the physical, radiographic and ultrasonographic examinations are documented. CT in combination with CT arthrography showed multiple lesions in the stifle: a traumatic osteochondrosis like lesion of the medial femoral condyle, bony fragments, cartilage trauma and caudal cruciate ligament injury. The prognosis for continuing use as a

sports horse was regarded as unfavourable. Therefore, the horse was subjected to euthanasia. All CT findings could therefore be confirmed by gross pathology.

In conclusion, based on this case, a CT and CT arthrography examination is able to provide a diagnosis, which is not achieved with other conventional imaging techniques.

In the **sixth chapter**, an intravenous (IV) and an intra-arterial (IA) contrast-enhancement CT protocol of the head are evaluated. The normal and abnormal soft-tissue contrast-enhancement of the head after systemic IV and direct IA injection are described and comparatively evaluated. All 24 horses that underwent an IV (n=12) or IA (n=12) contrast-enhanced CT of the head recovered well without complications from the procedures. Compared to the pre-contrast studies, post-contrast studies showed significant contrast enhancement in the pituitary gland (IA: $p < 0.0001$; IV: $p < 0.0001$), IA nose septum ($p = 0.002$), nose mucosa (IA: $p < 0.0001$; IV: $p = 0.02$), parotid salivary gland (IA: $p < 0.0001$; IV $p < 0.0001$), cerebrum (IA: $p < 0.0001$; IV: $p < 0.0001$), longus capitis muscle (IA: $p < 0.0001$; IV $p = 0.001$), IA temporal muscle ($p < 0.0001$), IA masseter muscle ($p <0.0001$) and IV brainstem ($p = 0.01$). No significant contrast enhancement was seen in the eye (IA: $p = 0.23$; IV $p = 0.33$), tongue (IA $p = 0.2$; IV $p = 0.57$), IA brainstem ($p = 0.88$), IV nose septum ($p = 0.26$), IV temporal muscle ($p = 0.09$) and IV masseter muscle ($p = 0.46$). Three different categories of abnormal enhancement were detected: a strong vascularised mass, an enhanced rim surrounding an unenhanced structure and an inflamed anatomical structure with abnormal contrast enhancement.

In conclusion, using the intra-arterial technique, similar contrast enhancement is achieved using less contrast medium compared to the intravenous technique. A potential major advantage of the IA technique is the ability to evaluate lesions that are characterised by increased blood flow. Using the intravenous technique, a symmetrical and homogenous enhancement is achieved, however timing is more crucial and the contrast dosage is more of influence in the IV protocol. A potential major advantage of the IV technique is the ability to evaluate lesions that are characterised by increased vascular permeability. Knowledge of the

different normal contrast enhancement patterns will facilitate the recognition of abnormal contrast enhancements.

The objective of the study in the **seventh chapter** is to examine the influence of the size, age and sex of the horse on the size of the pituitary gland and determine the possibility of using the pituitary gland height-to-brain area ratio (P:B ratio) to allow comparison of different sized and aged horses. This cross-sectional study included 32 horses without pituitary pars intermedia dysfunction (PPID), that underwent a contrast-enhanced CT examination. The pituitary gland height was measured in these horses and the P:B ratio was calculated. These measurements were correlated to the size, age and sex of the horses. The pituitary gland height was significantly associated with the size ($p<0.001$) and the age ($p<0.001$), but not with the sex ($p=0.40$) of the horses. No significant association was found between the P:B ratio and the size ($p=0.25$), the age ($p=0.06$) or the sex ($p=0.25$) of the horses.

In conclusion, the pituitary gland size varies between different sized and aged horses. The use of the P:B ratio is a valuable metric for making comparisons between the pituitary glands of these horses.

The **eighth** and **last chapter** is the general discussion. The results of this PhD research provided additional insight in the capabilities and advantages of CT in equine medicine. The major disadvantage of CT however is the need for general anaesthesia. Standing low-field MRI has therefore been used to diagnose subtle prodromal fractures. Further research between CT and MRI will have to demonstrate which modality is more suited to diagnose these prodromal pathologies. Although at the moment it is not possible to exam the distal limb on a standing sedated horse, for head structures the ability to perform CT examination on the standing sedated horse is a possibility and therefore a major advantage. The ability to improve soft tissue contrast of the head structures however is clearly dependent on the contrast enhancement protocol used. Further research improving the contrast enhancement protocols are needed to further ameliorate contrast-enhanced CT.

SAMENVATTING

In de afgelopen decennia heeft de medische beeldvorming in de diergeneeskunde een enorme ontwikkeling doorgemaakt. Radiografie en echografie behoren nog steeds tot de primaire diagnostische modaliteiten en zijn ruim beschikbaar in de paardengeneeskunde. Daarnaast beschikken steeds meer paardenklinieken ook over geavanceerde beeldvormingsmodaliteiten zoals computertomografie (CT) of magnetische resonantie (MR). Om een correcte keuze te maken tussen de verschillende onderzoeksmodaliteiten, afhankelijk van de aan te tonen pathologie, is het noodzakelijk dat de dierenarts op de hoogte is van de mogelijkheden en beperkingen van iedere modaliteit. Het algemene doel van dit doctoraatswerk was om een beter inzicht te verkrijgen in het gebruik, de mogelijkheden en de voordelen van CT voor de paardengeneeskunde.

In het **eerste hoofdstuk** van dit proefschrift worden eerst de algemene principes van CT bij het paard beschreven. Daarna wordt er een overzicht gegeven van de meest voorkomende toepassingen van CT in de paardengeneeskunde, met name de diagnostiek van orthopedische-, hoofd en hals-, dentale- en sinusaandoeningen.

In het **tweede hoofdstuk** worden de wetenschappelijke doelstellingen van dit doctoraatsonderzoek geformuleerd. De doelstelling van het eerste deel van dit proefschrift is na te gaan in hoeverre botletsels bij paarden op basis van radiografie en CT kunnen worden beschreven en gediagnosticeerd. De doelstelling van het tweede deel van dit proefschrift is het ontwikkelen en evalueren van contrastprotocollen en applicaties voor CT van het hoofd bij paarden.

In het **derde hoofdstuk** van dit proefschrift worden de verschillen onderzocht tussen radiografie en CT in het detecteren, beschrijven en diagnosticeren van onderbeenfracturen bij het paard. In dit onderzoek werden de radiografische en CT-beelden van 27 paarden met een onderbeenfractuur en 3 controle paarden, door 4 evaluatoren retrospectief beoordeeld en op tien verschillende punten gescoord. De Cohen's kappa en gewogen kappa statistieken werden gebruikt om de onderlinge verschillen tussen de evaluatoren en de modaliteiten te beoordelen. Zowel voor

radiografie als CT was de “intramodaliteit”-betrouwbaarheid zeer goed, de “intermodaliteit”-betrouwbaarheid was echter lager. Zowel de “intra-“ als de “intermodaliteit”-betrouwbaarheid voor het anatomisch lokaliseren en identificeren van verplaatsingen van fracturen waren goed. De betrouwbaarheid voor het beoordelen van: betrokkenheid van een gewricht, het herkennen van verbrijzeling en het aantal aanwezige fragmenten was aan de ondergrens van goed. De “intermodaliteit”-betrouwbaarheid voor het bepalen van de fractuur configuratie, de fractuur “gap” en het identificeren van extra fissuren in de nabijheid van de fractuur was slecht tot matig, de “intramodaliteit”-betrouwbaarheid van CT was voor deze punten steeds hoger dan voor radiografie.

De conclusie van deze studie is dat CT, vergeleken met radiografie, extra diagnostische informatie oplevert met betrekking tot onderbeenfracturen bij paarden. CT is beter in het detecteren en het visualiseren van deze fracturen vergeleken met radiografie.

In het **vierde hoofdstuk** van dit proefschrift zijn de verschillen tussen radiografie en CT in het detecteren, beschrijven en diagnosticeren van fracturen ter hoogte van het hoofd bij het paard beschreven. In dit onderzoek werden de radiografische en CT-beelden van 18 paarden met een schedelfractuur door 2 evaluatoren retrospectief bekeken en op zes verschillende punten gescoord. Om de beoordelingen van de evaluatoren met elkaar te kunnen vergelijken werd een vereenvoudigd fractuurclassificatiesysteem gebruikt. Op basis van de radiografische beelden werd in 3/18 gevallen geen fractuur gedetecteerd. In 2/15 gevallen werd er geen weke delen betrokkenheid gediagnosticeerd en in 7/15 gevallen werd de uitgebreidheid van het letsel onderschat op basis van de radiografische beelden. Daarnaast werd in 4/10 gevallen radiografisch een enkelvoudige fractuur gediagnosticeerd in plaats van een multipele fractuur en in 5/15 gevallen werd een fractuur als eenvoudig radiografisch geclassificeerd in plaats van verbrijzeld. Het aantal fragmenten dat werd gedetecteerd met behulp van radiografie was in 14/15 gevallen lager vergeleken met CT.

De conclusie van deze studie is dat men met behulp van radiografie in staat is om de meeste schedelfracturen te diagnosticeren. Het classificeren van deze

schedelfracturen op basis van radiografie en CT verschilt echter duidelijk. Hierdoor kan naargelang de modaliteit die gebruikt wordt de interpretatie en perceptie van de schedelfractuur duidelijk verschillen.

In het **vijfde hoofdstuk** wordt bij een volwassen warmbloedpaard de diagnostische waarde van CT in combinatie met CT-artrografie bij een knieletsel vergeleken ten opzichte van het klinisch, radiografisch en echografisch onderzoek. Met behulp van CT in combinatie met CT-artrografie werden verschillende letsels gedetecteerd in het kniegewricht, namelijk een traumatisch osteochondrosis-achtig letsel aan de caudo-axiale rand van de mediale femurcondyl, een mineralisatie tussen de mediale meniscus en de mediale femurcondyl met een groefvormige beschadiging van het kraakbeen van dezelfde condyl en een letsel in de caudale kruisband. De ernst van de letsels en bijbehorende slechte prognose als sportpaard hebben uiteindelijk geleid tot euthanasie. Een postmortaal onderzoek dat werd uitgevoerd op het gewricht bevestigde de op basis van het CT-onderzoek gestelde diagnose.

Op basis van deze casus kan men concluderen dat men met behulp van CT in combinatie met CT-artrografie een diagnose heeft kunnen stellen die op basis van de andere beeldvormende modaliteiten niet mogelijk is.

In het **zesde hoofdstuk** worden een intraveneus (IV) en een intra-arterieel (IA) contrastprotocol voor CT van het hoofd bij paarden geëvalueerd. De normale en abnormale aankleuring van de weke delen van het hoofd zij beschreven en vergeleken na het toedienen van een systemische IV contrastbolus en een directe IA contrast toediening. Hiervoor werden 24 paarden bestudeerd: 12 paarden ondergingen het IV-protocol en 12 paarden het IA-protocol. Er werden geen complicaties opgemerkt tijdens en na de recovery van de paarden. In vergelijking met de native-CT studies, werd een significante contrast aankleuring opgemerkt van de hypofyse (IA: $p < 0,0001$; IV: $p < 0,0001$), het neusseptum (IA: $p = 0,002$), de neusmucosa (IA: $p < 0,0001$; IV: $p = 0,02$), parotis speekselklier (IA: $p < 0,0001$; IV $p < 0,0001$), het cerebrum (IA: $p < 0,0001$; IV: $p < 0,0001$), de longus capitis spier (IA: $p < 0,0001$; IV $p = 0,001$), de temporaal spier (IA: $p < 0,0001$), de masseter spier (IA p

<0,0001) en de hersenstam (IV: p = 0,01). Er werd geen significante aankleuring opgemerkt van de ogen (IA: p = 0,23; IV p = 0,33), de tong (IA p = 0,2; IV p = 0,57), de hersenstam (IA: p = 0,88), het neusseptum (IV: p = 0,26), de temporal spier (IV: p = 0,09) en de masseter spier (IV: p = 0,46). Op basis van beide protocollen konden er drie verschillende abnormale aankleuringspatronen worden geïdentificeerd: een sterk gevasculariseerde massa, een massa waarbij enkel de rand duidelijk aankleurde en een ontsteking van een normale anatomische structuur die duidelijker aankleurde dan normaal.

De conclusies van deze studie zijn dat men minder contrastvloeistof nodig heeft voor het IA-protocol vergeleken met het IV-protocol, om een vergelijkbare aankleuring van de weke delen structuren te bekomen. Het potentieel belangrijkste voordeel van het IA-protocol is dat men structuren met een verhoogde bloedvoorziening gemakkelijker kan detecteren. Het IV-protocol toont een symmetrische en homogene aankleuring van de weke delen structuren. Een correcte timing is echter van cruciaal belang en de contrastdosis beïnvloedt het IV-protocol meer dan het IA protocol. Het potentieel belangrijkste voordeel van het IV-protocol is dat men extravasatie gemakkelijker kan detecteren. Kennis van de normale aankleuringspatronen beschreven in deze studie zal het herkennen van abnormaliteiten vergemakkelijken.

In het **zevende hoofdstuk** zijn de invloeden van de lichaamsgrootte, leeftijd en geslacht op de grootte van de hypofyse bij het paard bestudeerd. Daarnaast is de mogelijkheid beoordeeld om de ratio tussen de hoogte van de hypofyse en het hersenoppervlak (de P:B-ratio) te gebruiken om de hypofyse van paarden van verschillende grootten en leeftijden met elkaar te vergelijken. Hiervoor werden 32 paarden zonder hypofyse pars intermedia dysfunctie (PPID – of misschien beter gekend onder de naam Cushing), die een contrast-CT ondergingen bestudeerd. De gemeten hoogte van de hypofyse en de bijbehorende berekende P:B-ratio werd gecorreleerd met de lichaamsgrootte, de leeftijd en het geslacht van de paarden. Hieruit kwam naar voren dat er een significante correlatie bestond tussen de hoogte van de hypofyse enerzijds en de lichaamsgrootte (p<0,001) en de leeftijd (p<0,001) van de paarden anderzijds. Deze correlatie bestond niet voor het geslacht (p=0,40).

Er was geen significante correlatie tussen de P:B-ratio enerzijds en de lichaamsgrootte (p=0,25), de leeftijd (p=0,06) of het geslacht (p=0,25) anderzijds.

De conclusie van deze studie is dat de grootte van de hypofyse varieert tussen paarden van verschillende grootten en leeftijden. Door gebruik te maken van de P:B-ratio kan de hypofyse van paarden van verschillende omvang gemakkelijk met elkaar vergeleken worden.

De algemene discussie van dit proefschrift is vervat in het **achtste** en **laatste hoofdstuk**. De resultaten van dit proefschrift geven meer inzicht in de mogelijkheden en voordelen van het gebruik van CT in de paardengeneeskunde. Hierbij moet echter opgemerkt worden dat het grootste nadeel van een CT-onderzoek de algemene anesthesie is. Om deze redenen wordt staande laagveld-MR dan ook gebruikt om bijvoorbeeld subtiele onderbeenfracturen bij staande gesedeerde paarden te diagnosticeren. Om na te gaan of CT dan wel MR de meest geschikte modaliteit is om deze subtiele letsels te diagnosticeren zijn er bijkomende vergelijkende studies nodig. Alhoewel het op dit moment nog niet mogelijk is om onderzoeken van de ledematen op het staande, gesedeerde paard uit te voeren, is het wel reeds mogelijk om CT-onderzoek van het hoofd op het staande gesedeerde paard uit te voeren. Het verbeteren van het zichtbare contrast tussen de weke delen van het hoofd is echter duidelijk afhankelijk van het gebruikte contrastprotocol. Bijkomende studies zullen moet uitwijzen welke protocollen dit zichtbare contrast nog verder kunnen verbeteren.

CURRICULUM VITAE

Casper Paul Crijns werd geboren op 9 april 1985 te Veldhoven, Nederland. Tijdens zijn jeugd heeft hij in Nederland, Frankrijk en Duitsland gewoond, om uiteindelijk zijn middelbareschooldiploma voorbereidend wetenschappelijk onderwijs ("VWO"), met als profiel natuur en gezondheid, te behalen aan het Kandinsky College te Nijmegen. Niet huiverig om opnieuw naar het buitenland te verhuizen, startte hij in 2003 met de studies Diergeneeskunde aan de Universiteit Antwerpen. In 2011 studeerde hij af als dierenarts optie paard aan de Universiteit Gent. Het tweede deel van zijn uit drie delen bestaande Masterproef is nog tijdens zijn studie gepubliceerd in Equine Veterinary Journal.

Onmiddellijk na het afstuderen startte hij een internship paard aan de vakgroep Medische Beeldvorming van de Huisdieren en Orthopedie van de Kleine Huisdieren onder leiding van Prof. Dr. H. van Bree. Geboeid door het wetenschappelijke onderzoek trad hij op 1 oktober 2012 in dienst bij dezelfde vakgroep als wetenschappelijk medewerker. Naast het verrichten van zijn wetenschappelijk onderzoek hield hij zich voornamelijk bezig met de computer tomografische onderzoeken bij de paarden. Als wetenschapper met een groot hart voor de praktijk kon hij het aanbod om zijn werk aan de Universiteit te combineren met een praktijkfunctie in een grote paardenkliniek niet afslaan. Op 1 juni 2013 trad hij als dierenarts in dienst bij DAP Bodegraven BV met als taak de medische beeldvorming en orthopedie van de paarden.

Casper Paul Crijns is auteur van verschillende wetenschappelijke publicaties in internationale tijdschriften en was spreker op verschillende internationale congressen.

BIBLIOGRAPHY

Publications in International Journals

Crijns, Casper P.; Gielen, Ingrid M.V.L.; van Bree, Henri J.J.; Bergman, Erik, 2010. The use of CT and CT arthrography in diagnosing equine stifle injury in a Rheinlander gelding. *Equine Veterinary Journal* 42(4):367-371.

Crijns, Casper P.; Martens, Ann; Bergman, Erik H.J.; van der Veen, Henk; Duchateau, Luc; van Bree, Henri J.J.; Gielen, Ingrid M.V.L., 2014. Intra-modality and inter-modality agreement in radiography and computed tomography of equine distal limb fractures. *Equine Veterinary Journal* 46(1):92-96.

Crijns, Casper P.; Vlaminck, Lieven; Verschooten, Francis; van Bergen, Thomas; de Cock, Hilde E.; Huylebroek, Frits; Pool, Roy; Gielen, Ingrid M.V.L., 2015. Multiple mandibular ossifying fibroma in a yearling Belgian Draught horse filly. *Equine Veterinary Education* 27(1);11-15.

Crijns, Casper P.; Baeumlin, Yseult; De Rycke, Lieve; Broeckx, Bart J.G.; Vlaminck, Lieven; Bergman, Erik H.J.; van Bree, Henri J.J.; Gielen, Ingrid M.V.L., 2016. Intra-arterial versus intra venous contrast-enhanced computed tomography of the equine head. *BMC Veterinary Research* 12.

Crijns, Casper P.; Vanderperren, Katrien; Weller, Renate; Martens, Ann; Vlaminck, Lieven; Verschooten, Francis; van Bree, Henri J.J.; Gielen, Ingrid M.V.L., 2016. The use and advantages of computed tomography in equine medicine. *The Australian Equine Veterinarian*, 35(2);50-61.

De Rycke, Lieve; **Crijns, Casper P.**; Chiers, Koen; van Bree, Henri J.J. ; Gielen, Ingrid M.V.L. Late onset wedge-shaped thoracic vertebrae in a 6 month-old Pug. *Veterinary Record Case Reports*, review submitted.

Crijns, Casper P.; van Bree, Henri J.J.; Broeckx, Bart J.G.; Schauvliege, Stijn; van Loon, Gunther; Martens, Ann; Vanderperren, Katrien; Dingemanse, Walter B.; Gielen, Ingrid M.V.L. Computed tomographic findings on the size, age and sex influencing the size of the pituitary gland in normal horses. *Anatomia, Histologia, Embryologia,* submitted.

Pollaris, Elke; Vandervekens, Elke; Gielen, Ingrid M.V.L.; **Crijns, Casper P.**; Vlaminck L. Equine dentistry in the 21st century 2. Dental examination of the horse's mouth and diagnostic techniques for detection of dental disease. *Vlaams Diergeneeskundig Tijdschrift,* submitted.

Crijns, Casper P.; Weller, Renate; Vlaminck, Lieven; Verschooten, Francis; Schauvliege, Stijn; Powell, Sarah E.; van Bree, Henri J.J.; Gielen, Ingrid M.V.L. Comparison between radiography and computed tomography for diagnosis of equine head fractures. In preparation.

Publications in Proceedings of International Scientific Meetings

Crijns, Casper P.; Gielen, Ingrid M.V.L.; Bergman, Erik H.J.; Martens, Ann; van der Veen, Henk; Duchateau, Luc; van Bree, Henri J.J. Radiography and computed tomography for the diagnosis of distal limb fractures in equines: a comparative study. *American Association of Equine Practioners, Annual convention*, Anaheim, California, United States of America, December 1-5, 2012, p.537-538.

Crijns, Casper P.; Vlaminck, Lieven; Verschooten, Francis; van Bergen, Thomas; de Cock, Hilde E.; Pool, Roy; Gielen, Ingrid M.V.L. Multiple mandibular ossifying fibromas in a yearling Belgian draft horse. *CT-User, 3rd International meeting*, Ghent, Belgium, November 30-December 1, 2013, p.16.

Crijns, Casper P.; Martens, Ann; Bergman, Erik H.J.; van der Veen, Henk; Duchateau, Luc; van Bree, Henri J.J.; Gielen, Ingrid M.V.L. Comparison of radiography vs. CT in equine orthopaedic trauma: intramodality and intermodality agreement in radiography and computed tomography of equine distal limb fractures. *CT-User, 3rd International meeting*, Ghent, Belgium, November 30-December 1, 2013, p.146-147.

Crijns, Casper P.; Vlaminck, Lieven; Picavet, Tresemiek; de Vries, Cynthia; Gielen, Ingrid M.V.L. Progressive ethmoidal hematoma originating from the rostral maxillary sinus in a 18-year-old Warmblood gelding. *CT-User, 3rd International meeting*, Ghent, Belgium, November 30-December 1, 2013, p.17.

Vlaminck, Lieven; **Crijns, Casper P.**; Gielen, Ingrid M.V.L. Nasal cavity and sinuses in equines. *CT-User, 3rd International meeting*, Ghent, Belgium, November 30-December 1, 2013, p.148-149.

Crijns, Casper P.; Gielen, Ingrid M.V.L. CT in equine brain diseases. *CT-User, 3rd International meeting*, Ghent, Belgium, November 30-December 1, 2013, p.148-149.

Crijns, Casper P.; Hofland, Leendert-Jan; Veldeman, Bart; De Blaauw, Sander J.A.; Sterk, Teun. Successful closed reduction of an atlantoaxial luxation in a Dutch Warmblood gelding with long-term follow-up. *European Veterinary Conference: Voorjaarsdagen*, Amsterdam, The Netherlands, April 17-19, 2014, p.278.

De Blaauw, Sander J.A.; Verschoor, I.; **Crijns, Casper P.** Ultrasonographic artefacts appearance in the collateral ligaments of the distal interphalangeal joint with the ligament under different tension levels. *EVDI Annual congress*, Utrecht, The Netherlands, August 27-30, 2014.

Crijns, Casper P.; van Bree, Henri J.J.; van Loon, Gunther; Schauvliege, Stijn; Martens, Ann; Gielen, Ingrid M.V.L. Computed tomographic pituitary gland height-to-brain area ratio measurements in healthy equines. *EVDI Annual congress*, Utrecht, The Netherlands, August 27-30, 2014.

Crijns, Casper P.; Martens, Ann; Bergman, Erik H.J.; van der Veen, Henk; Duchateau, Luc; van Bree, Henri J.J.; Gielen, Ingrid M.V.L. Comparison of radiography vs. CT in equine orthopaedic trauma: intramodality and intermodality agreement in radiography and computed tomography of equine distal limb fractures. *Turkish Small Animal Veterinary Association, Continuing Education congress*, Istanbul, Turkey, October 31-November 1, 2014, p.196.

Crijns, Casper P.; Gielen, Ingrid M.V.L. A lethargic foal. *Equine MR and CT Imaging Days*, Bonn, Germany, February 19-21, 2015.

Crijns, Casper P.; Gielen, Ingrid M.V.L. An Arabian foal with epileptic seizures. *Equine MR and CT Imaging Days*, Bonn, Germany, February 19-21, 2015.

Crijns, Casper P.; Hofland, Leendert-Jan Diagnostic applications of MMEP and therapeutic management: theory and case presentations. *Focus on the Equine Spine Advanced Course Part Two,* Utrecht, The Netherlands, April 5-8, 2016.

DANKWOORD

Dan rest mij nu enkel nog om eenieder te bedanken die direct of indirect heeft meegeholpen aan het tot stand komen van dit doctoraatsproefschrift. Een werk waar veel uren in zijn gaan zitten, maar waar ik onmogelijk van kan zeggen dat ik dit alleen gedaan heb.

Een doctoraat schrijven gaat niet zonder de toegewijde begeleiding van promotoren. Ingrid daarom wil ik beginnen met jou hartelijk te bedanken voor de jarenlange, zeer aangename samenwerking. Een samenwerking die begonnen is in het voorlaatste jaar van mijn studies. Ik kan me onze eerste ontmoeting nog goed herinneren. Er moest een literatuurstudie geschreven worden over CT van de knie bij het paard. Maar gelukkig stond je vanaf het begin open voor andere ideeën en hebben we een mooi case report geschreven. Terugkijkend was dat het begin van dit avontuur. Ingrid, het eindwerk dat vandaag voor ons ligt zou zeker en vast niet tot stand zijn gekomen zonder jouw gedrevenheid en toewijding. Ik ben je daarom zeer dankbaar voor de kansen die je me vanaf het begin geboden hebt, je niet nalatende steun en de wijze raad die je altijd paraat hebt. Maar natuurlijk ook voor het altijd nalezen en verbeteren van de verschillende manuscripten en de verschillende brieven aan de editors die daarbij meegestuurd moesten worden.

Ann vanaf het begin, toen je gevraagd werd om mee te werken aan het eerste fracturen onderzoek heb je dat met veel enthousiasme en toewijding gedaan. Om met de woorden van Prof. Verschooten te spreken, de samenwerking tussen de radioloog en de chirurg is onontbeerlijk voor de patiënt. In casus betekent dit, dat ik je zeer dankbaar ben voor de inzichten en kennis die ik van je heb mogen leren. En ik ben je uiteraard ontzettend dankbaar dat je me geïntroduceerd hebt bij Teun en Leendert-Jan.

Katrien, jij bent als derde toegevoegd bij de promotoren, maar in de afgelopen jaren heb ik zowel voor je officiële aanstelling als promotor van dit proefschrift als erna ontzettend veel van je geleerd, bedankt voor alles.

Em. Prof. Dr. Henri van Bree, beste Piet, als oud-vakgroepvoorzitter heeft u - voor een groot deel op de achtergrond - dit proefschrift maar ook mijn carrière met een gerichte visie aangestuurd. U heeft de mogelijkheid gecreëerd om bij de vakgroep te beginnen en in de loop van de tijd het idee ondersteund om, naast mijn wetenschappelijke werkzaamheden, in de praktijk te gaan werken. Terugkijkend op de verschillende gebeurtenissen kan ik u enkel en alleen uitermate dankbaar zijn.

Prof. Dr. De Backer, voorzitter van de examencommissie, dank u wel voor het opnemen van deze taak en het zorgen dat de officiële bijeenkomsten en verplichtingen in goede banen zijn geleid met dit werk als eindresultaat.

Prof. Dr. Vlaminck, secretaris van de examencommissie, lid van de begeleidingscommissie, maar ook de clinicus die de afgelopen jaren de meeste patiënten voor CT heeft doorverwezen. Naast de belangrijke officiële taak waarvoor ik je bedank, wil ik je vooral ook bedanken voor alle case besprekingen die we de afgelopen jaar gehad hebben.

Em. Prof. Dr. Verschooten, beste Francis, uw gedrevenheid, passie en uitgesproken mening over het vak en uw bereidheid om altijd langs te komen om beelden, casus of manuscripten te bespreken was uitermate leerzaam en waardeer ik ontzettend. Eigenlijk kan ik enkel zeggen dat ik het een eer vind dat u hier altijd tijd voor heeft willen nemen. Ik voel me bevoorrecht dat uw gesorteerd archief van enkel in “hardcopy” te verkrijgen oude artikelen nu in mijn werkkamer staat. Dank u voor het zetelen in de begeleidingscommissie en examencommissie van mijn doctoraat.

Prof. Dr. Weller, dear Renate, your work drive but above all your great personality are to admire. Your comments were always correct and to the point, but with the necessary humour (I quote: “Wouldn’t it be better to use proper English?”). Thank you very much to be part of my doctoral advisory committee and the examination board and I hope we will be able to work on some projects together in the future.

Prof. Dr. Pille, Prof. Dr. Cornillie, Prof. Dr. van Weeren en Drs. Hofland wil ik bedanken voor hun bijdrage in de examencommissie, de kritische verbeteringen van dit proefschrift en scherpe opmerkingen tijdens de interne verdediging hebben dit werk zonder enige twijfel verder verbeterd.

Walter, Annemie, Aqui, Lieve, Kaatje en Billy, mijn directe collega's van de CT MRI unit en voor een groot deel van jullie mijn (ex-)bureaugenoten, met jullie heb ik de afgelopen jaren het meest en vooral zeer aangenaam samengewerkt. Of het nu ging om even de kliniek te bespreken, een opmerking van een reviewer door te nemen, een tekstuele vraag op te lossen of gewoon om even een frustratie te luchten, onderling ging dat prima! Bedankt daarvoor! Walter en Billy nog even doorzetten en heel erg veel succes met het afronden van jullie doctoraten! Walter vanaf het begin hebben we altijd goed kunnen samenwerken en kunnen lachen, die agility moet ik echter toch nog een keer live komen zien. Annemie vanaf dag één was ik welkom om een bureau met je te delen, alhoewel ik het waarschijnlijk niet vaak laat merken apprecieer ik je enorm. Aqui wherever you go in the future, I will come and visit! Lieve en Kaatje succes met jullie verdere carrière. Collega's, we houden contact!

Kim en Marnix, ik denk dat er in de kliniek weinig zou gebeuren mochten jullie er niet zijn. Kim je hebt me, op een altijd vrolijke manier, geleerd hoe je een goede foto moet nemen, je kritische blik en het inzicht om een net niet goede foto te verbeteren zijn vaardigheden waarvoor ik je zeer dankbaar ben. Marnix de luxe die we bij de beeldvorming hebben om altijd direct van je technische ondersteuning gebruik te kunnen maken is een groot voorrecht en het maakt ons leven in ieder geval een stuk gemakkelijker. Uiteraard ook een grote dank voor het ontwerpen van de cover van dit proefschrift! Het is altijd een plezier geweest om met jullie te mogen samenwerken en daar ben ik zeer dankbaar voor. Mochten jullie in Nederland passeren staat de kreeft (het oranje op het bord Kim…) altijd klaar.

De collega radiologen voor paard, Els, Stijn, Sarah, Elke, Lise, Fred en Prof. Dik, ik heb van jullie veel mogen leren de afgelopen jaren, de structurele, kritische interpretatie van de kleinste details op een radiografie is een vaardigheid, die ik voornamelijk door jullie geleerd heb, waarvoor dank. Ik hoop dat we elkaar in de toekomst nog gaan tegenkomen en dat we nog wat interessante gevallen kunnen bespreken. Els, Lise en Fred good luck with the exams, don't forget to sleep so now and then…

Als radiologen maken we voornamelijk plaatjes voor andere diensten, maar voor de CT-studies hebben we toch altijd hulp nodig van de anesthesisten. Stijn de rust en kalmte die je uitstraalt ook als het even iets spannender wordt is bewonderingswaardig en ik heb in de loop van de jaren gezien dat je de vaardigheden van een goede anesthesist en deze rust op alle jonge residenten hebt overgedragen, chapeau en heel veel dank daarvoor. Hoewel het altijd even spannend was om met een nieuwe anesthesist voor het eerst een paard vanuit de recovery box naar de CT-ruimte te transporteren en daarbij, mijn favoriet, op het laatste moment toch een katheter in de cephalica te vragen, is het toch altijd goed afgelopen. Miguel, Barbara, Sanne, Daphne, Diego, Ilaria, Anne, Anja, Charlotte en de anesthesisten van kleine huisdieren, Tim, Tim, Koen, Virginie, Annika, Inge, Alix, Alessandra, Anouk, Caroline en Katrien, bedankt voor de vele uren die jullie bij ons doorbrengen, zonder jullie geen CT's en MRI's!

Het transporteren van de paarden ging ook zeker niet zonder de hulp van de assistentes van de operatiezaal, Carolien, Valerie en Cindy en de agenda planning van de Heidi en Veerle op het secretariaat. Dames bedankt om dit altijd met een glimlach te regelen, Cindy voortaan gebruiken we enkel nog de hoge kar!

Mijn collega interns, Thomas, Véronique, Kris, Thomas, Kimry, Jan, Dimitri en Kim jullie wil ik bedanken voor een fantastische eerste jaar!

De huidige en vroegere collega's van de medische beeldvorming en orthopedie van de kleine huisdieren, laat ik beginnen bij het kliniek secretariaat, met Marleen, bedankt voor de warme koffie die 's ochtend vroeg altijd al klaar stond en

de talloze opbeurende woorden waar iedereen voor bij je langs mag komen. En dan uiteraard het secretariaat boven, Sandra, Claudine en Natasja, men moest letterlijk langs jullie zien te geraken om mij te storen. Maar veel belangrijker naast de vrolijke goede morgen, de (volledig logische) administratieve zaken van de universiteit worden door jullie fantastisch geregeld, waardoor de rest van de vakgroep zich in onze ogen op “belangrijkere” zaken kan focussen. Uiteraard ook een grote dank aan de collega radiologen voor de kleine huisdieren, Emmelie, Eva, Kathelijne, Ines, Yseult, Pascaline, Anais, Caroline, Laure, Olivia, Blandine en de orthopeden Bernadette, Yves, Geert, Stijn, Evelien, Eva, Delphine en Kathelijn. En last but not least, uiteraard Prof. Saunders, de huidige vakgroep voorzitter, beste Jimmy succes met de niet gemakkelijke taak om deze veelzijdige groep van mensen en karakters succesvol te laten samenwerken. Collega’s succes in de toekomst!

De collega’s van de dienst Heelkunde Maarten, Kelly, Michele, Maarten, Eva, Helga, Julie en Elke en de collega’s van de dienst Inwendige ziekten Laurence, Dominique, Joke, Caroline, Gunther, Hans en de talloze interns van jullie diensten, bedankt voor de goede samenwerking de afgelopen jaren op de faculteit.

In de verschillende artikelen die zijn geschreven is de statistiek door Prof. Dr. Duchateau of door Dr. Bart Broeckx uitgevoerd. Men zegt weleens dat men met statistiek alles kan aantonen, dat wil echter niet zeggen dat dit ook kan wanneer men de statistiek correct toepast. Ik ben jullie daarom zeer dankbaar met jullie zeer kundige hulp met dit lastige onderdeel van elke studie.

Erik je aanstekelijk enthousiasme over de praktijk in combinatie met de wetenschap zijn van grote invloed geweest op mijn carrière. Het ’s avonds nog even “hobbyen” om gemakkelijker inzicht in de anatomie/pathologie te krijgen is een bezigheid die ik zeker van jou heb overgenomen en ik doe het nog steeds graag. Ik dank je voor de waardevolle kennis die ik van je heb mogen leren, heel veel succes met de nieuwe kliniek.

Zoals eerder vermeld ben ik deeltijds, met veel plezier in Bodegraven gaan werken. Teun ons eerste contact ligt ondertussen alweer enkele jaren achter ons, maar ik denk dat we het erover eens kunnen zijn dat de visie voor de toekomst die we toen een keer 's avonds laat samen met Leendert-Jan besproken hebben, steeds meer invulling begint te krijgen en dat we een zeer mooie toekomst tegemoet gaan. Bart, Sander, Hans, Hanneke, Dick, Charissa, Ilse, Eddy, Doreen, Wouter, Nathan, Dominique, Inge, Berend, Kimberley, Jomy, Madeleine, Anoeska, Sander, Marloes, Jolien, Yvonne, Stevine, Jorienke, Romy, Ellen, Katja, Regina, Ellen, Simone, Miranda, Inger, Ton, Wouter, bedankt voor de afgelopen jaren en ik verheug me er al op om in dit hechte team voltijds bij de DAP te komen werken.

Oud-studiegenoten en goede vrienden, ik wil jullie allereerst bedanken voor jullie vriendschap. Jan en Barbara sinds het begin van de studie zijn jullie zeer goede vrienden waardoor we een fantastische studententijd gehad hebben, ik moet er nog vaak aan terugdenken, veel geluk met de kleine Gust en we moeten zeker nog een keer samen gaan skiën. Wouter we kunnen wel concluderen dat we gelijkaardig terecht zijn gekomen, Lolkje ik zal zien dat ik me wat vaker, iets ruimer op voorhand, aanmeld om langs te komen, veel geluk samen met Noortje en haar toekomstige kleine broertje of zusje. Thomas hopelijk blijven onze gelijkgezinde wegen zich in de toekomst kruisen. Kaatje, ook al zijn we ieder een andere richting uitgegaan, wil ik je zeer hartelijk bedanken voor alles dat we samen hebben meegemaakt. Ik wens je het allerbeste toe voor je residency, je doctoraat en je toekomst. Brecht, ik denk nog regelmatig met plezier terug naar de weken dat we samen intern hebben gezeten in het laatste jaar van de studie.

Daniel, Joey, Edwin, Booy, Nikay, Rob, Harrie, Guido en de rest van de jongens ook al gaat er soms een hele tijd overheen dat we elkaar zien, het weerzien is altijd van harte.

Broertjes, tijdens onze studententijd moesten we aardige afstanden afleggen om een biertje met elkaar te kunnen drinken, gelukkig worden die afstanden kleiner nu we alle drie in de randstand gaan werken. Peter dat betekent dat we vaker zullen komen barbecueën. Jeroen en Sophie er komt leuke tijd aan met een extra welkome

aanvulling van de familie. Maar of het nu ver weg is of dichtbij, ik waardeer jullie enorm!

Papa en mama, jullie voorbeeld volgende en een eigen (wijze) weg in het leven te kiezen, met een duidelijk doel voor ogen, is een van de belangrijke redenen dat we vandaag bij deze mijlpaal zijn aangekomen. De wetenschap dat jullie altijd klaar staan met raad en ondersteuning maakt het leven een stuk gemakkelijker. Ik kan jullie voor zoveel specifieke zaken bedanken, maar ik zal het samenvatten in “Bedankt voor alles!”.

Met het einde van een doctoraat, komt er ook een eind aan het dankwoord, liefste Charlotte, voor jou de laatste woorden, de laatste fase van een doctoraat schijnt niet altijd gemakkelijk te zijn en de kandidaat schijnt dan af en toe humeurig en verstrooid te kunnen reageren. Gelukkig heb jij daar geen last van gehad… Liefste bedankt voor je steun en raad, ik ben ervan overtuigd dat we samen een mooie toekomst tegemoet gaan!

“The important thing is not to stop questioning. Curiosity has its own reason for existing.”

Albert Einstein